INVESTIGATION OF THE REACTIVITY OF POLYHEDRAL BORANE ANIONS WITH CARBON-BASED NUCLEOPHILES AND ELECTROPHILES

by

Sedriel J. Montalvo, B.S.

A thesis submitted to the Graduate Council of
Texas State University in partial fulfillment
of the requirements for the degree of
Master of Science
with a Major in Chemistry
August 2015

Committee Members:

Debra A. Feakes, Chair

Todd W. Hudnall

Jennifer Irvin

COPYRIGHT

by

Sedriel J. Montalvo

2015

FAIR USE AND AUTHOR'S PERMISSION STATEMENT

Fair Use

This work is protected by the Copyright Laws of the United States (Public Law 94-553, section 107). Consistent with fair use as defined in the Copyright Laws, brief quotations from this material are allowed with proper acknowledgment. Use of this material for financial gain without the author's express written permission is not allowed.

Duplication Permission

As the copyright holder of this work I, Sedriel J. Montalvo, refuse permission to copy in excess of the "Fair Use" exemption without my written permission.

ACKNOWLEDGEMENTS

I would like to acknowledge my committee members: Dr. Jennifer Irvin, Dr. Todd Hudnall, and Dr. Debra A. Feakes. All of you have contributed to my graduate career. Dr. Irvin, you always gave me your opinion no matter how small the question was. Dr. Feakes and Dr. Hudnall, I would not be the chemist I am today without the guidance from both of you. Dr. Hudnall, you took me under your wing and treated me as one of your group members and taught me advanced techniques that I would have never stumbled upon alone while at Texas State. Honestly, from the time spent in your lectures and with you in the laboratory, I know that a Ph.D. is attainable. Dr. Feakes, you gave me a chance to prove myself when I was not sure anyone else would have and for that, amongst other reasons, you are irreplaceable in my life. I can never express how much appreciation I have for you allowing me to join you group after an unsuccessful undergraduate career. You were not only a fantastic mentor, but you will also be a lifelong friend that I will hold close to my heart. Thank you. I would like to thank Martin Mantz for his preliminary work investigating the nucleophilic attack of the [*trans*-$B_{20}H_{18}]^{2-}$ ion with carbon nucleophiles. I would like to thank Dr. Christopher Dorsey for assistance with the NMR. I would also like to thank the Department of Chemistry and Biochemistry and the Graduate Department at Texas State University for financial support.

I would like to recognize my family for their support during my career, especially Abuney, Avier, and Edris for giving me advice when I needed it and when I did not. I

would also like to thank my friends James Titus and Julia Lara. Julia, the countless nights in the lab would have been much more unbearable without a partner in crime. The brainstorming you helped with, brought to light new perspectives on experiments and helped me develop my ability to convey chemistry. James, the late nights helping each other stay up working, along with helping me learn that sometimes you have to call it a night, helped me finish. You will always be a brother in my eyes. A special thanks to Michelle Mindieta. Michelle, as you and I progressed through our academic careers, the support you have given me allowed me to look at problems from different angles and remember to have fun. You were indispensable over the past two years. To all of you, thank you.

This manuscript was submitted on July 9, 2015.

TABLE OF CONTENTS

Page

LIST OF TABLES

Table **Page**

LIST OF FIGURES

Figure **Page**

LIST OF SCHEMES

Scheme **Page**

ABSTRACT

The substitution chemistry of the [*trans*-$B_{20}H_{18}]^{2-}$ ion was first investigated by Hawthorne and coworkers The nucleophilic attack of the [*trans*-$B_{20}H_{18}]^{2-}$ ion by a hydroxide ion, alkoxide ion, thiolate ion, and amine ion have been reported in the literature. To date, there have been no reports in the literature of nucleophilic attack of the [*trans*-$B_{20}H_{18}]^{2-}$ ion with carbon nucleophiles. Previous investigations of the interaction of the [*trans*-$B_{20}H_{18}]^{2-}$ ion with carbon nucleophiles have not been completely characterized. Initial characterization using X-ray diffraction has been complicated due to difficulty in obtaining singles crystals of the reduced derivatives. Single crystals of the oxidized derivatives, $[B_{20}H_{17}X]^{2-}$, are more easily acquired. However, when characterized using X-ray diffraction, unexpected results were obtained, presumably as a result of the harsh reaction conditions of the oxidation reaction. Therefore, an investigation of alternative oxidizing agents is warranted. As a result, the overall goal of the research project is to create a series of $[B_{20}H_{17}X]^{4-}$ ions and $[B_{20}H_{17}X]^{2-}$ ions where X is a carbon-based nucleophile. Specific aims for the research project are:

1) Investigate the reaction of the [*trans*-$B_{20}H_{18}]^{2-}$ ion with a variety of carbon nucleophiles,
2) Investigate the oxidation of the resulting $[B_{20}H_{17}X]^{4-}$ ions to form a series of $[B_{20}H_{17}X]^{2-}$ ions, restoring the three-center two-electron bond, and
3) Characterize the $[B_{20}H_{17}X]^{2-}$ ions by single crystal X-ray diffraction.

A series of reactions were completed which yielded reduced, substituted derivatives of the $[B_{20}H_{18}]^{4-}$ ion where the substituent is a carbon-based nucleophile. Carbon nucleophiles investigated included the acetylide ion, the methyl anion, the acetonitrile anion, and the cyanide ion. Due to the difficulty of growing single crystals, suitable for characterization by X-ray crystallography, the resulting products were oxidized with an organic oxidizing agent, *p*-benzoquinone, which allowed the react accomplished under significantly milder conditions than the previously used oxidizing agent, ferric chloride. The location of the substituent appears to be a result of the hardness or the softness of the nucleophile utilized. As a result of the research, a new theory regarding the factors that control the location of the substituent has been proposed. Further characterization of several products, using X-ray diffraction, will be needed to provide supporting evidence.

The oxidation of the reduced product in the presence of an electrophile was investigated using several electrophiles in order to investigate the potential to selectively substitute the resulting product. Reaction conditions necessary for the formation of the products have been determined. Preliminary results indicate that the substituted [*trans*-$B_{20}H_{18}]^{4-}$ ion may be successfully oxidized to a substituted [*trans*-$B_{20}H_{18}]^{2-}$ ion. The data also suggest that the reactions yield a bridge complex instead of a doubly substituted product as hypothesized. However, final verification by X-ray diffraction needs to be completed.

CHAPTER I

INTRODUCTION

1.1 Boron Neutron Capture Therapy

Boron neutron capture therapy (BNCT) is a binary cancer therapy that utilizes a neutron capture reaction to initiate a cytotoxic fission.[1, 2] The therapy was first proposed by Locher in 1936 and was made possible, in part, by the rise of nuclear energy from World War II.[3] To initiate the reaction, the boron-10 isotope is irradiated with thermal neutrons (0.025 eV).[1, 2] The outcome is a linear dispersion of alpha particles, ^{4}He, recoiling lithium, ^{7}Li, and 2.28 MeV of kinetic energy. The reaction is represented by the following equation: ${}^{10}_{5}\mathrm{B} + {}^{1}_{0}\eta \rightarrow {}^{4}_{2}He^{2+} + {}^{7}_{3}Li^{3+} + \gamma$.[1, 2] The linear energy transfer (LET), denoted as γ, dissipates within approximately one cell diameter (~10 μm) and, theoretically, the limited distance results in the destruction of an individual cell and prevents damage to cells in immediate proximity.[1, 4, 5] Boron-10 is ideal for the neutron capture reaction because its high neutron capture cross section is orders of magnitude greater than other elements found in mammalian tissue, the isotopic abundance of boron-10 is relatively high, and boron has a wide derivative chemistry which enables its incorporation into biologically active compounds.[2] In order for the treatment to be successful, approximately 20 μg of boron-10 per g of tumor must be selectively delivered to and retained by the tumor cells. Along with this, the boron within the tumor cell must absorb enough thermal neutrons to cause lethal damage to the tumor cells.[1] The novel approach of the binary cancer therapy provides a direct method of attack on the tumor cell. This therapy is designed to be selective towards malignant cells and provides an

alternate approach to current cancer therapies. Agents to be used in BNCT must meet a series of requirements such as: 1) a low toxicity, 2) a low normal tissue uptake (including blood), 3) a high uptake in tumor tissue, 4) rapid clearance of agent from normal cells and tissues, and 5) retention of agent within tumor cells during irradiation.[1] Two agents have been approved for clinical trials: mercaptoundecahydrododecaborate ($Na_2B_{12}H_{11}SH$) commonly known as sodium borocaptate (BSH), and l-4-dihydroxy-borylphenyalanine (BPA), a boron derivative of an amino acid. The [*closo*-$B_{10}H_{10}]^{2-}$ ion, commonly abbreviated as GB-10, has also been used in human clinical trials.[1] None of these compounds fulfill all of the requirements needed to be an ideal agent for BNCT. As a result, research has resulted in a new generation of compounds involving one or more polyhedral boranes or polyhedral carboranes coined as the "third generation" of BNCT agents.[3] Polyhedral borane or carborane-containing compounds are attractive for potential BNCT agents due to their high concentration of boron atoms, the ability to be modified in several locations, and the moderate molecular weight.[2, 3, 6]

1.2 **Boranes**

Boron's history dates back to the ancient era with the compound borax, which was used to form borosilicate glass. The name, boron, was proposed by H. Davy and is a combination of its original source, borax, and the name of its neighbor on the periodic table, carbon. Boron is a nonmetal that is a member of group III on the periodic table. Boron differs from carbon by having one less valence electron. Additionally, since boron is less electronegative than carbon, the B-H bond has a reversed polarity as compared to the C-H bond. Boron has several common similarities to its neighbor, carbon, such as the

fact they both form covalent molecules.[7] Boron is known to catenate, similar to carbon and in turn, compounds that contain only carbon and hydrogen are called alkanes and compounds that contain only boron and hydrogen are called boranes.[7, 8] The catenation creates polyhedral borane compounds which are described as having three-dimensional aromaticity and larger boron cages are analogous to buckeyball.[9] These polyhedral boranes are referred to as boron clusters. Not all polyhedral boranes are aromatic. Aromaticity, along with the classification of polyhedral cluster compounds, is accomplished with a set of rules established by Dr. Kenneth Wade.[10] In 1971, Wade described three classifications of polyhedral borane compounds: *closo, nido,* and *arachno*.[11] The compounds are classified by the number of skeletal bonding electron pairs they contain. If held together by (n + 1) pairs of electrons, where n is the number of vertices within the skeletal structure of the borane, the compound is classified as *closo*; if held together by (n + 2) pairs of electrons, the compound is classified as *nido*; and, if held together by (n + 3) pairs of electrons, the compound is classified as *arachno*. The rules and additional classifications were further developed by D. M. P. Mingos in 1972 by expanding on the principle of counting skeletal electrons pairs.[10, 11] Alfred Stock began investigating borane chemistry in 1912. He pioneered synthetic borane procedures for 20 years.[7, 8] Techniques that he developed included the air sensitive techniques necessary when handling the hazardous and potentially explosive compounds *nido*-B_6H_{10}, *arachno*-B_5H_{11}, *nido*-B_5H_9, *closo*-B_4H_{10}, and *nido*-B_2H_6. Stock was also recognized for the synthesis of decaborane ($B_{10}H_{14}$) whose chemical structure is depicted in **Figure 1.**[13, 14] Stock's introductory work led to the work of Lipscomb, who was awarded the Nobel prize in Chemistry in 1976.[12] Lipscomb's work described the bonding and structure of

complex boranes, specifically the investigation of compounds with three-center two-electron bonds.[12]

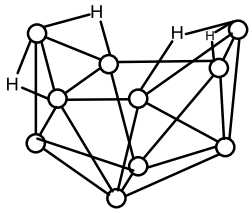

Figure 1: Structure of decaborane, $B_{10}H_{14}$.

In Figure 1 and throughout, an open circle in a figure represents a B-H vertex. Therefore, decaborane is characterized by ten B-H vertices bonded together through a web of B-B-B and B-H-B bonds. The structure is classified as a *nido* polyhedral borane by Wade's rules.[11] Decaborane is synthesized by the pyrolysis of smaller boranes under a vacuum free of any halogens and is later isolated by sublimation to form a white crystalline solid.[15] When decaborane is placed in the presence of a two electron donor, a new complex is formed, $B_{10}H_{12}X_2$, where X is the two-electron donor, as an intermediate. Upon heating, the intermediate will then undergo an internal conversion to form a [*closo*-$B_{10}H_{10}$]$^{2-}$ anion (**Figure 2**).[12]

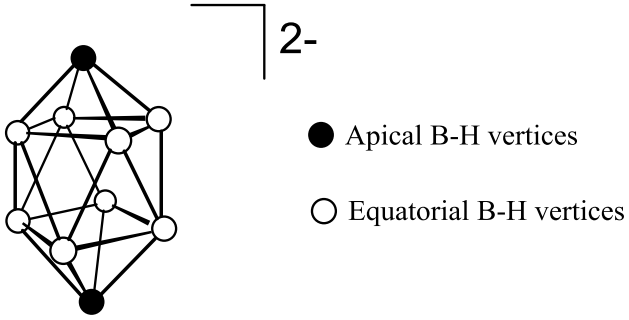

Figure 2: Structure of the [*closo*-$B_{10}H_{10}$]$^{2-}$ anion.

Oxidation of the [*closo*-$B_{10}H_{10}]^{2-}$ anion using a suitable oxidizing agent in a refluxing aqueous environment results in the formation of the $[B_{20}H_{18}]^{2-}$ ion. The reaction scheme is represented in **Scheme 1.**

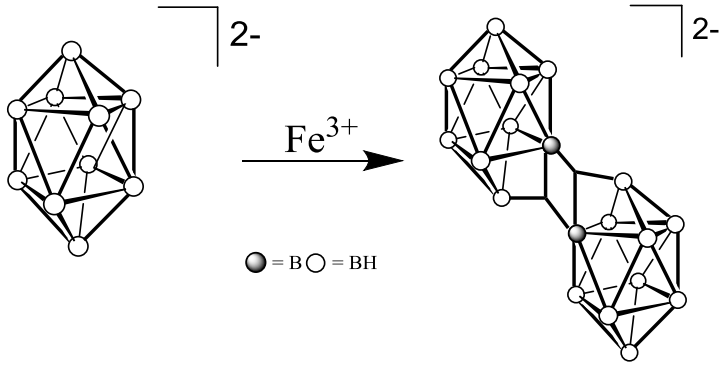

Scheme 1. The oxidation of the [*closo*-$B_{10}H_{10}]^{2-}$ ion to yield the $[B_{20}H_{18}]^{2-}$ ion.

The $[B_{20}H_{18}]^{2-}$ ion was first synthesized by Kaczmarczyk and coworkers in 1962 (**Scheme 1)**.[15] Originally, Lipscomb suggested that the structure of the oxidized species contained a doubly-bridged hydrogen atom; however, the ion has now been characterized by X-ray crystallography and the two polyhedral borane cages are known to be linked by two three-center two-electron bonds.[16]

Three isomers of the $[B_{20}H_{18}]^{2-}$ anion are known to exist (**Figure 3**): [*trans*-$B_{20}H_{18}]^{2-}$ (equivalent to the normal isomer, [*n*-$B_{20}H_{18}]^{2-}$), [*cis*-$B_{20}H_{18}]^{2-}$, and [*iso*-$B_{20}H_{18}]^{2-}$. All of the isomers are characterized by the presence of two polyhedral $[B_{10}H_9]^-$ anions tethered by two three-center two-electron bonds. The unique location and linkage of the three-center two-electron bonds determines the isomeric conformation of the polyhedral borane anion. The *cis* isomer is characterized by having one of the polyhedral

borane cages perpendicular to the position in the *trans* isomer, while the [*iso*-$B_{20}H_{18}]^{2-}$ is identified by its parallel B-H-B linkages between the two $[B_{10}H_9]^-$ cages.[4,17-19]

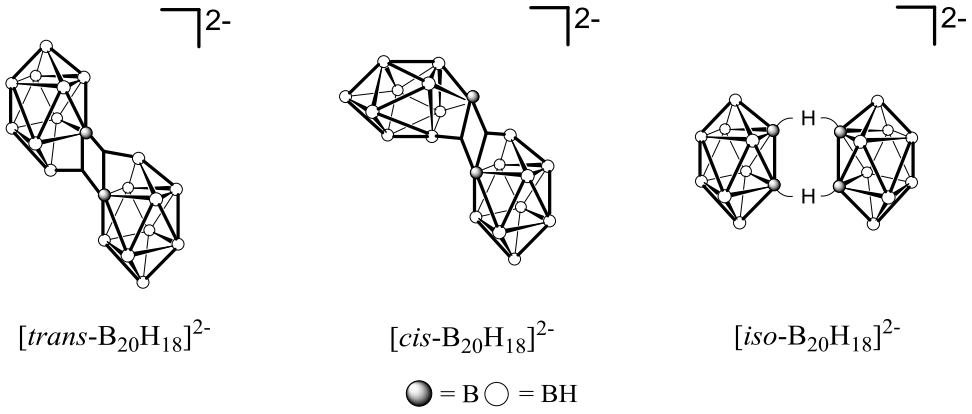

Figure 3: Structures of three isomers of the $[B_{20}H_{18}]^{2-}$ ion.

Each of the isomeric forms is synthesized differently. The [*trans*-$B_{20}H_{18}]^{2-}$ ion was first prepared from the Fe^{3+} oxidation of the $[B_{10}H_{10}]^{2-}$ ion.[16, 17] Treatment of [*trans*-$B_{20}H_{18}]^{2-}$ with ultraviolet light in acetonitrile yields the [*iso*-$B_{20}H_{18}]^{2-}$, a photoisomer of the [*trans*-$B_{20}H_{18}]^{2-}$ ion. The formation of the [*iso*-$B_{20}H_{18}]^{2-}$ is reversible and the reformation of the [*trans*-$B_{20}H_{18}]^{2-}$ ion is accomplished through thermal soaking of the [*iso*-$B_{20}H_{18}]^{2-}$ ion in water at 100 ^oC for 36 hours.[20] The *cis* isomer is formed by treating the $[B_{10}H_{10}]^{2-}$ ion with two equivalents of Ce^{4+} ion in acidic aqueous conditions.[20]A summary of conversions is depicted in **Scheme 2**.

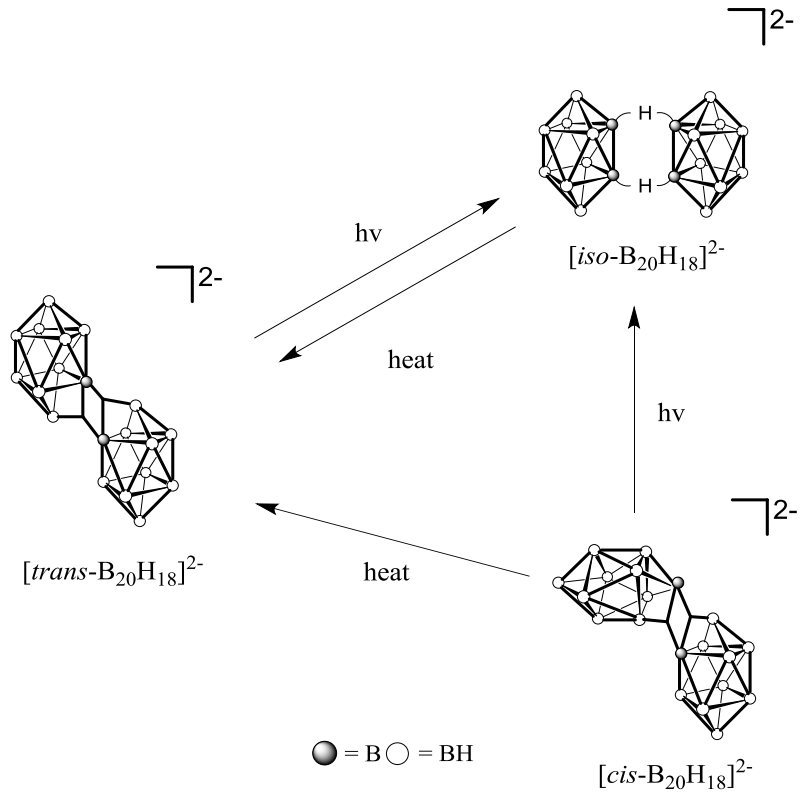

Scheme 2. Summary of the conversion reactions between the *trans*, *cis* and *iso* $[B_{20}H_{18}]^{2-}$ isomers.

Treatment of the $[trans\text{-}B_{20}H_{18}]^{2-}$ ion with sodium in liquid ammonia yields a reduced polyhedral borane anion, the $[B_{20}H_{18}]^{4-}$ ion. The $[B_{20}H_{18}]^{4-}$ ion is characterized by the presence of a B-B linkage between the equatorial boron atoms and referred to as $[e^2\text{-}B_{20}H_{18}]^{4-}$. When the $[e^2\text{-}B_{20}H_{18}]^{4-}$ ion is subjected to an acidic solution, an acid catalyzed rearrangement is induced and forms a second isomer, referred to as the $[a^2\text{-}B_{20}H_{18}]^{4-}$ ion (**Figure 4)**. The $[a^2\text{-}B_{20}H_{18}]^{4-}$ ion is characterized by having a B-B linkage between the apical boron atoms of the polyhedral borane cages. A third isomer, the $[ae\text{-}B_{20}H_{18}]^{4-}$ ion, is also possible and is characterized by having a B-B linkage between an apical boron atom and an equatorial boron atom on the respective polyhedral borane cages.[20]

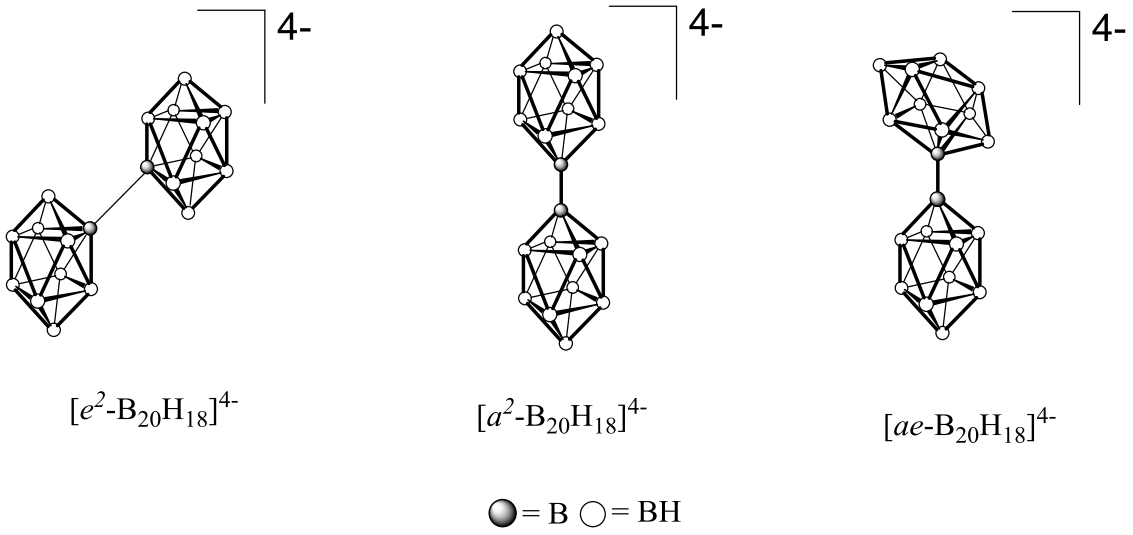

Figure 4: Isomers of the reduced $[B_{20}H_{18}]^{4-}$ ion.

1.3 Nucleophilic Attack on the $[B_{20}H_{18}]^{2-}$ Ion

The three-center two-electron bond present in all three isomers of the $[B_{20}H_{18}]^{2-}$ ion provide an electron-deficient location within the compound that is susceptible to nucleophilic attack.[1] Nucleophilic attack is initiated by the attack on the equatorial boron atom in one of the electron-deficient, three-center, two-electron bonds by the nucleophile followed by a migration of one of the cages. A second equivalent of the nucleophile is required to remove the bridging hydrogen and convert the $[B_{20}H_{18}X]^{3-}$ ion into the $[B_{20}H_{17}X]^{4-}$ ion (**Scheme 3)**.[21]

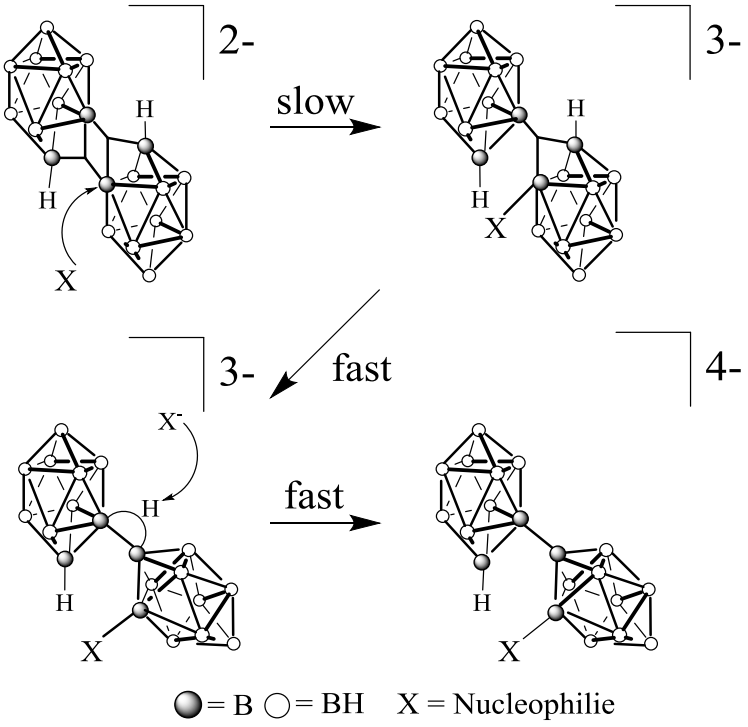

Scheme 3. Mechanism of nucleophilic attack proposed by Hawthorne in 1965.[22]

The resulting [*ae*-$B_{20}H_{17}X]^{4-}$ ion, the kinetic isomer, is also susceptible to acid-catalyzed rearrangement, forming the thermodynamic isomer, [a^2-$B_{20}H_{17}X]^{4-}$. The [*cis*-$B_{20}H_{18}]^{2-}$ and the [*iso*-$B_{20}H_{18}]^{2-}$isomers are also susceptible to nucleophilic attack.[2] Reductive substitution of the [*iso*-$B_{20}H_{18}]^{2-}$ yields a substituted [e^2-$B_{20}H_{17}X]^{4-}$ ion.[21] The substituent is located on the equatorial belt adjacent to the terminal boron apex as seen in **Scheme 4**. The [e^2-$B_{20}H_{17}X]^{4-}$ ion can undergo an acid-catalyzed rearrangement to yield the [a^2-$B_{20}H_{17}X]^{4-}$ ion.[21]

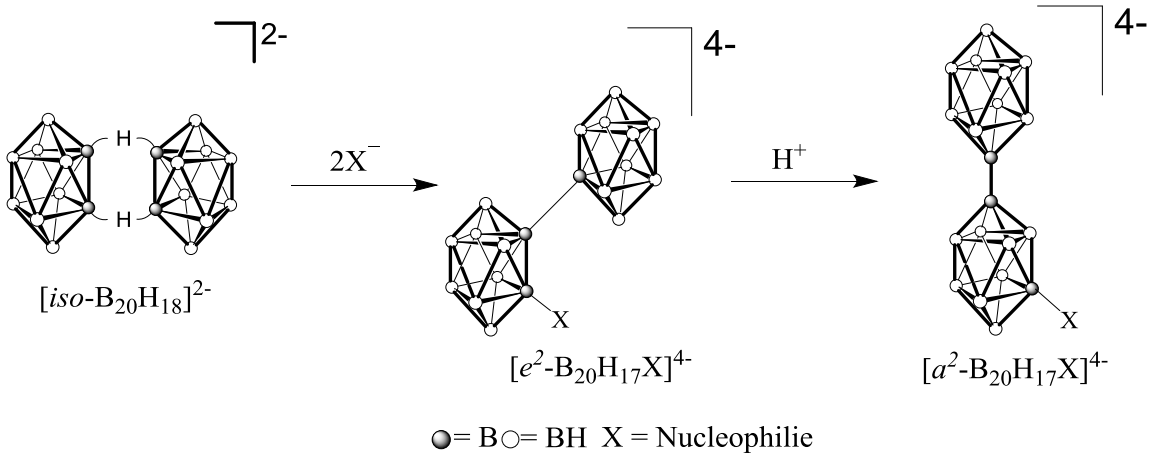

Scheme 4. Conversion of $[a^2\text{-}B_{20}H_{17}X]^{4-}$ from $[e^2\text{-}B_{20}H_{17}X]^{4-}$ generated from $[iso\text{-}B_{20}H_{18}]^{2-}$ ion.

Reactions involving the polyhedral borane anions are monitored by ^{11}B nuclear magnetic resonance (NMR) spectroscopy. The $^{11}B\{^1H\}$ NMR spectrum of the starting material for current investigations, the $[trans\text{-}B_{20}H_{18}]^{2-}$ ion, is characterized by a seven peak pattern (**Figure 5**).

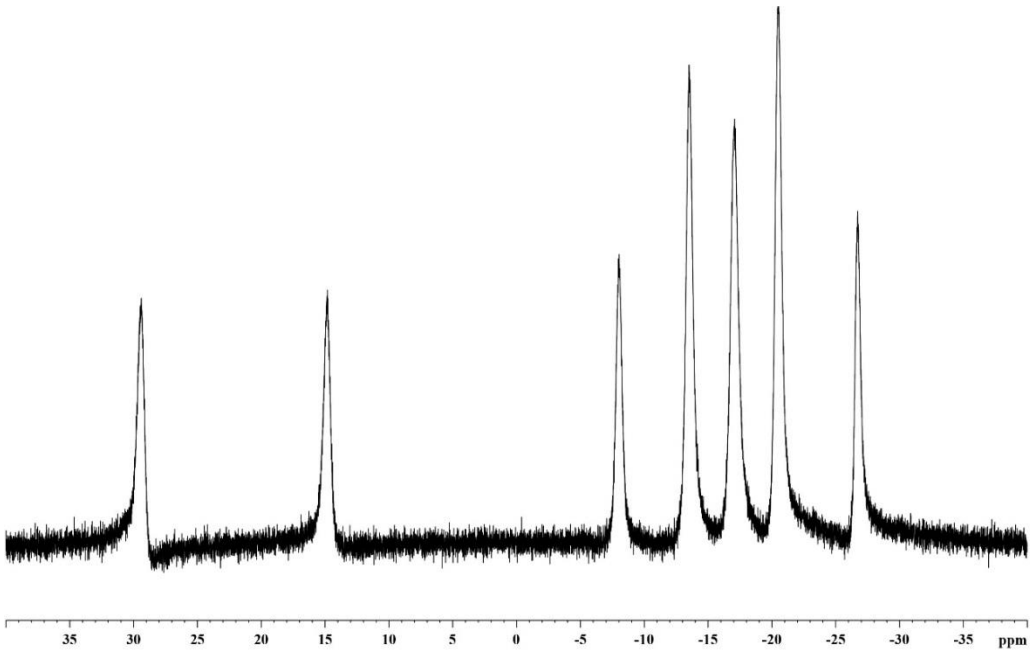

Figure 5: $^{11}B\{^1H\}$ NMR spectrum of the $[trans\text{-}B_{20}H_{18}]^{2-}$ ion.

Conversion of the [*trans*-$B_{20}H_{18}$]$^{2-}$ ion to a substituted product is easily observed in the ^{11}B NMR spectrum. Signals associated with apical boron atoms and substituted boron atoms are observed downfield of -15 ppm, while the signals associated with the equatorial boron atoms are observed upfield of -15 ppm. An *ae*-isomer is characterized by three apical B-H singlets in a ^{11}B{^{1}H} NMR spectrum (**Figure 6)** and as doublets in the ^{1}H coupled ^{11}B NMR spectrum (**Figure 7)**. An a^2-isomer is characterized by two singlets due to the presence of only two apical B-H vertices (**Figure 8)**.

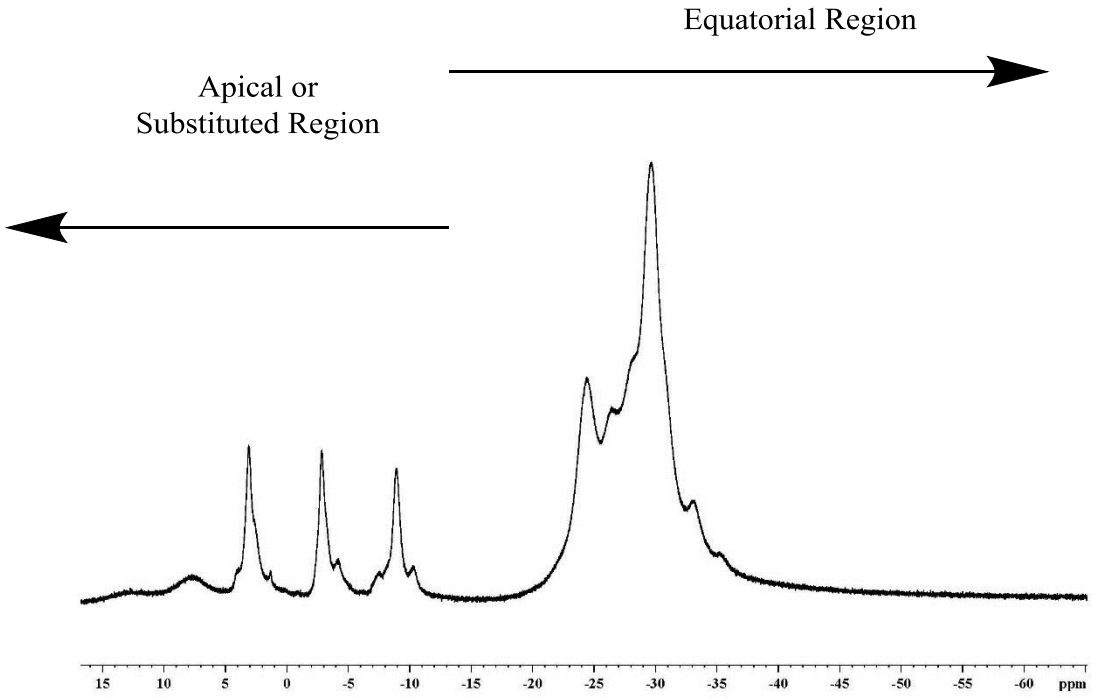

Figure 6: Representative^{11}B{^{1}H} NMR spectrum of an apical-equatorial isomer of [$B_{20}H_{17}X$]$^{4-}$ (X is a generic nucleophile) indicating the apical or substituted region and the equatorial region of the spectrum.

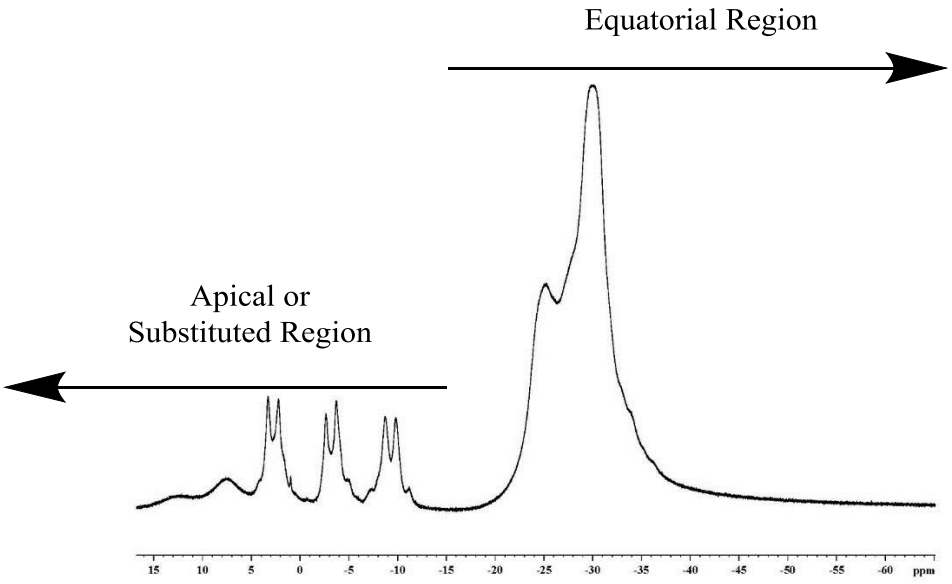

Figure 7: Representative ^{1}H coupled ^{11}B NMR spectrum of an apical-equatorial isomer of $[B_{20}H_{17}X]^{4-}$ (X is a generic nucleophile) indicating the apical or substituted region and the equatorial region of the spectrum.

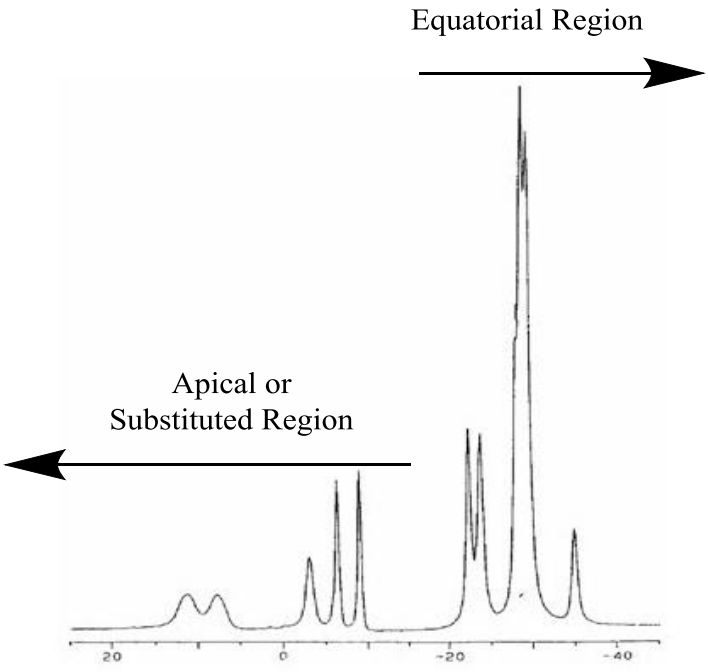

Figure 8: Representative ^{1}H decoupled ^{11}B NMR spectrum of an apical-apical isomer of $[B_{20}H_{17}X]^{4-}$ (X is a generic nucleophile) indicating the apical or substituted region and the equatorial region of the spectrum.

The derivatives of the $[B_{20}H_{18}]^{2-}$ ion have the potential to react with nucleophilic substituents on intracellular proteins and, as a result, increase their *in vivo* retention. As a result, investigation of the oxidation of the reduced substituted derivatives may lead to new compounds with the desired characteristics for potential BNCT agents.[3] For example, the retention of the $[B_{20}H_{17}NH_3]^{3-}$ ion has been attributed to an *in vivo* oxidation of the ion to the more reactive $[B_{20}H_{17}NH_3]^{-}$ ion which is susceptible to nucleophilic attack.[2] The laboratory preparation of the oxidized species has been reported for the [*ae*-$B_{20}H_{17}OH]^{4-}$ ion. The conversion is achieved at low temperatures in an aqueous solution of ferric chloride to yield the [*trans*-$B_{20}H_{17}OH]^{2-}$ ion (**Scheme 5**).[20] Ferric chloride is extremely acidic in aqueous solution and the harsh reaction conditions are not always desirable.

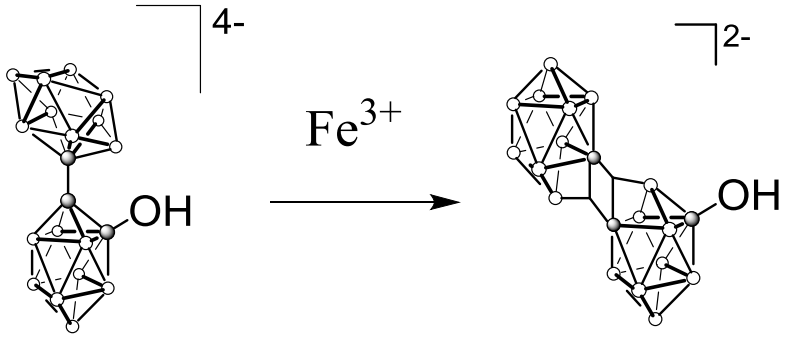

Scheme 5. Oxidation of [*ae*-$B_{20}H_{17}OH]^{4-}$ ion to form the [*trans*-$B_{20}H_{17}OH]^{2-}$ ion.

In an attempt to investigate alternative oxidizing agents that can be used in milder aqueous and organic solvents, Watson-Clark and coworkers have reported the oxidation of the [e^2-$B_{20}H_{18}]^{4-}$ ion at room temperature with *p*-benzoquinone to yield the [*trans*-$B_{20}H_{18}]^{2-}$ ion (**Scheme 6)** in aqueous solution.[22] The oxidation of the [a^2-$B_{20}H_{18}]^{4-}$ ion

using *p*-benzoquinone, to produce the [*trans*-$B_{20}H_{18}]^{2-}$ ion, also occurs in a 4:1 mixture of refluxing dichloromethane/acetonitrile (**Scheme 6).**[22]

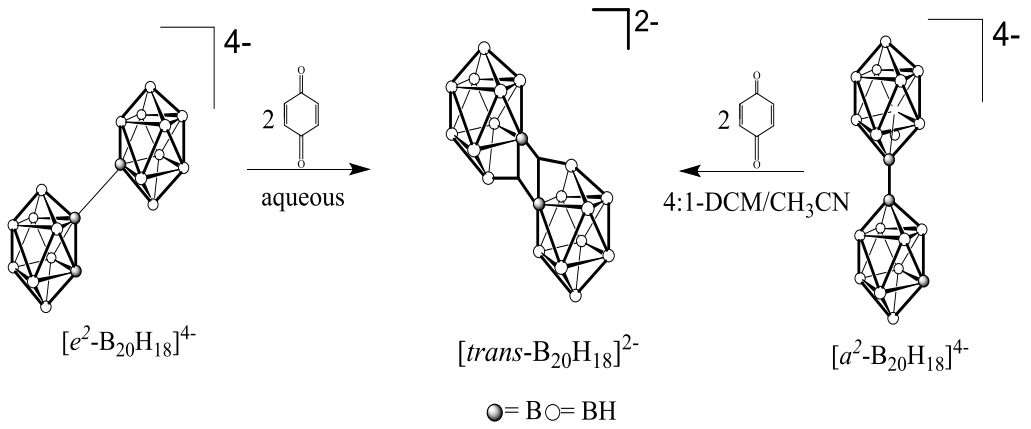

Scheme 6. Oxidation of the [e^2-$B_{20}H_{18}]^{4-}$ ion and the [a^2-$B_{20}H_{18}]^{4-}$ ion to form the [*trans*-$B_{20}H_{18}]^{2-}$ion using two equivalences of *p*-benzoquinone.

Warson-Clark and coworkers also reported that 1,4-tetrachloro-*p*-benzoquinone could be used to oxidize the [*closo*-$B_{10}H_{10}]^{2-}$ ion in acetonitrile at room temperature to yield the [*trans*-$B_{20}H_{18}]^{2-}$ ion (**Scheme 7**).[22] This is noteworthy due to unsuccessful oxidation attempts using azobenzene, nitrobenzene, benzophenone and *p*-benzoquinone.[22]

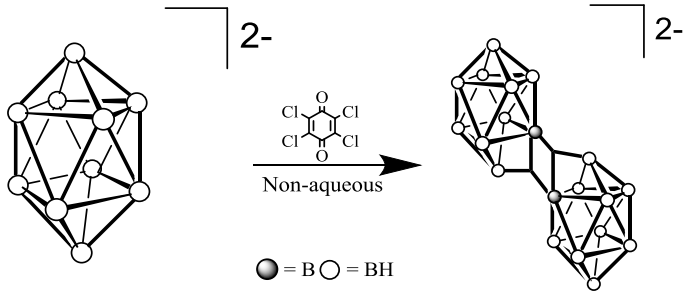

Scheme 7: Oxidation of the [*closo*-$B_{10}H_{10}]^{2-}$ ion to yield the [*trans*-$B_{20}H_{18}]^{2-}$ ion using 1,4-tetrachlorobenzoquinone.

The oxidation of the reduced substituted ions, $[B_{20}H_{17}X]^{4-}$, to form the $[B_{20}H_{17}X]^{2-}$ ions, has gained interest due to the potential application in BNCT. The oxidized compounds can be incorporated into the delivery vessel of choice, for example, liposomes, at a higher concentration. Additionally, the electron-deficient bonds characteristic of the oxidized ions have the potential to react with nucleophiles on intracellular proteins and allow for both retention of the ions in the cell as well as provide more specific binding to target systems.[4]

1.4 **Carbon Nucleophiles**

Polyhedral borane ions initially were of interests in the 1960's because of their potential to be used as high energy fuels.[23] The diminishing interest in polyhedral borane anions as fuel led to a declining interest in polyhedral borane chemistry until the 1990's where interest rose again based on the potential application of polyhedral borane ions in BNCT.[24, 25] Researchers have successfully synthesized several substituted ions of the form $[B_{20}H_{17}X]^{4-}$ where X is –OH,[20, 21] –OR,[20, 21] $–NH_3$,[4] –NHRR′,[26] and –SH.[6] To date, no reactions of the $[B_{20}H_{18}]^{2-}$ ion with a carbon nucleophile have been reported in the literature. As investigations of the nucleophilic attack of the $[trans\text{-}B_{20}H_{18}]^{2-}$ ion using varying nucleophiles proceeded, evidence arose that the original mechanism could not explain all of the observed chemistry.[3, 6] Nitrogen and oxygen nucleophiles follow the proposed mechanism in **Scheme 3**; however, sulfur nucleophiles do not appear to follow this mechanism.[6] The reaction of the $[trans\text{-}B_{20}H_{18}]^{2-}$ ion with the Bender's salt, $KSC(O)OC(CH_3)_3$, yielded an a^2 isomer directly and, based on two-dimensional ^{11}B NMR spectroscopy, the substituent is believed to be located on the equatorial belt

adjacent to the terminal boron apex (**Scheme 8)**. This isomeric assignment would be expected from the photoisomer, but not from the [*trans*-$B_{20}H_{18}]^{2-}$ ion.[19] Additionally, an unexpected and novel solvent-coordinated species, $[B_{20}H_{17}O(CH_2)_4]^{3-}$ was obtained when the [*trans*-$B_{20}H_{18}]^{2-}$ ion was allowed to react with a variety of nucleophiles in tetrahydropyran (THP) as the solvent.[27] Although not isolated, a similar solvent-coordinated species was proposed for reactions conducted in tetrahydrofuran (THF). While the solvent-coordinated species could not be isolated for the THF reactions, a ring opening event took place which resulted in the nucleophile bound to the terminal end of the ring-opened THF.[27] Hawthorne and coworkers proposed a revised mechanism in 2002 in an attempt to explain the nucleophile-solvent interactions (**Scheme 9**).[2]

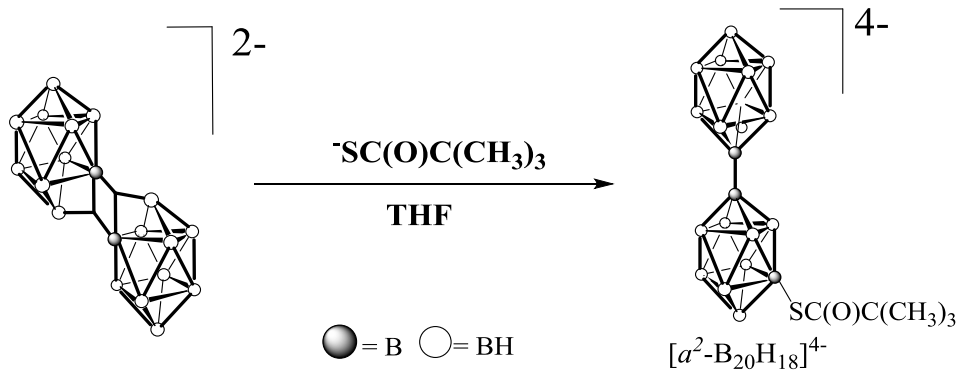

Scheme 8: Product of the reaction with the protected thiol nucleophile.

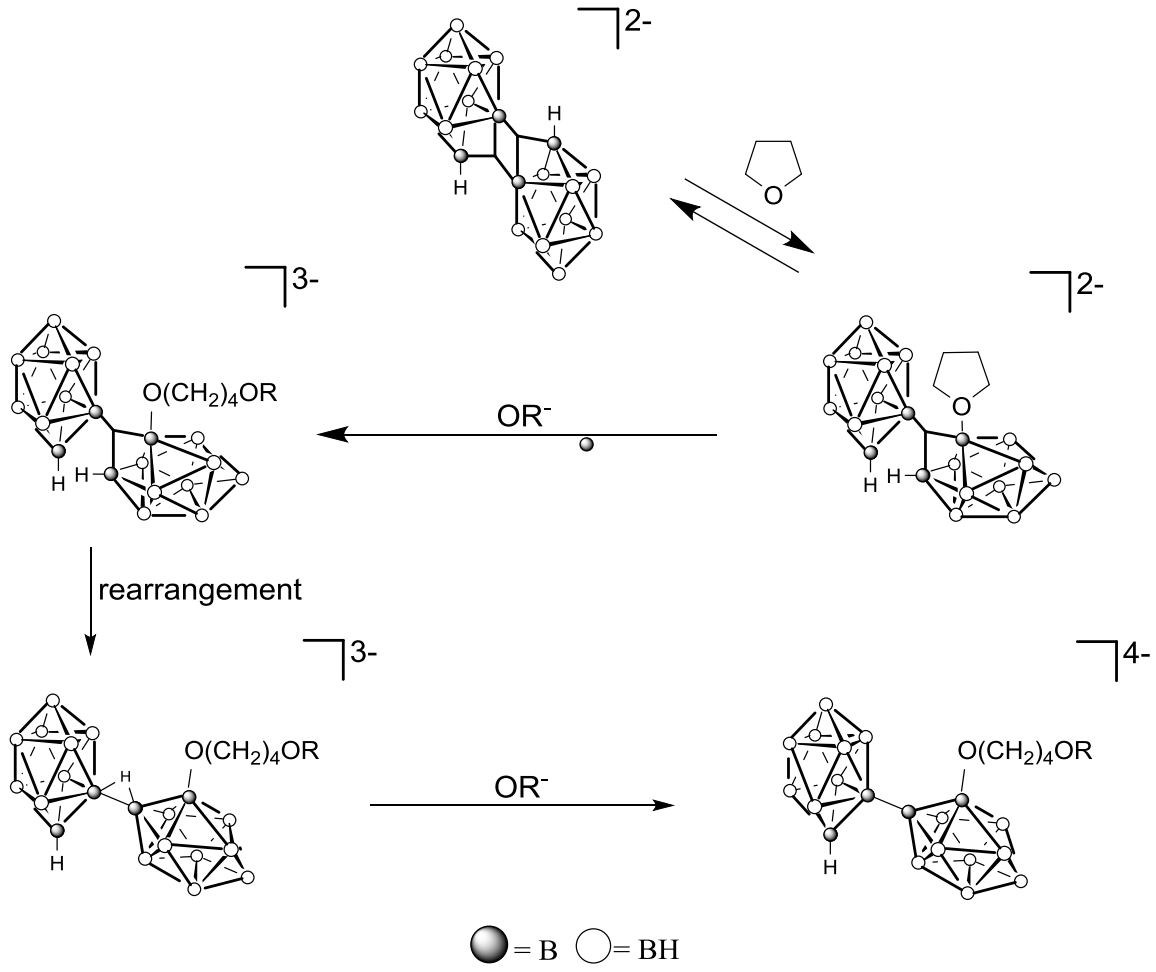

Scheme 9: Mechanism of solvent coordination with [*trans*-$B_{20}H_{18}$]$^{2-}$ion.

In 2013, Martin Mantz, a MS student at Texas State University, investigated a series of reactions based on the nucleophilic attack of the [*trans*-$B_{20}H_{18}$]$^{2-}$ ion by a series of carbon nucleophiles.[28] To our knowledge, this is the first investigation of its type. Mantz investigated three nucleophiles: $^{-}C{\equiv}CH$, $^{-}CH_2CN$, and $^{-}CH_2CH_2CH_2CH_3$. The products were characterized by ^{11}B NMR spectroscopy and the spectra of the resulting compounds were consistent with previously reported $[B_{20}H_{17}X]^{4-}$ species.[28] While the compounds were characterized by ^{11}B NMR spectroscopy, complete characterization

including high resolution mass spectrometry and/or elemental analysis had not been completed; however, the results were promising and further investigation was warranted. The $-CH_2CN$ derivative and the $-C\equiv CH$ derivative were particularly interesting because of their potential for derivatization to acid and amide derivatives and their potential application in BNCT. Mantz initiated investigations of the oxidation of the $[B_{20}H_{17}X]^{4-}$ anion resulting from the reaction of the $[trans\text{-}B_{20}H_{18}]^{2-}$ ion and the *n*-butyl ion and a single crystal, suitable for characterization by X-ray crystallography was grown; however, the resulting compound was not the anticipated $[B_{20}H_{17}(CH_2)_3CH_3]^{2-}$ ion but the $[\mu\text{-}OCH_2CH_3\text{-}B_{20}H_{17}]^{2-}$ ion which had been already reported (**Figure 9)**.[29]

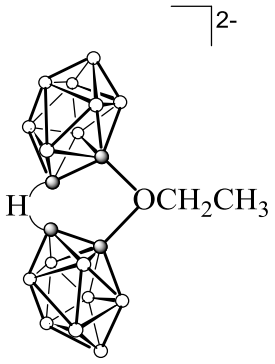

$[\mu\text{-}OCH_2CH_3\text{-}B_{20}H_{17}]^{2-}$

Figure 9: Structure of the $[\mu\text{-}OCH_2CH_3\text{-}B_{20}H_{17}]^{2-}$ ion.

As a result of the unanticipated outcome, a reinvestigation of the compounds produced in the earlier was initiated. Few $[B_{20}H_{17}X]^{4-}$ derivatives have been characterized by X-ray crystallography because of the difficulty in growing suitable crystals; however, the single crystals of the $[B_{20}H_{17}X]^{2-}$ ions are more easily obtained. As a result, the research proposed herein is based on the reinvestigation of the reactions of the $[trans\text{-}B_{20}H_{18}]^{2-}$ ion with carbon nucleophiles, followed by the oxidation of the

resulting products in an attempt to characterize each of the products by X-ray crystallography. New synthetic routes will be investigated and developed to generate the carbon-substituted $[B_{20}H_{17}X]^{4-}$ ions and further oxidize the products to produce the substituted $[B_{20}H_{17}X]^{2-}$ ions for potential application in BNCT.

CHAPTER II

STATEMENT OF PROBLEM

In spite of the fact that polyhedral borane anions have been under investigation since the 1960's and mechanisms have been proposed for the reactivity of the [*trans*-$B_{20}H_{18}]^{2-}$ ion with nucleophiles, several questions remain for further investigation. The nucleophilic attack of the [*trans*-$B_{20}H_{18}]^{2-}$ ion by a hydroxide ion, alkoxide ion, thiolate ion, and amine ion have been reported in the literature.[23, 27, 28, 29, 30] To date, there have been no reports in the literature of nucleophilic attack of the [*trans*-$B_{20}H_{18}]^{2-}$ ion with carbon nucleophiles. Ideally, the products of the reactions, $[B_{20}H_{17}X]^{4-}$, would be fully characterized, including single crystal X-ray diffraction; however, single crystals of the reduced derivatives are particularly difficult to obtain. Single crystals of the oxidized derivatives, $[B_{20}H_{17}X]^{2-}$, are more easily obtained. Therefore, an investigation of alternative oxidizing agents is warranted because of the harsh reaction conditions which exist with the ferric ion.[23] As a result, the overall goal of the research project is to create a series of $[B_{20}H_{17}X]^{4-}$ and $[B_{20}H_{17}X]^{2-}$ derivatives where X is a carbon-based nucleophile. Specific aims for the research project are:

1) investigate the reaction of the [*trans*-$B_{20}H_{18}]^{2-}$ ion with a variety of carbon nucleophiles,
2) investigate the oxidation of the resulting $[B_{20}H_{17}X]^{4-}$ ions to form a series of $[B_{20}H_{17}X]^{2-}$ ions, restoring the three-center two-electron bond, and
3) characterize the $[B_{20}H_{17}X]^{2-}$ ions by single crystal X-ray diffraction.

The proposed research will contribute to the understanding of the reactivity of the [*trans*-$B_{20}H_{18}$]$^{2-}$ ion and add to the current understanding of the factors which control the formation of the products of the reactions, including the electronic factors, steric effects, and impact of the solvent. Additionally, the resulting compounds may prove to be useful and also provide the starting materials for the production of more efficient agents for potential application in BNCT.

CHAPTER III

METHODOLOGY

3.1 **Materials**

Sublimed decaborane, $B_{10}H_{14}$, was obtained from Dr. Lee J. Todd at Indiana University (Bloomington, IN). **DISCLAMER**: **decaborane is extremely toxic and impact sensitive. It is known to form explosive mixture especially when mixed with halogenated materials.** Sodium acetylide (18% slurry in xylenes), CD_3CN, *n*-butyllithium (1.6 M solution in hexanes), methyllithum (1.6 M solution in diethyether, ±5% w/v), were purchased from Acros Organics (New Jersey, United States). Acetyl chloride (99+%), *p*-benzoquinone (98+%), ethyl magnesiumbromide (3 M in diethylether), iodomethane (99+% stab. with copper), methyl magnesiumbromide (3 M in diethylether), potassium hydroxide (85%), and rubidium acetate (99.8% metals basis) were purchased from Alfa Aesar (Ward Hill, Massachusetts). The iodomethane was packed under argon and used without any additional purification. Acetonitrile, ferric chloride hexahydrate, and methanol were purchased from VWR (Radnor or West Chester, Pennsylvania). Dichloromethane and sodium hydroxide were purchased from EM science (Gibbstown, New Jersey). Acetonitrile and dichloromethane were distilled in the presence of calcium hydride. Anhydrous diethylether , and triethylamine were purchased from J.T. Baker (Center Valley, Pennsylvania or Phillipsburg, New Jersey). The diethylether was distilled in the presence of sodium metal. The triethylamine was dried over molecular sieves. Dimethylformamide (DMF 99.9+%), D_2O, methyltriphenylphosphonium bromide ($MePPh_3$ 98%), and trifluroacetic acid were

purchased from Sigma-Aldrich Chemical Company (St. Louis, MO). The DMF was dried over molecular sieves. Copper (I) cyanide (99%), was purchased from Strem Chemicals (Newburry Port, Massachusetts). Benzoyl chloride (98%) was purchased from Tokyo Chemical Industry (TCI) (Tokyo, Japan). Absolute ethanol was provided by the Texas State University stockroom.

3.2 **General Technique**

Synthetic reactions were performed under an argon atmosphere using Schlenk techniques when necessary. The polyhedral borane starting materials, $(Et_3NH)_2[B_{10}H_{10}]$ and $(Et_3NH)_2[B_{20}H_{18}]$, were prepared using published methods.[1,16,17]

3.3 **Physical Measurements**

NMR Spectroscopy. The $^{11}B\{^1H\}$ and ^{11}B Fourier transform NMR spectra were obtained using a Bruker Avance III spectrometer, operating at 128 MHz ^{11}B . ^{11}B NMR spectra were obtained using quartz tubes. Boron chemical shifts were externally referenced to $BF_3{\cdot}Et_2O$ in C_6D_6; peaks up-field of the reference are designated as negative.

X-Ray Crystallography. All crystallographic measurements were carried out on a Rigaku Mini CCD area detector diffractometer using graphite-monochromated Mo Kα radiation (λ = 0.71073 Å) at 223 K using an Oxford Cryostream low-temperature device. A sample of suitable size and quality was selected and mounted onto a nylon loop. Data reductions were performed using Crystal Clear Expert 2.0. The structures were solved by direct methods, which successfully located most of the non-hydrogen atoms. Subsequent

refinements on F^2 using the SHELXTL/PC package (version 5.1) allowed location of the remaining non-hydrogen atoms. Colorless, single crystals of $[MePPh_3]_2[B_{20}H_{17}CH_3]$, $[MePPh_3]_2[B_{20}H_{17}OH]$, and $[MePPh_3]_2[\mu\text{-}OCH_3\text{-}B_{20}H_{17}]$ were obtained by slow vapor diffusion of dry diethylether into a dry acetonitrile solution saturated with the compound. $[MePPh_3]_2[B_{20}H_{17}CH_3]$† († indicates methyl substituent located on equatorial belt adjacent to the terminal boron apex) and $[MePPh_3]_2[\mu\text{-}OCH_3\text{-}B_{20}H_{17}]$ crystallized in the monoclinic space group $P2_1/c$. The $[MePPh_3]_2[B_{20}H_{17}CH_3]$* (* indicates methyl substituent located on equatorial belt adjacent to the boron-boron linkage) and $[MePPh_3]_2[\mu\text{-}OCH_3\text{-}B_{20}H_{17}]$ produced colorless crystals of $[MePPh_3]_2[B_{20}H_{17}OH]$ crystalized in the triclinic space group *P–1*. The $[MePPh_3]_2[\mu\text{-}OCH_3\text{-}B_{20}H_{17}]$ crystal contained one interstitial molecule of acetonitrile in the asymmetric unit. Key details of the crystal and structure refinement data are summarized in **Table 1** and **Table 2**. Further crystallographic details may be found in the respective CIF files which were deposited at the Cambridge Crystallographic Data Centre, Cambridge, UK. The CCDC reference numbers for $[MePPh_3]_2[B_{20}H_{17}CH_3]$, $[MePPh_3]_2[B_{20}H_{17}OH]$, and $[MePPh_3]_2[\mu\text{-}OCH_3\text{-}B_{20}H_{17}]$ were assigned as 1057240, 1057241, and 1057242, respectively.

3.4 **Synthesis**

3.4.1 ***Preparation of $Rb_4[B_{20}H_{17}C_2H]$ using Sodium Acetylide.***

A clean, dry 100.0 mL Schlenk flask was equipped with a stir bar, stoppered, and flushed with argon gas. Dry triethylamine (15.0 mL, 107 mmol) was syringed into the reaction flask. An 18% by mass suspension of sodium acetylide (95% purity) in xylenes (3.00 mL, 0.011 mol) was syringed into the reaction mixture while stirring and being

sealed under vacuum. The reaction was placed under argon then allowed to stir for five minutes, the septum was removed under an increase flow of argon and $(Et_3NH)_2$[*trans*-$B_{20}H_{18}$] (0.257 g, 0.586 mmol) was added to the flask and the septum was replaced. The reaction was allowed to stir at room temperature for 96 h. Reaction completion was confirmed by ^{11}B NMR spectroscopy. The reaction mixture was dried *in vacuo*, dissolved in a minimum amount of distilled water, and the [*ae*-$B_{20}H_{17}C_2H]^{4-}$ anion was precipitated as a rubidium salt by adding a solution of $RbC_2H_3O_2$ (0.5 M,10.0 mL) in methanol to the aqueous product solution. The precipitate was filtered, dried, and recrystallized from water:methanol resulting in 0.293 g of pale yellow crystals of Rb_4[*ae*-$B_{20}H_{17}C_2H$] (83.4 % yield). $^{11}B\{^1H\}$ NMR (δ, D_2O) 2.36, 2.51, –9.84, –24.4, –27.3, –29.9, –35.2.

3.4.2 *Preparation of $(MePPh_3)_2$[ae-$B_{20}H_{17}CH_3$] using Aqueous Benzoquinone Oxidation*

The Rb_4[*ae*-$B_{20}H_{17}C_2H$] (0.105 g, .176 mmol) was dissolved in 10.0 mL of distilled water in a clean, dry 50.0 mL round bottom flask. While stirring, HCl (1.0 M, 1.0 mL) was added to the reaction mixture. Once dissolved, *p*-benzoquinone (0.046 g, .43 mmol) was added, and the reaction was allowed to stir at room temperature until the reaction reached completion, approximately 4 h. Completion was monitored using by ^{11}B NMR spectroscopy. Excess *p*-benzoquinone was filtered and the $[B_{20}H_{17}CH_3]^{2-}$ anion was precipitated as the methyltriphenylphosphonium, $MePPh_3^+$, salt by adding a solution of $MePPh_3Br$ (0.50 M) in distilled water to the filtered reaction mixture. The precipitate was filtered, dried, and recrystallized from acetonitrile:ether resulting in 0.110 g of dark

purple crystalline residue of $(MePPh_3)_2[B_{20}H_{17}CH_3]$, (78.6 % yield). $^{11}B\{^1H\}$ NMR (δ, acetonitrile) 29.3, 28.1, 14.0, 12.7, 11.3, 2.46 –4.98, –8.48, –11.8, –14.4, –15.7, –21.2, –23.6, –25.5, –29.4..

3.4.3 *Preparation of $(MePPh_3)_2[ae\text{-}B_{20}H_{17}CH_3]$ by $MgBrCH_3$.*

A clean, dry 100.0 mL Schlenk flask was equipped with a stir bar, stoppered, and flushed with argon gas. Diethylether (15.0 mL) was syringed into the reaction flask. A solution of methylmagnesium bromide (3.0 M, 1.4 mL, 4.2 mmol) was syringed into the reaction mixture while the solution was stirred. After stirring for five minutes, the septum was removed under an increased flow of argon and $(Et_3NH)_2[B_{20}H_{18}]$ (0.258 g, 0.588 mmol) was added to the flask and the septum was replaced. The reaction was allowed to stir at room temperature for 12 h. Reaction completion was confirmed by ^{11}B NMR spectroscopy. The reaction solvent was removed to yield a yellow/green residue. Distilled water was added to the residue and the solids were removed by filtration. The solution was used without further purification for the oxidation reaction in the formation of the $[B_{20}H_{17}CH_3]^{2-}$ ion. $^{11}B\{^1H\}$ NMR (δ, D_2O) 13.8, 2.2, –1.6, –7.6, –9.0, –27.1, –30.2.

$[B_{20}H_{17}CH_3]^{2-}$: The solution from the previous reaction was transferred to a clean, dry 50 mL round bottom flask. While stirring, HCl (1.0 M, l.0 mL) was added to the reaction mixture. Once dissolved, *p*-benzoquinone (0.185 g, 1.71 mmol) was added, and the reaction was allowed to stir at room temperature for 4 h. Reaction completion was confirmed by ^{11}B NMR spectroscopy. Excess *p*-benzoquinone was filtered and the $[B_{20}H_{17}CH_3]^{2-}$ anion was precipitated as the methyltriphenylphosphonium, $MePPh_3^+$, salt

by addition of a solution of $MePPH_3Br$ (0.5 M) in distilled water to the filtered reaction mixture. The precipitate was filtered, dried, and recrystallized from acetonitrile:ether, resulting in 0.362 g, (76.5% yield) of $(MePPh_3)_2[B_{20}H_{17}CH_3]$. $^{11}B\{^1H\}$ NMR (δ, CD_3CN) 32.0, 30.6, 18.2, 16.1, –6.8, –12.4, –16.0, –19.4, –25.6, –28.3.

3.4.4 *Preparation of $(MePPh_3)_2[ae\text{-}B_{20}H_{17}CH_3]$ by $LiCH_3$.*

A clean, dry 100 mL Schlenk flask was equipped with a stir bar and $(Et_3NH)_2[trans\text{-}B_{20}H_{18}]$ (0.256 g, 0.584 mmol) was stoppered, and flushed with argon gas. Dry diethylether (15.0 mL) was syringed into the reaction flask. A 1.6 M room temperature solution of methyllithium (2.00 mL, 3.20 mmol) was syringed into the reaction mixture while the reaction mixture was stirred under argon. The reaction was allowed to stir at room temperature for 4 h. Reaction completion was confirmed by ^{11}B NMR spectroscopy. The product of the reaction, $Li_4[ae\text{-}B_{20}H_{17}CH_3]$ was isolated by extracting the reaction mixture with distilled water. $^{11}B\{^1H\}$ NMR (δ, D_2O) 8.06, 3.11, –2.87, –8.93, –24.2, –29.6, –33.1.

$[B_{20}H_{17}CH_3]^{2-}$: After verification by $^{11}B\{^1H\}$ NMR that the $[ae\text{-}B_{20}H_{17}C_2H]^{4-}$ was in solution, the solution was transferred to a clean, dry 50 mL round bottom flask and dissolved in 9 mL of deionized water. While stirring, HCl (1.0 mL, 1.0 M) was added to the reaction mixture. Once dissolved, *p*-benzoquinone (0.156g, 1.44 mmol) was added and the reaction was allowed to stir at room temperature for 4h. Quantitative conversion was observed by ^{11}B NMR spectroscopy. Excess *p*-benzoquinone was filtered and the $[B_{20}H_{17}CH_3]^{2-}$ anion was precipitated as a methyltriphenylphosphonium, $MePPh_3^+$, salt by adding a solution of $MePPh_3Br$ (0.5 M) in distilled water to the filtered reaction mixture.

The precipitate was filtered, dried, and recrystallized from acetonitrile:ether resulting in 0.35 g (75.4 % yield) of a dark purple crystalline residue of $(MePPh_3)_2[trans\text{-}B_{20}H_{17}CH_3]$. $^{11}B\{^1H\}$ NMR (δ, CD_3CN) 30.2, 29.0, 15.6, 13.8, 6.92, 4.43, 2.66, 1.77, – 0.44, – 3.01, – 3.81, – 4.97, – 7.01, – 10.2, – 13.2, – 16.6, – 20.8, – 22.9, – 24.0, – 27.1, – 28.1, – 29.8, – 20.8.

3.4.5 *Preparation of $(MePPh_3)_2[ae\text{-}B_{20}H_{17}CH_2CH_3]$ using $MgBrCH_2CH_3$.*

A clean, dry 100.0 mL Schlenk flask was equipped with a stir bar, stoppered, and flushed with argon gas. Diethylether (15.0 mL) was syringed into the reaction flask. A solution of ethylmagnesium bromide (3.0 M, 1.0 mL, 4.2 mmol) was syringed into the reaction mixture while the solution was stirred. After stirring for five minutes, the septum was removed under an increased flow of argon and $(Et_3NH)_2[B_{20}H_{18}]$ (0.248 g, 0.565 mmol) was added to the flask and the septum was replaced. The reaction was allowed to stir at room temperature for 12 h. Reaction completion was confirmed by ^{11}B NMR spectroscopy. The reaction solvent was removed y reduced pressure. Distilled water (20 mL) was added to the residue and the solids were removed by filtration. The solution containing the $[B_{20}H_{17}CH_2CH_3]^{4-}$ ion was used without further purification for the oxidation reaction in the formation of the $[B_{20}H_{17}CH_2CH_3]^{2-}$ ion. $^{11}B\{^1H\}$ NMR (δ, D_2O) 13.2, 3.16, –3.09, –7.55, –8.65, –26.1, –29.8.

$[B_{20}H_{17}CH_2CH_3]^{2-}$: The solution containing the $[B_{20}H_{17}CH_2CH_3]^{4-}$ ion from the previous reaction was transferred to a clean, dry 50 mL round bottom flask. While stirring, HCl (1.0 M, 2.0 mL) was added to the reaction mixture. Once dissolved, *p*-benzoquinone (0.193g, 1.79 mmol) was added, and the reaction was allowed to stir at

room temperature for 4 h. Reaction completion was confirmed using ^{11}B NMR spectroscopy. Excess *p*-benzoquinone was filtered and the $[B_{20}H_{17}CH_2H_3]^{2-}$ anion was precipitated as the methyltriphenylphosphonium, $MePPh_3^+$, salt by addition of a solution of $MePPh_3Br$ (0.5 M) in distilled water to the filtered reaction mixture. The precipitate was filtered, dried, and recrystallized from acetonitrile:ether, resulting in 0.34 g (75.5% yield) of $(MePPh_3)_2[B_{20}H_{17}CH_2CH_3]$. $^{11}B\{^1H\}$ NMR (δ, CD_3CN) 30.4, 15.9, 7.04, 0.08, –6.96, –12.5, –16.0, –19.5, –22.4, –25.5, –26.7, –28.1. $^{11}B\{^1H\}$ NMR (δ, CD_3CN)

3.4.6 *Preparation of $K_4[B_{20}H_{17}OH]^{4-}$ using KOH.*

A clean and dry 250 mL Beaker was equipped with a stir bar, and KOH (3.23 g, 57.6 mmol) which had been dissolved in minimal amount of distilled water. $(Et_3NH)_2$[*trans*-$B_{20}H_{18}$] (5.00 g, 11.4 mmol) was added to the solution and was allowed to stir for one hour. After the reaction was completed, the reaction was cooled to 0 C^o and cold ethanol was added until a fine white solid precipitated. The precipitate was filtered, dried, and recrystallized from water:ethanol resulting in 4.15 g of white crystals of K_4[*ae*-$B_{20}H_{17}OH$], **(**89.6 % yield). $^{11}B\{^1H\}$ NMR (δ, D_2O) 9.83, 2.75, –2.04, –3.16, –5.43, –8.46, –9.44, –23.5, –27.0, –29.5, –34.5.

3.4.7 *Preparation of $(MePPh_3)_2[B_{20}H_{17}OH]$ using Aqueous Benzoquinone Oxidation* $[B_{20}H_{17}OH]^{2-}$**:**

K_4[*ae*-$B_{20}H_{17}OH$] (0.105 g, 0.258 mmol) was dissolved in 10.0 mL of distilled water in a 50 mL round bottom flask. HCl (1.0 M, 1 mL) was added to the stirred reaction mixture. After, *p*-benzoquinone (0.084 g, 0.78 mmol) was added, the reaction

was allowed to stir at room temperature for approximately 4 h. Reaction completion was confirmed by ^{11}B NMR spectroscopy. Excess *p*-benzoquinone was removed by filtration and the $[B_{20}H_{17}OH]^{2-}$ anion was precipitated as a methyltriphenylphosphonium salt by the addition of a solution of $MePPh_3Br$ (0.5 M) in distilled water. The precipitate was filtered, dried, and recrystallized from acetonitrile:ether, resulting in 0.125 g (57.8% yield) of $(MePPh_3)_2[B_{20}H_{17}OH]$. $^{11}B\{^1H\}$ NMR (δ, CD_3CN) 30.1, 29.0, 24.1, 20.7, 15.0, 13.8, –7.5, –10.8, –13.5, –14.8, –16.7, –20.2, –22.7, –24.7, –29.5.

3.4.8 *Preparation of $(MePPh_3)_4[B_{20}H_{17}OH]$*

In a clean, dry round bottom flask, $K_4[B_{20}H_{17}OH]$ (0.13 g, 0.096mmol) was dissolved in a minimal amount of distilled water. The $[B_{20}H_{17}OH]^{4-}$ ion was precipitated as a methyltriphenylphosphonium, $MePPh_3^+$, salt by adding a solution of $MePPh_3Br$ (0.5 M, 2.5 mL) in distilled water. The yellow precipitate was filtered, dissolved in acetonitrile, and the by-products were removed by washing the product with dichloromethane. The solution was precipitated by adding diethylether and the product was filtered and dried *in vacuo* resulting in 0.334 g bright yellow powder of $(MePPh_3)_4[ae\text{-}B_{20}H_{17}OH]$, (80.1 % yield). $^{11}B\{^1H\}$ NMR (δ, acetonitrile) 5.08, 1.72 0.08, 3.84, –7.30, –23.1, –25.7, –28.9, –33.8.

3.4.9 *Preparation of $(MePPh_3)_2[B_{20}H_{17}OH]$ using Benzoquinone Oxidation*

$K_4[B_{20}H_{17}OH]$ (0.13 g, 0.096mmol) was placed in a 250 mL round bottom flask, equipped with a stir bar, and dissolved with a mixture of dichloromethane (80 mL) and acetonitrile (20 mL). Once dissolved, trifloroacetic acid (1 mL, 13.1 mmol) was added

and allowed to stir for 5 minutes until the solution appeared as translucent. Freshly sublimed *p*-benzoquinone (0.025g, 0.23 mmol) was added and the reaction was refluxed for 12 h. Completion was monitored using ^{11}B NMR spectroscopy. Once cooled, the reaction mixture was dried *in vacuo*, washed with diethylether to remove excess *p*-benzoquinone, and the product recrystallized from acetonitrile:ether resulting in 0.066 g dark purple crystalline residue of $(MePPh_3)_2[B_{20}H_{17}OH]$, (85.7 % yield). $^{11}B\{^1H\}$ NMR (δ, acetonitrile) 32.7, 21.1, 15.8, –5.2,–11.9, –15.8, –19.1, –21.5, –24.5.

3.4.10 ***Preparation of $(MePPh_3)_2[\mu\text{-}OCH_3\text{-}B_{20}H_{17}]$ using Electrophilic Benzoquinone Oxidation***

A clean, dry 100 mL Schlenk flask was equipped with $(MePPh_3)_4[ae\text{-}B_{20}H_{17}OH]$ (0.163 g, 0.120 mmol) and a stir bar and was stoppered and flushed with argon gas. Dry dichloromethane (80 mL) and dry acetonitrile (20 mL) was syringed into the reaction flask. Once dissolved, iodomethane (1.00 mL, 16.1 mmol) were syringed into the reaction flask and allowed to stir for five minutes. The septum was removed under an increased flow of argon and freshly sublimed *p*-benzoquinone (0.069g, 0.64 mmol) was added to the mixture. The mixture was refluxed for approximately 12 h. Reaction completion was confirmed using ^{11}B NMR spectroscopy. Once cooled, the reaction mixture was dried *in vacuo*, washed with distilled water to remove excess methyliodide, dried, and the product recrystallized from acetonitrile:ether, resulting in 0.075 g (76% yield) of $(MePPh_3)_2[\mu\text{-}OCH_3\text{-}B_{20}H_{17}]$. $^{11}B\{^1H\}$ NMR (δ, CD_3CN) 29.9, 28.6, 15.7, 13.6, 12.0, 6.5, 3.7, –5.0, –7.8, –10.4, –13.9, –15.1, –16.8, –21.3, –22.7, –24.8, –27.3, –29.1, –30.5.

3.4.11 *Preparation of $(MePPh_3)_2[\mu\text{-}OCOCH_3\text{-}B_{20}H_{17}]$ using Electrophilic Organic Benzoquinone Oxidation*

A clean, dry 100 mL Schlenk flask was equipped with $(MePPh_3)_4[ae\text{-}B_{20}H_{17}OH]$ (0.148 g, 0.109 mmol) and a stir bar, and was stoppered and flushed with argon gas. Dry dichloromethane (80.0 mL) and dry acetonitrile (20 mL) were syringed into the reaction flask. Once dissolved, acetyl chloride (1.00 mL, 14.1 mmol) was syringed into the reaction flask and allowed to stir for five minutes. After stirring for five minutes, the septum was removed under an increased flow of argon. Freshly sublimed *p*-benzoquinone (0.023, 0.21 mmol) was added to the mixture and the mixture was refluxed until completion, approximately 12 h. Reaction completion was confirmed using ^{11}B NMR spectroscopy. Once cooled the reaction mixture was dried *in vacuo*, washed with distilled water to remove excess acetyl chloride in the form of acetic acid, dried and the product recrystallized from acetonitrile:ether resulting in 0.086 g (94 % yield) of dark purple crystalline residue of **$(MePPh_3)_2[\mu\text{-}OCOCH_3\text{-}B_{20}H_{17}]$**. $^{11}B\{^1H\}$ NMR (δ, acetonitrile) 32.9, 29.3, 19.7, 13.9, 9.68, 3.36, 0.28, –2.38, –7.44, –14.04, –16.7, –20.4, –24.8.

3.4.12 *Preparation of $(MePPh_3)_2[\mu\text{-}OCOC_6H_5\text{-}B_{20}H_{17}]$ using Electrophilic Benzoquinone Oxidation*

A clean, dry 100 mL Schlenk flask was equipped with $(MePPh_3)_4[ae\text{-}B_{20}H_{17}OH]$ (0.147 g , 0.108 mmol) and a stir bar and was stoppered and flushed with argon gas. Dry dichloromethane (80 mL) and dry acetonitrile (20 mL) were syringed into the reaction

flask. Once dissolved, benzoyl chloride (1.00 mL, 8.60 mmol) was syringed into the reaction flask and allowed to stir for five minutes. The septum was removed under an increased flow of argon, and freshly sublimed *p*-benzoquinone (0.023g, 0.21 mmol) was added to the mixture The mixture was refluxed for approximately 12 h. Reaction completion was confirmed using ^{11}B NMR spectroscopy. Once cooled, the reaction mixture was dried *in vacuo*, washed with distilled water to remove excess benzoyl chloride, dried, and the product recrystallized from acetonitrile:ether resulting in 0.076 g (78 % yield) of $(MePPh_3)_2[\mu\text{-}OCOC_6\text{-}H_5B_{20}H_{17}]$. $^{11}B\{^1H\}$ NMR (δ, CD_3CN) 31.1 29.5, 20.7, 15.8, 11.4, 3.18, –0.12, –7.01, –12.4, –16.0, –17.8, –19.3, –21.8, –24.3, –25.3, –28.9, –30.3.

3.4.13 ***Preparation of $Rb_4[B_{20}H_{17}CH_2CN]$ using $^-CH_2CN$***

A clean, dry 100 mL Schlenk flask was equipped with a stir bar, stoppered, and flushed with argon gas. A syringe was used to transfer a 1.6 M solution of *n*-butyllithium in hexanes (3.5 mL, 6.00 mmol) to the reaction flask. The solution was dried *in vacuo* to remoe the hexanes resulting in a dry white solid *n*-butyllithium. Freshly distilled diethylether (10.0 mL) was added to the flask via syringe. The mixture was cooled to -78 ºC by surrounding the reaction flask with a dry ice-acetone bath. Freshly distilled acetonitrile (0.50 mL, 6.7 mmol) was added to the flask and the mixture was allowed to stir for 30 minutes. Afterwards, the reaction flask was allowed to warm to room temperature over a period of 2h. Once at room temperature $(Et_3NH)_2[trans\text{-}B_{20}H_{18}]$ was added (0.501 g, 1.14 mmol). The reaction was allowed to stir for 36 h. Completion of the reaction was confirmed using ^{11}B NMR spectroscopy. The reaction mixture was dried *in*

vacuo and the $Li_4[B_{20}H_{17}CH_2CN]$ residue was dissolved in a minimum amount of distilled water. The $[B_{20}H_{17}CH_2CN]^{2-}$ ion was precipitated as the methyltriphenylphosphonium, $MePPh_3^+$, salt by addition of a solution of $MePPh_3Br$ (0.5 M) and recrystallized from acetonitrile:ether, resulting in 0.682 g (91.8 % yield) of $(MePPh_3)_4[ae\text{-}B_{20}H_{17}CH_2CN]$. $^{11}B\{^1H\}$ NMR (δ, CD_3CN) 0.355, –5.37, –7.54, –7.81, –12.9, –27.3, –30.0, –32.8, –37.9.

3.4.14 *Preparation of $(MePPh_3)_2$ $[B_{20}H_{17}CH_2CN]$*

A clean, dry 100 mL Schlenk flask was equipped with $(MePPh_3)_4[ae\text{-}B_{20}H_{17}CH_2CN]$ (0.147 g, 0.108 mmol), and dry dichloromethane (20 mL) and dry acetonitrile (5 mL) were added into the reaction flask. Once dissolved, trifluoroacetic acid (1.00 mL, 8.60 mmol) was added to the reaction flask and allowed to stir for five minutes. The septum was removed under an increased flow of argon, and freshly sublimed *p*-benzoquinone (0.023g, 0.21 mmol) was added to the mixture. The mixture was refluxed for approximately 12 h. Reaction completion was confirmed by ^{11}B NMR spectroscopy. Once cooled, the reaction mixture was dried *in vacuo*, washed with distilled water to remove excess diethylether to remove excess *p*-benzoquinone, dried, and the product recrystallized from acetonitrile:ether, resulting in 0.702g (74.3 % yield) of $(MePPh_3)_2[B_{20}H_{17}CH_2CN]$. $^{11}B\{^1H\}$ NMR (δ, CD_3CN) 33.8, 32.0, 30.8, 29.3, 28.2, 25.7, 23.5, 17.8, 16.1, 13.1, 9.85, 1.28, –3.45, –6.76, –9.76, –13.5, –17.0, –19.7, –27.3.

3.4.15 *Preparation of $(MePPh_3)_4[B_{20}H_{17}CN]$ using CuCN*

A clean, dry 25. mL two neck flask was equipped with a stir bar and an adapter

and stoppered. $(Et_3NH)_2[B_{20}H_{18}]$ (0.501 g, 1.14 mmol) and copper (I) cyanide (0.523, 5.84mmol) were added to the flask. The flask was evacuated and flushed with argon. Dry dimethylformamide (DMF) (15 mL) was syringed into the reaction flask. Under an increased flow of argon, the adaptor was replaced with a condenser and the reaction was allowed to reflux for 6 h. Reaction completion was confirmed using ^{11}B NMR spectroscopy. Once cooled, distilled water (50 mL) was added to the reaction drop wise by pressure equalized dropping funnel (PED). The precipitate was filtered until the filtrate appeared translucent and discarded. The $[B_{20}H_{17}CN]^{2-}$ anion was precipitated as the methyltriphenylphosphonium, $MePPh_3^+$, salt by addition of a solution of $MePPh_3Br$ (0.5 M) and recrystallized from acetonitrile:ether resulting in 0.510 g (32.7 % yield) of $(MePPh_3)_4$[*ae*-$B_{20}H_{17}CN$]. $^{11}B\{^1H\}$ NMR (δ, CD_3CN) 4.88, –2.50, –4.88, –6.40, –10.2, –23.5, –25.0, –28.9, –33.7.

3.4.16 ***Preparation of $(MePPh_3)_2[B_{20}H_{17}CN]$***

A clean, dry 100 mL Schlenk flask was equipped with $(MePPh_3)_2$[*ae*-$B_{20}H_{17}CN$] (0.510 g, 0.372 mmol), and dry dichloromethane (20.0 mL) and dry acetonitrile (5.00 mL) were added to the reaction flask. Once dissolved, trifluoroacetic acid (1.00 mL, 8.60 mmol) was added to the reaction flask and allowed to stir for five minutes. The septum was removed under an increased flow of argon, and freshly sublimed *p*-benzoquinone (0.023g, 0.21 mmol) was added to the mixture. The mixture was refluxed for approximately 12 h. Reaction completion was confirmed using ^{11}B NMR spectroscopy. Once cooled, the reaction mixture was dried *in vacuo*, washed with distilled water to remove excess trifluoroacetic acid, washed with diethylether to remove excess *p*-benzoquinone, dried, and the product recrystallized from acetonitrile:ether resulting in

0.08 g, (26 % yield) of $(MePPh_3)_2[B_{20}H_{17}CN]$. $^{11}B\{^1H\}$ NMR (δ, CD_3CN) 29.3, 19.3, –14.8, –8.08,–13.5, –17.1, –20.5, –22.3, –25.1, –26.7, –30.9.

CHAPTER IV

RESULTS

Preliminary experiments, conducted as part of Mr. Martin Mantz's thesis in 2013, reported the reaction of the [*trans*-$B_{20}H_{18}]^{2-}$ ion with three carbon nucleophiles.[28] The carbon nucleophiles under investigation were deprotonated acetonitrile ($^{-}CH_2CN$), the butyl anion ($^{-}CH_2CH_2CH_2CH_3$), and the acetylide ion ($^{-}C{\equiv}CH$). Although the results of the investigation clearly indicated, using ^{11}B NMR spectroscopy, the formation of [*ae*-$B_{20}H_{17}X]^{4-}$ ions, the products were not fully characterized. Additionally, a single crystal of the product resulting from the oxidation of the butyl derivative yielded an unexpected ion, [μ-OCH_2CH_3-$B_{20}H_{17}]^{2-}$. As a result, a reinvestigation of the previous reactions in order to verify the identity of the products was initiated.

4.1 Reinvestigation of [*trans*-$B_{20}H_{17}C{\equiv}CH]^{2-}$

The reaction of the [*trans*-$B_{20}H_{18}]^{2-}$ ion with sodium acetylide was reinvestigated first because of the interest in converting the desired product, [*ae*-$B_{20}H_{17}C{\equiv}CH]^{4-}$, into agents with potential application in BNCT. The original reaction was accomplished by allowing a slurry of 18% sodium acetylide in xylenes to react with the [*trans*-$B_{20}H_{18}]^{2-}$ ion in refluxing trimethylamine for 96 hours (**Scheme 10**). Complete reaction was confirmed by ^{11}B NMR spectroscopy. The product of the reaction was an *ae* isomer, identified by three singlets at 2.8, -2.2, and -9.6 ppm in the proton-decoupled ^{11}B NMR spectrum (**Figure 10**) which correspond to the apical boron atoms.[28] Other peaks observed are the broad signal attributed to the B-B linkage between cages at 8.4, and a

substituted boron peak at -4.3. The product isolated from the initial reaction, an [*ae*-$B_{20}H_{17}X]^{4-}$ ion, was treated with an aqueous solution of ferric chloride and was precipitated as the tetrabutylammonium salt from water:methanol to generate the [*trans*-$B_{20}H_{17}X]^{2-}$ ion (**Scheme 10)**. Oxidation of the product was confirmed using ^{11}B NMR spectroscopy by comparison of the ^{11}B NMR spectrum of the starting material (**Figure 5**), the [*trans*-$B_{20}H_{18}]^{2-}$ ion, and the ^{11}B NMR spectrum of the resulting [*trans*-$B_{20}H_{17}X]^{2-}$ ion (**Figure 11**). The oxidized species exhibit consistent signals at ~30 ppm and ~15 ppm corresponding to the apical boron atoms and the equatorial boron atoms participating in the three center two electron bond. The product exhibited signals at 29.4 ppm and 14.3 ppm (**Figure 11).**

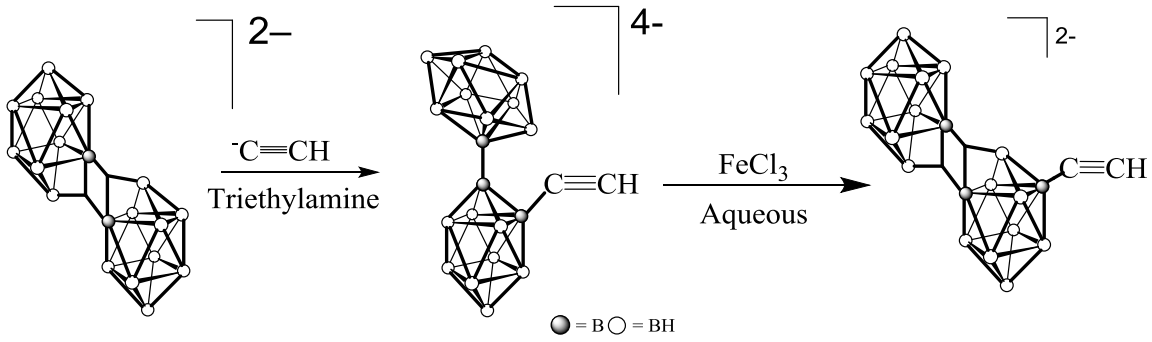

Scheme 10: Proposed reaction of the nucleophilic attack of the [*trans*-$B_{20}H_{18}]^{2-}$ ion by $^{-}C{\equiv}CH$. The reduced ion was oxidized using ferric chloride in aqueous solution.

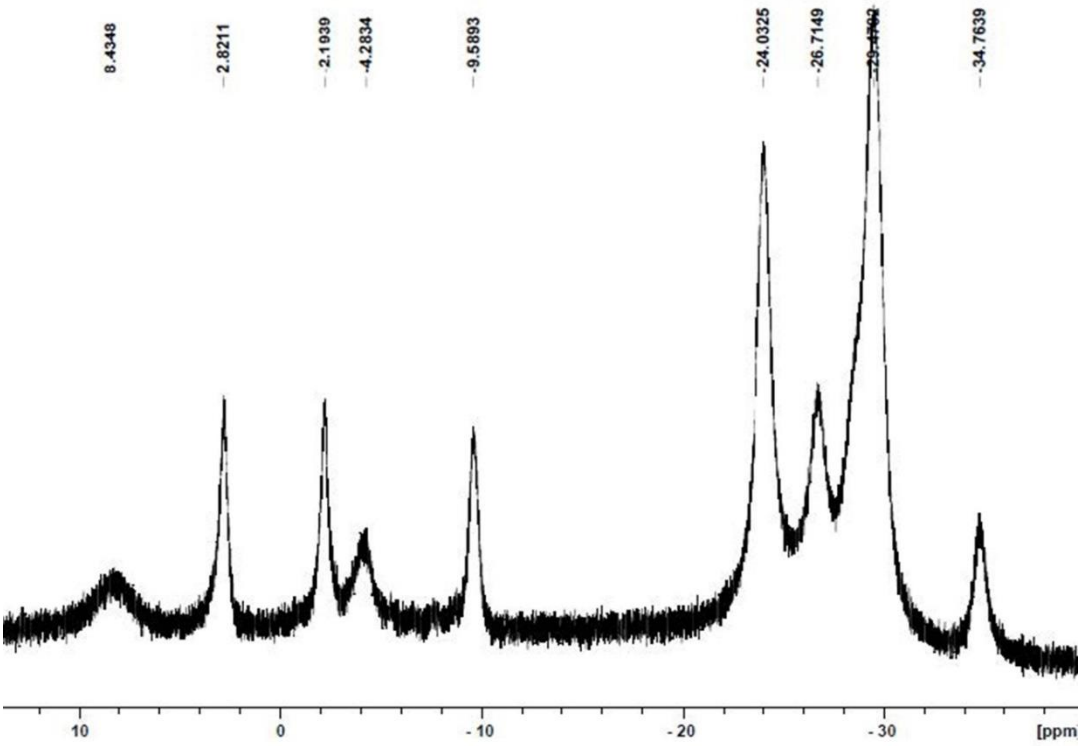

Figure 10: $^{11}B\{^{1}H\}$ spectrum of the product formed from the reaction of the [*trans*-$B_{20}H_{18}]^{2-}$ ion and sodium acetylide.

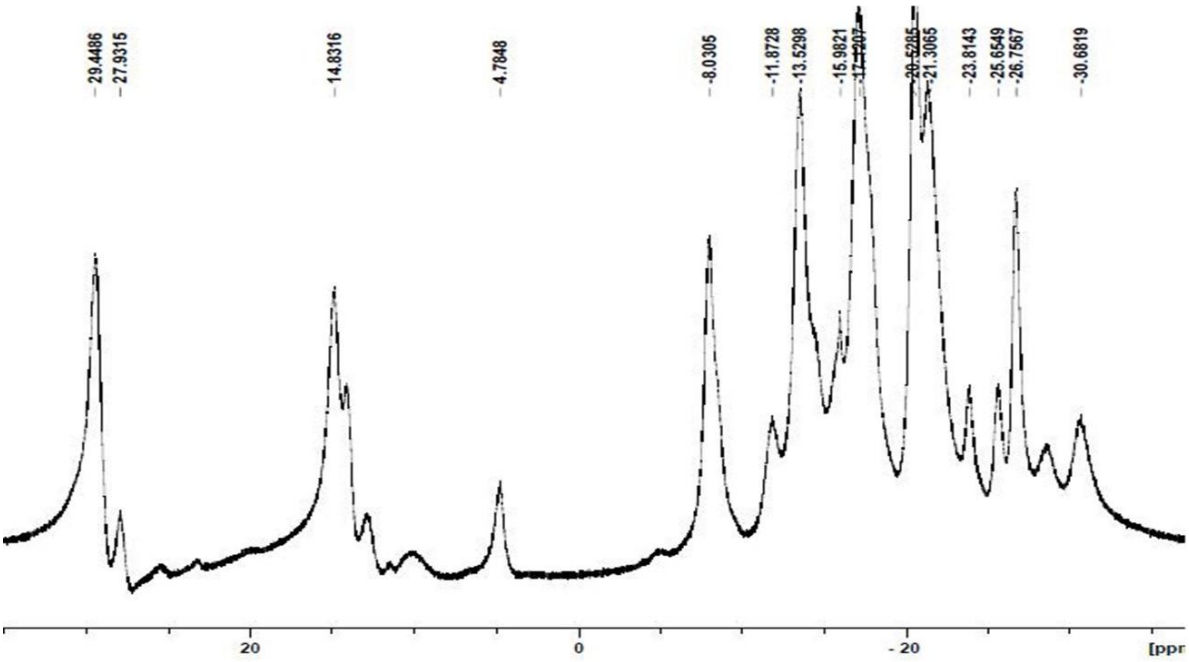

Figure 11: $^{11}B\{^{1}H\}$ spectrum of the product formed from the oxidation of the reduced ion by ferric chloride.

The reinvestigation of the nucleophilic attack of the [*trans*-$B_{20}H_{18}]^{2-}$ ion by an acetylide ion yielded similar results by $^{11}B\{^1H\}$ NMR spectroscopy (**Figure 12).** Quantitative conversion to the [*ae*-$B_{20}H_{17}X]^{4-}$ ion, as observed in the $^{11}B\{^1H\}$NMR spectrum, was achieved at room temperature, without the need of additional energy in the system, provided that the 96 hour reaction time was still utilized. The oxidation of the reduced ion with aqueous ferric chloride to form the oxidized ion produced results, by $^{11}B\{^1H\}$ NMR, consistent with an oxidized species (**Figure 13)**. The oxidized product was isolated as the methyltriphenylphosphonium salt to facilitate the growth of a single crystal for characterization by X-ray crystallography. Single crystals of the product were subjected to X-ray diffraction analysis which revealed the formation of the [*trans*-$B_{20}H_{18}]^{2-}$ ion. This result is consistent with results seen in the literature suggesting that the $FeCl_3$ reaction conditions are harsh enough to cleave substituents.[22]

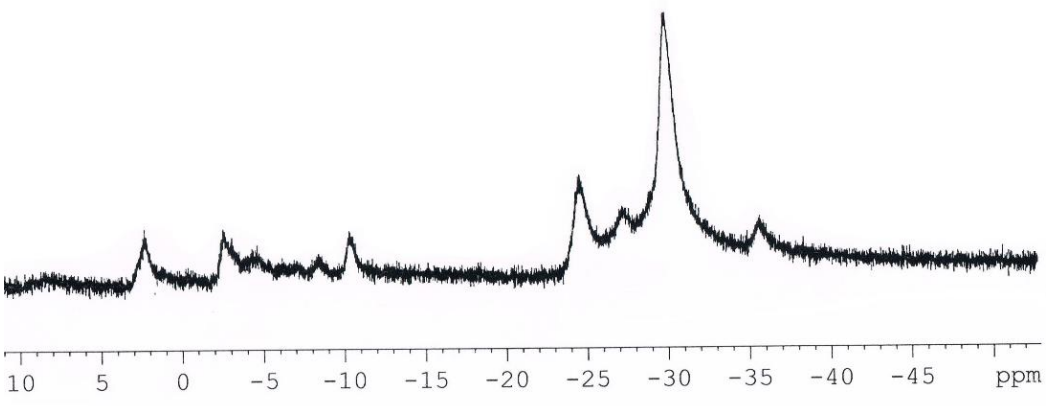

Figure 12: $^{11}B\{^1H\}$ spectrum of the product formed from in the reinvestigation of the reaction of the [*trans*-$B_{20}H_{18}]^{2-}$ ion and sodium acetylide.

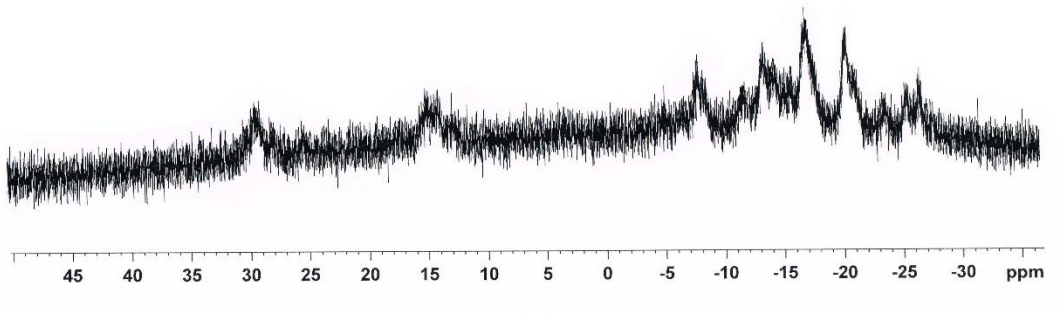

Figure 13: $^{11}B\{^{1}H\}$ spectrum of the product formed from the reinvestigation of the oxidation of the reduced ion by ferric chloride.

As a result of the cleavage of the substituent, a new synthetic scheme was developed where the ferric chloride oxidizing agent was replaced by *p*-benzoquinone in acidic aqueous conditions (**Scheme 11**).

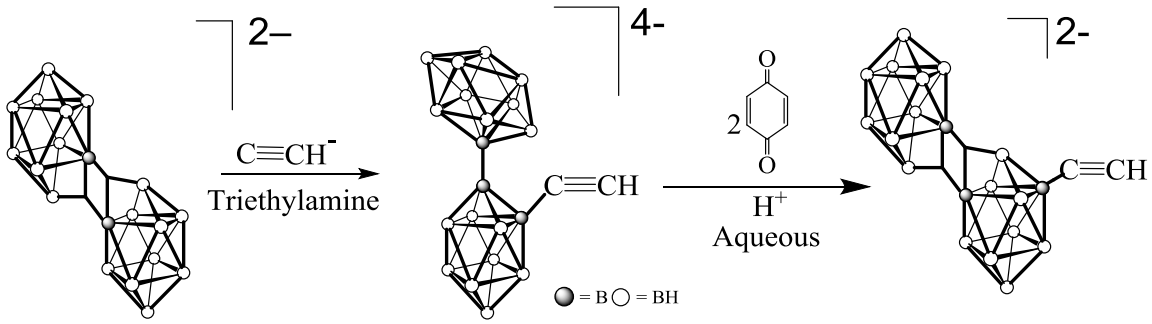

Scheme 11: Proposed reaction scheme for the preparation of the $[B_{20}H_{17}C{\equiv}CH]^{4-}$ and the oxidation of the resulting product using *p*-benzoquinone in acidic aqueous conditions to form the $[trans\text{-}B_{20}H_{17}C{\equiv}CH]^{2-}$ ion.

The $^{11}B\{^{1}H\}$ NMR spectrum of the oxidized product was consistent with the formation of a substituted oxidized product of the form $[B_{20}H_{17}X]^{2-}$ based on the presence of the peaks at ~30 ppm and ~15 ppm which are characteristic of these ions (**Figure 14**). A single crystal of the product was grown by slow vapor diffusion of diethylether into a

solution of the salt in acetonitrile and characterized by X-ray diffraction. Crystallographic data resulted in a structure of the [*trans*-$B_{20}H_{17}CH_3$]$^{2-}$ ion (**Figure 15**). The crystal structure appears to have two methyl substituents; however, this is a result of the crystallographic data processing. Only one methyl substituent is actually present.

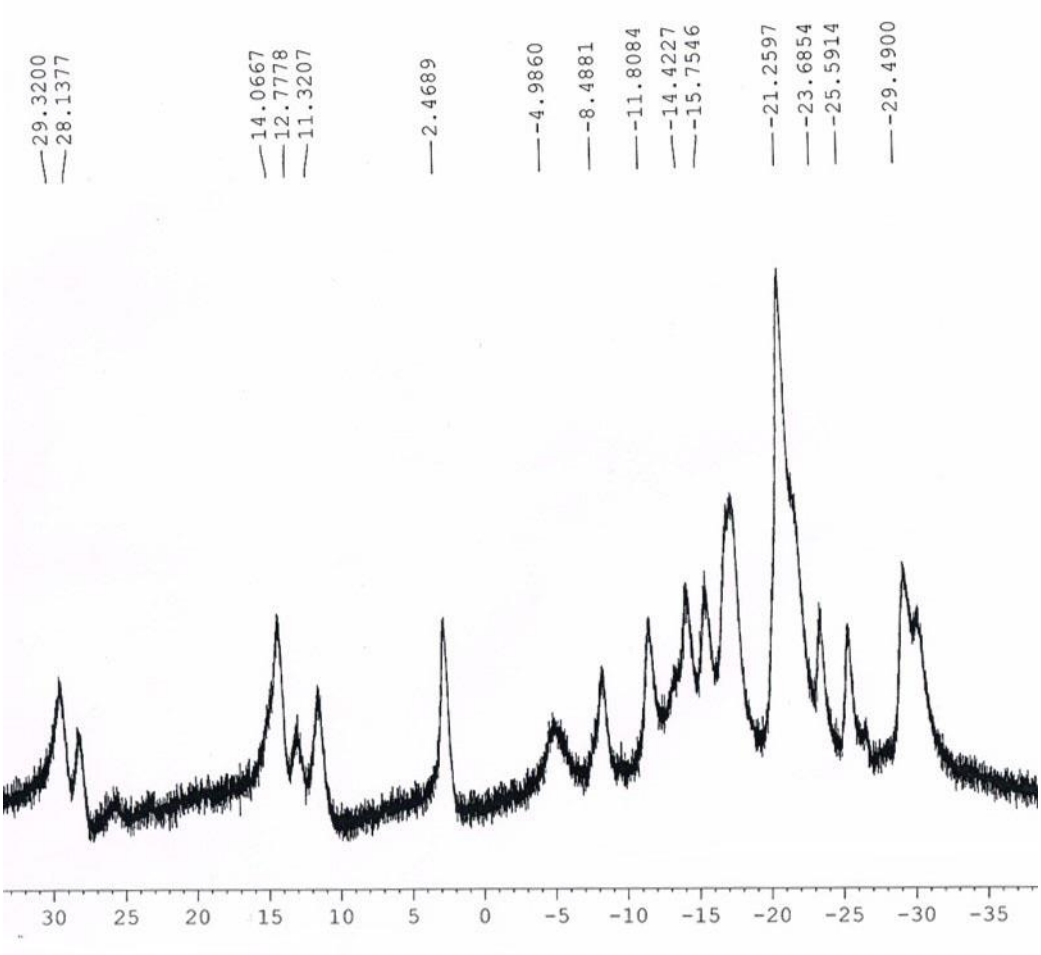

Figure 14: $^{11}B\{^1H\}$ spectrum of the product of the oxidation of the compound formed from the reaction of the [*trans*-$B_{20}H_{18}$]$^{2-}$ ion and the acetylide ion using *p*-benzoquinone.

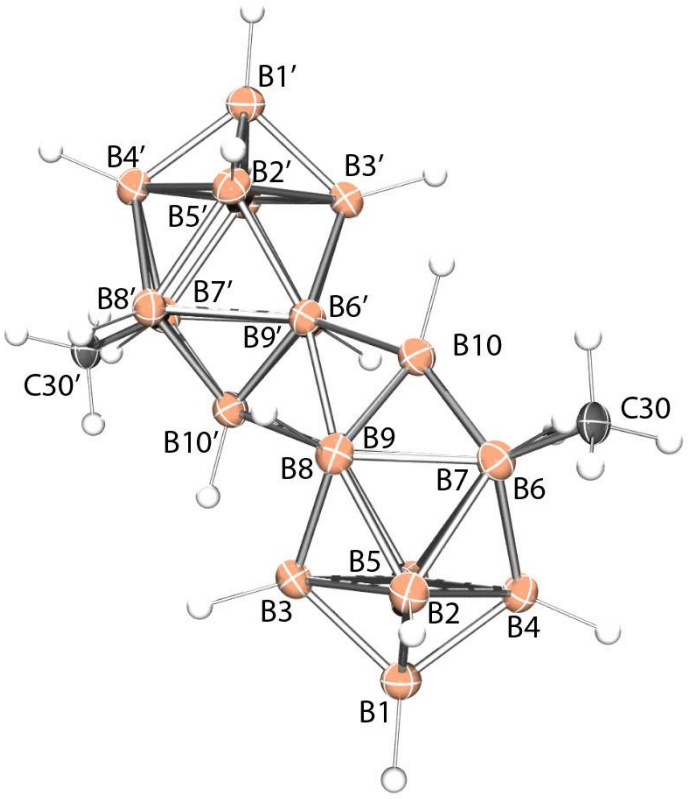

Figure 15. ORTEP drawing (ellipsoids set at 50% probability) of the crystal structure of the $[B_{20}H_{17}CH_3]^{2-}$ ion from the acetylide ion reaction. Relevant bond lengths include: B6–C30 1.433(8) Å, B9′-B10 1.914(3) Å, B9-B10′ 1.914(3) Å, and B9-B9′ 1.697(5) Å.

Since a single crystal of the reduced product of the acetylide reaction, the $[B_{20}H_{17}X]^{4-}$ ion, has not been obtained, it is unclear whether the acetylide substituent is present in the reduced product and the methyl substituent is a result of the oxidation process or if the acetylide substituent was never fully incorporated into the reduced ion. The methyl group was not observed in either the ^{1}H NMR spectrum or the ^{13}C NMR spectrum, presumably due to coupling to the adjacent and neighboring boron atoms which have large quadrupolar moments and nuclear spins $I = 3/2$.

4.2 Investigation of the [*trans*-$B_{20}H_{17}CH_3]^{2-}$ Ion

Based on the unexpected results obtained from the acetylide reaction, we set out to rationally synthesize the reduced methyl-substituted ion, the $[B_{20}H_{17}CH_3]^{4-}$ ion, and the oxidized methyl-substituted ion, the [*trans*-$B_{20}H_{17}CH_3]^{2-}$ ion (**Scheme 12**). The [*trans*-$B_{20}H_{18}]^{2-}$ ion was allowed to react with methylmagnesium bromide in diethylether at room temperature for 12 h. Quantitative conversion was observed using $^{11}B\{^1H\}$ NMR spectroscopy. The production of an apical-equatorial isomer of a reduced, substituted ion was confirmed by the presence of three apical boron atom signals at 2.2, -1.6, and -7.6 ppm (**Figure 16**). The three apical boron atoms exhibit doublets in the proton-coupled ^{11}B NMR spectrum (**Figure 17**). The reduced species was treated with the oxidizing agent, *p*-benzoquinone, in acidic aqueous conditions. The mixture was allowed to stir for 4 h at room temperature. The $^{11}B\{^1H\}$NMR spectrum of the product were consistent with the formation of an oxidized ion. Signals at 32.7 and 16.0 ppm (**Figure 18**) are characteristic of the oxidized ions. Single crystals of the methyltriphenylphosphonium salt of the oxidized product were obtained by slow vapor diffusion of diethylether into a solution of the salt in acetonitrile and analyzed by X-ray crystallography. The crystal structure confirmed the formation of the expected product, the [*trans*-$B_{20}H_{17}CH_3]^{2-}$ ion (**Figure 19**). Although no significant structural differences were observed between the crystal structures of the [*trans*-$B_{20}H_{18}]^{2-}$ ion[23] and the crystal structure of the [*trans*-$B_{20}H_{17}CH_3]^{2-}$ ion regarding the polyhedral borane framework, it is noteworthy that the methyl substituent was located on the equatorial belt adjacent to the terminal boron apex rather than the equatorial belt adjacent to the electron-deficient bonding region. This location of the substituent is not consistent with the mechanism proposed by Hawthorne

for reactions of the [*trans*-$B_{20}H_{18}]^{2-}$ ion (**Scheme 3**). The B5–C1 distance is 1.497(7) Å, and is similar to reported B–C(sp^3) bond lengths in polyhedral boron clusters (ca. 1.53–1.59 Å).[30,31] A table with a summary of crystal data, data collection and structural refinement of [*trans*-$B_{20}H_{17}CH_3]^{2-}$ formed in the acetylide reaction and the [*trans*-$B_{20}H_{17}CH_3]^{2-}$ formed in the Grignard reaction is available in **Table 1**. In the absence of the acid, no oxidation was observed**.**

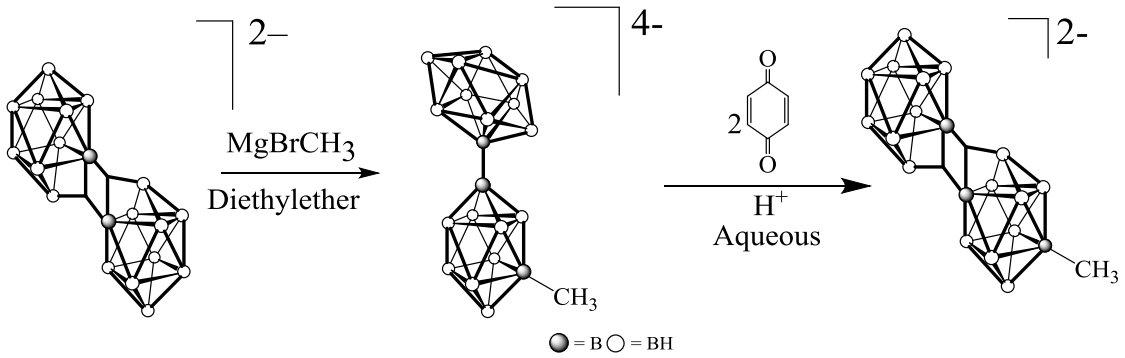

Scheme 12: Generation of $[B_{20}H_{17}CH_3]^{4-}$ ion by the nucleophilic attack of the [*trans*-$B_{20}H_{18}]^{2-}$ ion with $MgBrCH_3$. The $[B_{20}H_{17}CH_3]^{4-}$ ion was oxidized to the [*trans*-$B_{20}H_{17}CH_3]^{2-}$ ion by *p*-benzoquinone in acidic aqueous conditions.

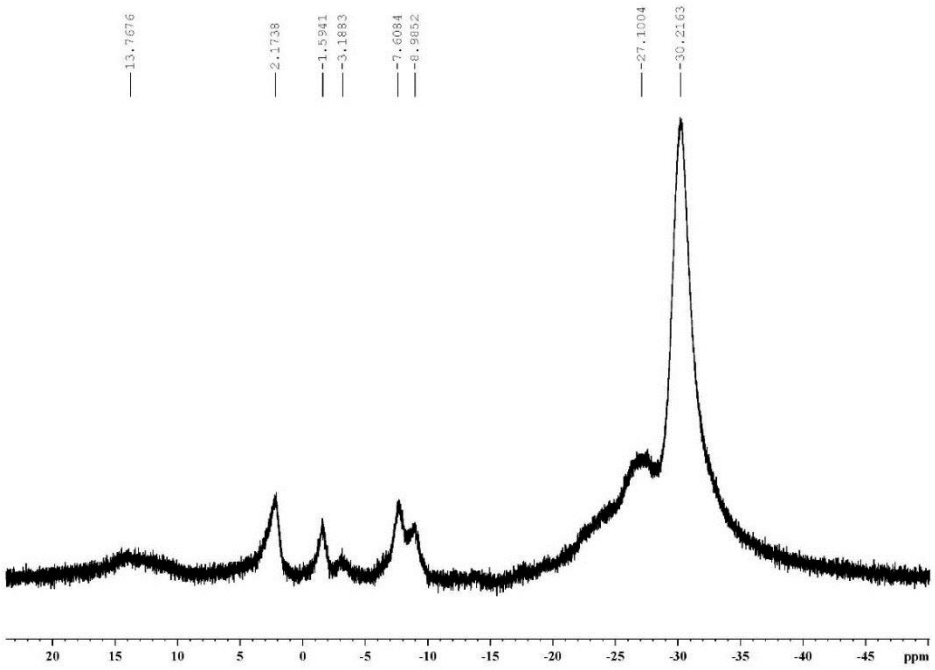

Figure 16: $^{11}B\{^{1}H\}$ spectrum of the product of the nucleophilic attack of $MgBrCH_3$ on the $[trans\text{-}B_{20}H_{18}]^{2-}$ ion.

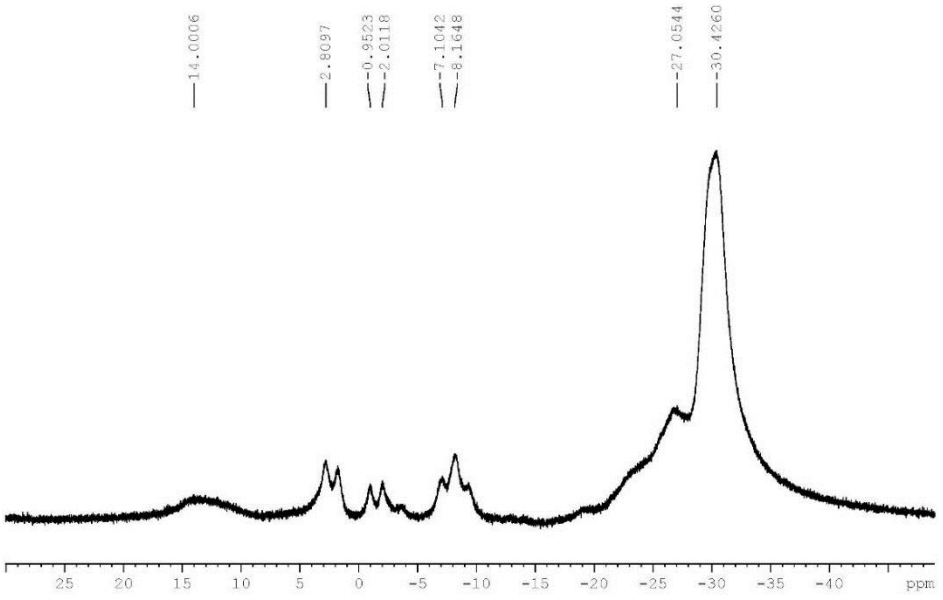

Figure 17: ^{11}B NMR spectrum of the product of the nucleophilic attack of $MgBrCH_3$ on the $[trans\text{-}B_{20}H_{18}]^{2-}$ ion.

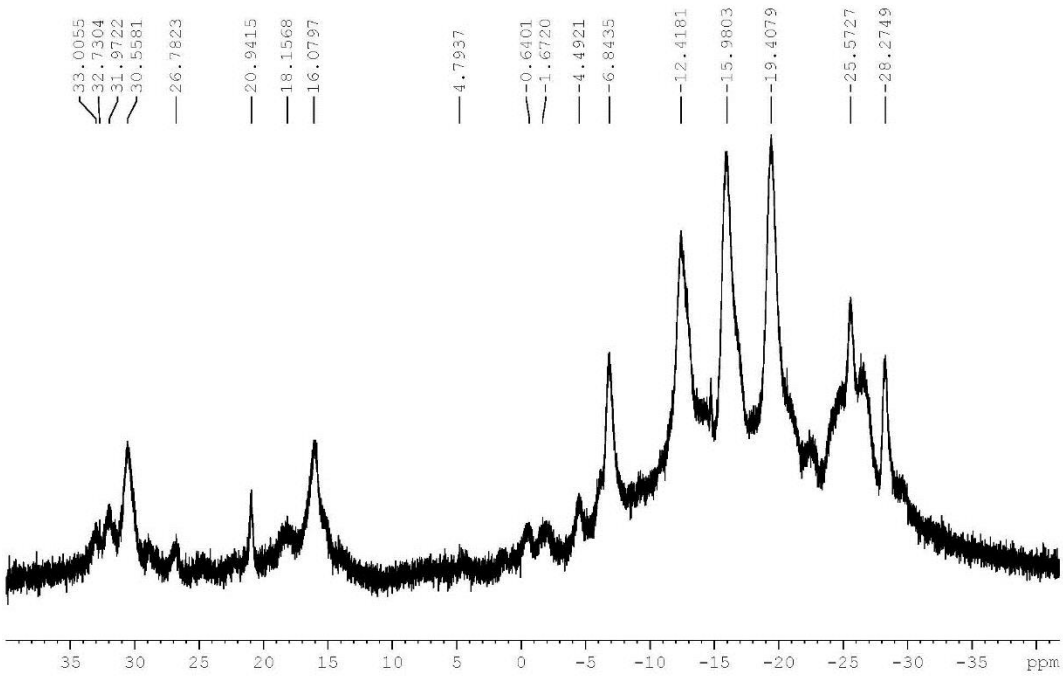

Figure 18: $^{11}B\{^{1}H\}$ spectrum of the resulting from the oxidation of the [*trans*-$B_{20}H_{17}CH_3]^{4-}$ ion to the [*trans*-$B_{20}H_{17}CH_3]^{2-}$ ion.

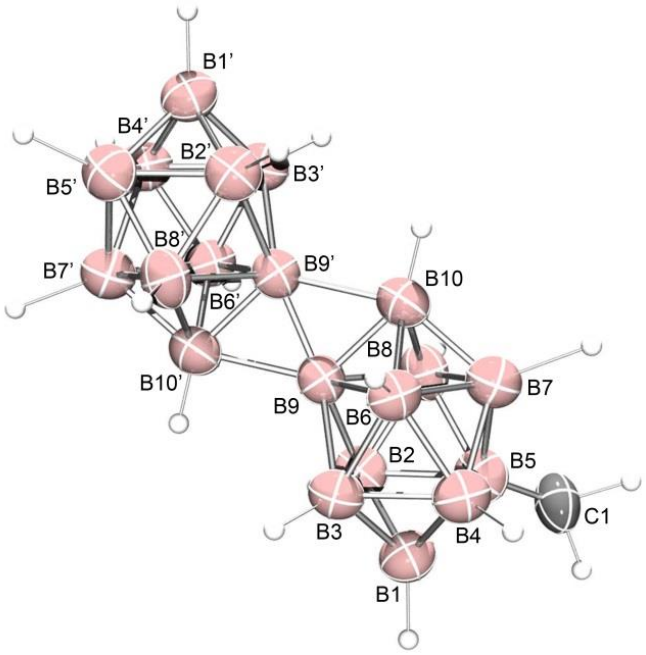

Figure 19: ORTEP drawing (ellipsoids set at 50% probability) of the crystal structure of the $[B_{20}H_{17}CH_3]^{2-}$ ion from the Grignard reaction. Relevant bond lengths include: B5–C1 1.497(7) Å, B9´-B10 1.916(5) Å, and B9-B10´ 1.916(5) Å.

Table 1. Crystal Data, Data Collection and Structure Refinement for $[B_{20}H_{17}CH_3]^{2-}$.

Molecule	$[MePPh_3]_2[B_{20}H_{17}CH_3]$*	$[MePPh_3]_2[B_{20}H_{17}CH_3]$†
Empirical Formula	C39 H56 B20 P2	$C_{39}H_{55}B_{20}P_2$
Formula Weight	802.98	801.97
Temperature	223(2) K	100(2) K
Wavelength	0.71075 Å	0.71075 Å
Crystal System	Triclinic	Monoclinic
Space Group	P1	P2(1)/c
Unit Cell Dimensions	a = 9.2999(10) Å b = 11.1821(12) Å c = 11.1998(12) Å a= 100.486(7)°. b= 90.306(6)°. γ= 92.223(7)°.	a = 12.0541(18) Å b = 15.440(2) Å c = 16.815(2) Å α= 90°. β= 132.961(7)°. γ = 90°
Volume	1144.3(2) Å3	2290.2(6) Å3
Z	1	2
Density (calculated)	1.165 Mg/m3	1.163 Mg/m3
Absorption coefficient	0.125 mm-1	0.125 mm-1
F(000)	420	838
Crystal size	0.2 x 0.2 x 0.2 mm3	0.1 x 0.1 x 0.1 mm3
Theta range for data collections	3.19 to 25.00°.	3.115 to 24.998°.
Index ranges	-11<=h<=11, -13<=k<=13, -13<=l<=13	-14<=h<=14, -18<=k<=18, -19<=l<=19
Reflections collected	9635	18690
Independent reflections	4020 [R(int) = 0.0272]	3981 [R(int) = 0.0862]
Completeness to theta = 26.00°	99.80%	98.60%
Refinement method	Full-matrix least-squares on F2	Full-matrix least-squares on F2
Data/restraints/parameters	4020 / 0 / 316	3981 / 0 / 300
GooF on F^2	1.019	1.003
Final R indices [I>2sigma(I)]	R1 = 0.0494, wR2 = 0.1260	R1 = 0.0627, wR2 = 0.1165
R indices (all data)	R1 = 0.0603, wR2 = 0.1339	
Largest diff. peak and hole	0.903 and -0.256 e.Å-3	0.235 and -0.191 e.Å-3

*Methyl substituent located on equatorial belt adjacent to the boron-boron linkage

† Methyl substituent located on equatorial belt adjacent to the terminal boron apex

4.3 Investigation of the Reaction of the [*trans*-$B_{20}H_{17}CH_3$]$^{2-}$ Ion with $LiCH_3$

The reaction of the acetylide ion with the [*trans*-$B_{20}H_{18}$]$^{2-}$ ion, followed by oxidation of the product, yielded an isomer of the [*trans*-$B_{20}H_{17}CH_3$]$^{2-}$ ion with the methyl substituent located on the equatorial belt adjacent to the electron-deficient bonds whereas the reaction of the methylmagnesium bromide with the [*trans*-$B_{20}H_{18}$]$^{2-}$ ion, followed by oxidation of the product, yielded an isomer of the [*trans*-$B_{20}H_{17}CH_3$]$^{2-}$ ion with the methyl substituent located on the equatorial belt adjacent to the terminal boron apex. The product of the first reaction is consistent with the mechanism proposed by Hawthorne; however the product of the second reaction is not. As a result, other methyl nucleophiles were investigated. The [*trans*-$B_{20}H_{18}$]$^{2-}$ ion was allowed to react with a solution of $LiCH_3$ (**Scheme 13**) in diethylether at room temperature for 12 h. Quantitative conversion to an apical-equatorial isomer of a reduced, substituted species was observed in the $^{11}B\{^1H\}$ NMR spectrum (**Figure 20**). The isomeric assignment was confirmed by the presence of three apical boron atoms signals observed at 3.1, -2.9, and -8.9 ppm. The three apical boron atoms exhibit doublets in the proton-coupled ^{11}B NMR spectrum (**Figure 21**). The reduced species was isolated and treated with the oxidizing agent, *p*-benzoquinone, in acidic aqueous conditions at room temperature for 4 h. The $^{11}B\{^1H\}$NMR (**Figure 22**) and ^{11}B NMR (**Figure 23**) spectra were consistent with similar oxidized ions with signals at 30.2 and 15.6 ppm. Further characterization by X-ray crystallography has yet to be conducted due to difficulty growing single crystals suitable for analysis.

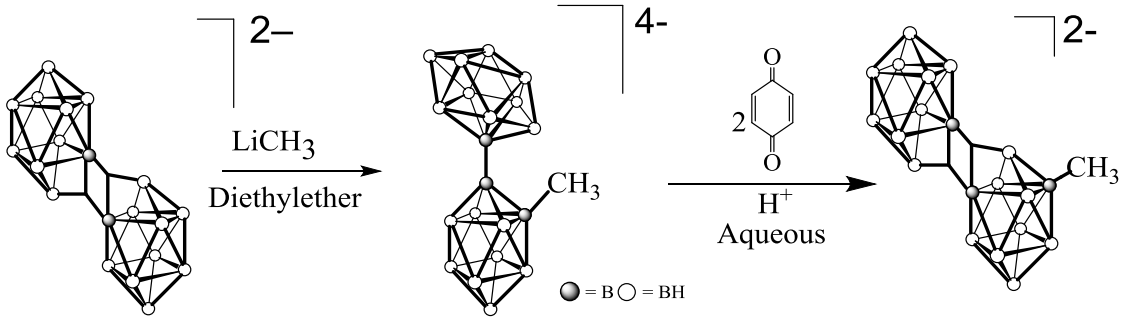

Scheme 13: Generation of the $[B_{20}H_{17}CH_3]^{4-}$ ion by the nucleophilic attack of $[trans\text{-}B_{20}H_{18}]^{2-}$ by $LiCH_3$. The $[B_{20}H_{17}CH_3]^{4-}$ ion was oxidized to the $[trans\text{-}B_{20}H_{17}CH_3]^{2-}$ ion using *p*-benzoquinone in acidic aqueous conditions.

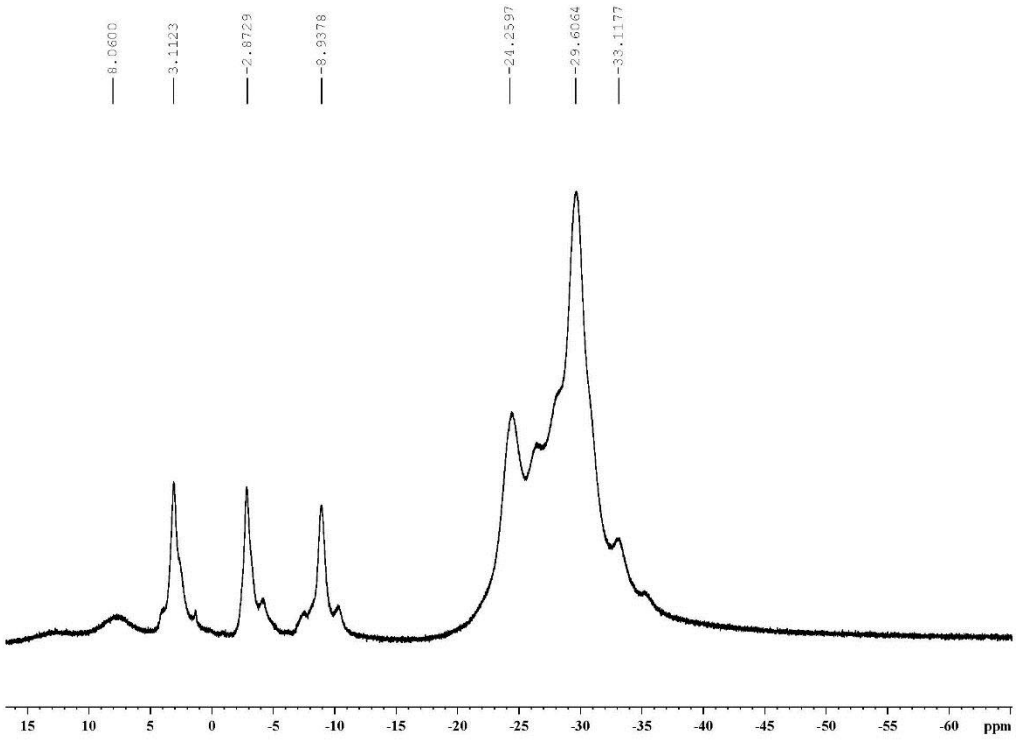

Figure 20: $^{11}B\{^1H\}$ NMR spectrum of the product resulting from the nucleophilic attack of $LiCH_3$ on the $[trans\text{-}B_{20}H_{18}]^{2-}$ ion.

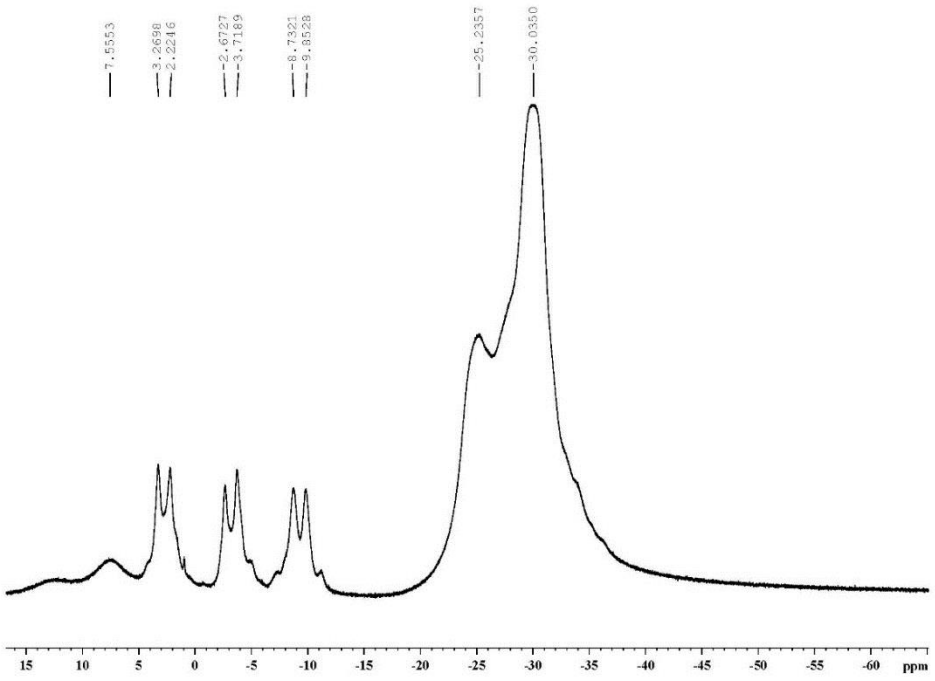

Figure 21: ^{11}B NMR spectrum of the product resulting from the nucleophilic attack of $LiCH_3$ on the $[trans\text{-}B_{20}H_{18}]^{2-}$ ion.

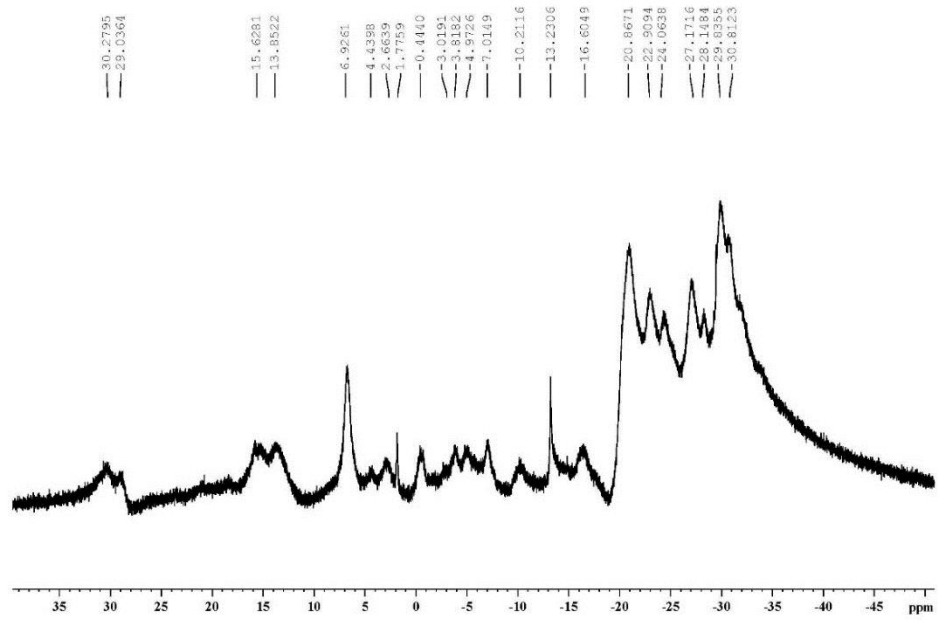

Figure 22: $^{11}B\{^1H\}$ NMR spectrum of the product formed from the oxidation of the $[trans\text{-}B_{20}H_{17}CH_3]^{4-}$ ion formed from the reaction with $LiCH_3$ to form the $[trans\text{-}B_{20}H_{17}CH_3]^{2-}$ ion.

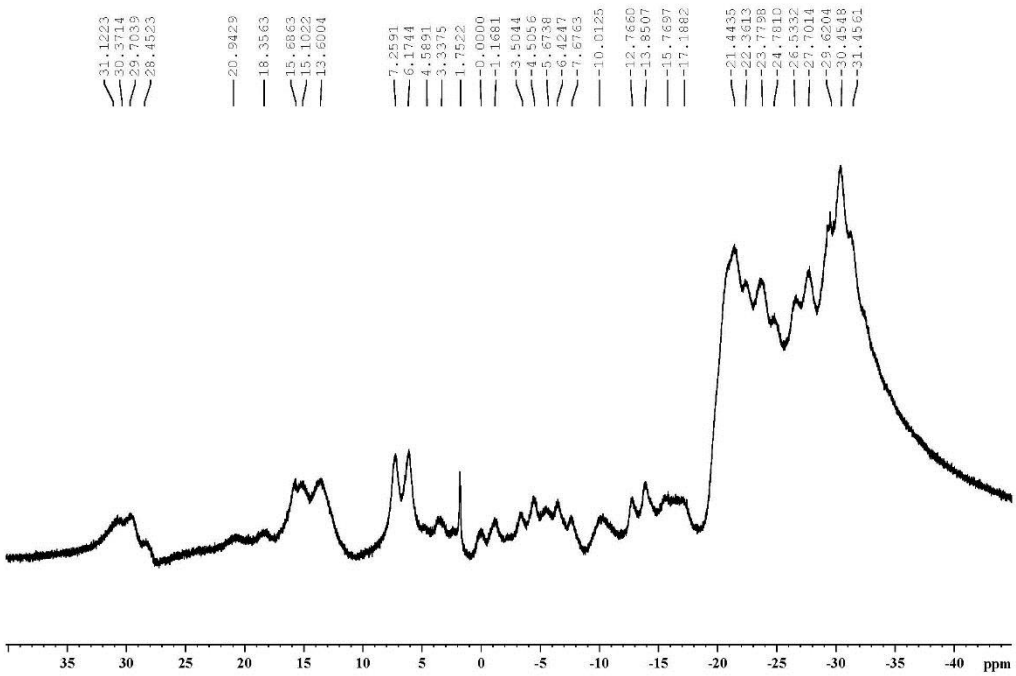

Figure 23: ^{11}B NMR spectrum of the product formed from the oxidation of the [*trans*-$B_{20}H_{17}CH_3$]$^{4-}$ ion formed from the reaction with $LiCH_3$ to form the [*trans*-$B_{20}H_{17}CH_3$]$^{2-}$ ion.

4.4 Investigation of [*trans*-$B_{20}H_{17}CH_2CH_3$]$^{2-}$

The reactivity of the [*trans*-$B_{20}H_{18}$]$^{2-}$ ion with Grignard reagents was unprecedented and provides a route to a wide variety of potential synthetic schemes. In order to investigate the reactivity more thoroughly, the reactivity of the [*trans*-$B_{20}H_{18}$]$^{2-}$ ion with ethylmagnesium bromide was also investigated (**Scheme 14**). The quantitative conversion of the [*trans*-$B_{20}H_{18}$]$^{2-}$ ion to the [*ae*-$B_{20}H_{17}CH_2CH_3$]$^{4-}$ ion was achieved by allowing the [*trans*-$B_{20}H_{18}$]$^{2-}$ ion to react with ethylmagnesium bromide in diethylether at room temperature for 12 h. Complete conversion was confirmed by ^{11}B{^{1}H} NMR

spectroscopy. The isomeric assignment was confirmed by the presence of three apical boron atoms signals observed at 3.2, -3.1, and -7.6 ppm (**Figure 24**). The three apical boron atoms exhibit doublets in the proton-coupled ^{11}B NMR spectrum (**Figure 25**) The reduced species was isolated and treated with the oxidizing agent, *p*-benzoquinone, in acidic aqueous conditions at room temperature for 4 h. The $^{11}B\{^{1}H\}$NMR (**Figure 26**) and ^{11}B NMR spectra (**Figure 27**) were consistent with the products of similar oxidation with signals at 30.4 and 15.9 ppm. Further characterization by X-ray crystallography has yet to be conducted due to difficulty growing single crystals suitable for analysis.

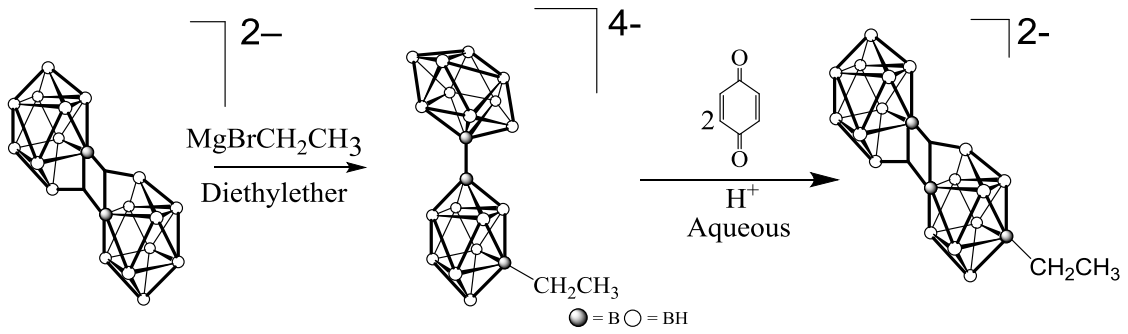

Scheme 14: Generation of [*ae*-$B_{20}H_{17}CH_2CH_3]^{4-}$ ion by the nucleophilic attack of [*trans*-$B_{20}H_{18}]^{2-}$ by $MgBrCH_2CH_3$. The $[B_{20}H_{17}CH_2CH_3]^{4-}$ ion was oxidized to form the [*trans*-$B_{20}H_{17}CH_2CH_3]^{2-}$ ion using *p*-benzoquinone in acidic aqueous conditions.

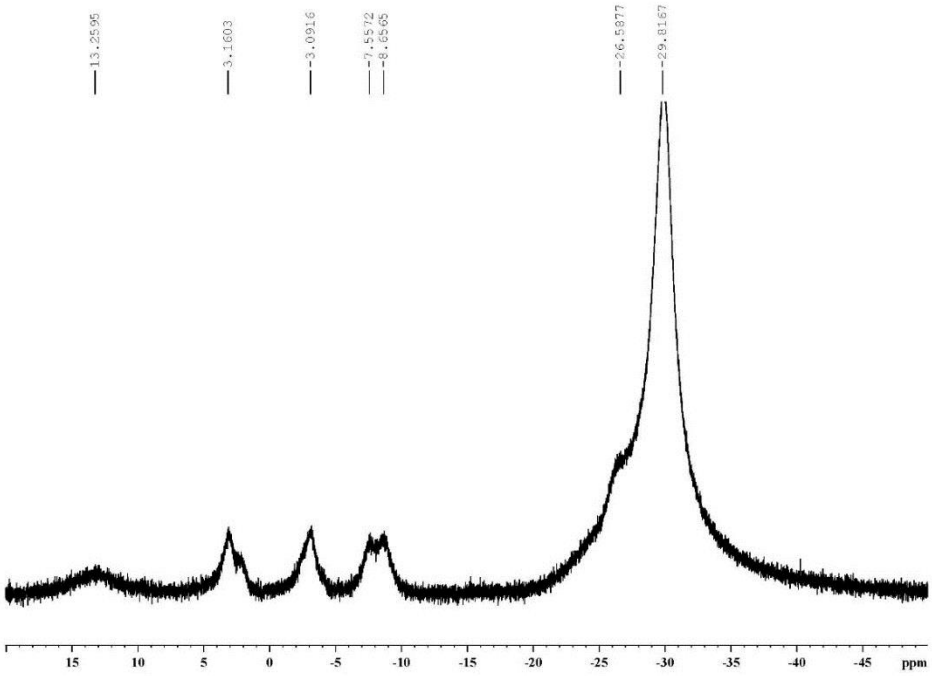

Figure 24: $^{11}B\{^{1}H\}$ NMR spectrum of the product resulting from the nucleophilic attack of $MgBrCH_2CH_3$ on the $[trans\text{-}B_{20}H_{18}]^{2-}$ ion.

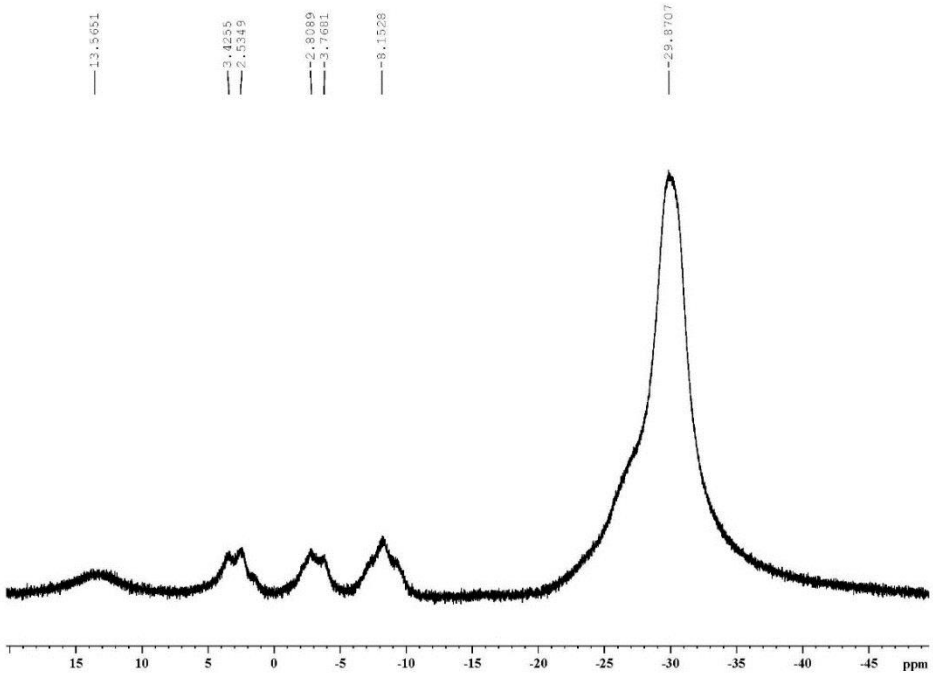

Figure 25: ^{11}B NMR spectrum of the product resulting from the nucleophilic attack of $MgBrCH_2CH_3$ on the $[trans\text{-}B_{20}H_{18}]^{2-}$ ion.

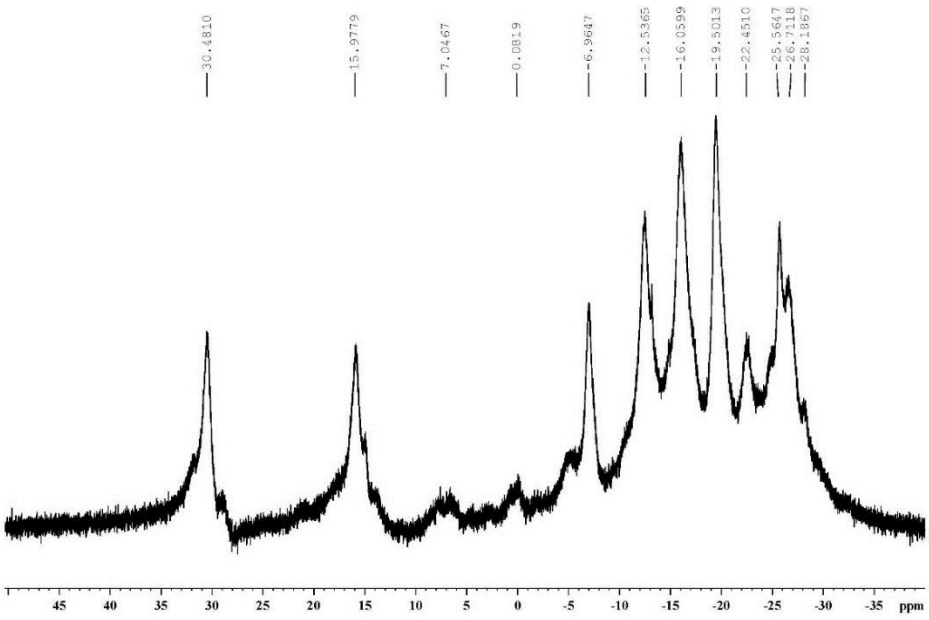

.

Figure 26: $^{11}B\{^{1}H\}$ NMR spectrum of the product of the oxidation of [*ae*-$B_{20}H_{17}CH_2CH_3]^{4-}$ ion to form the [*trans*-$B_{20}H_{17}CH_2CH_3]^{2-}$ ion.

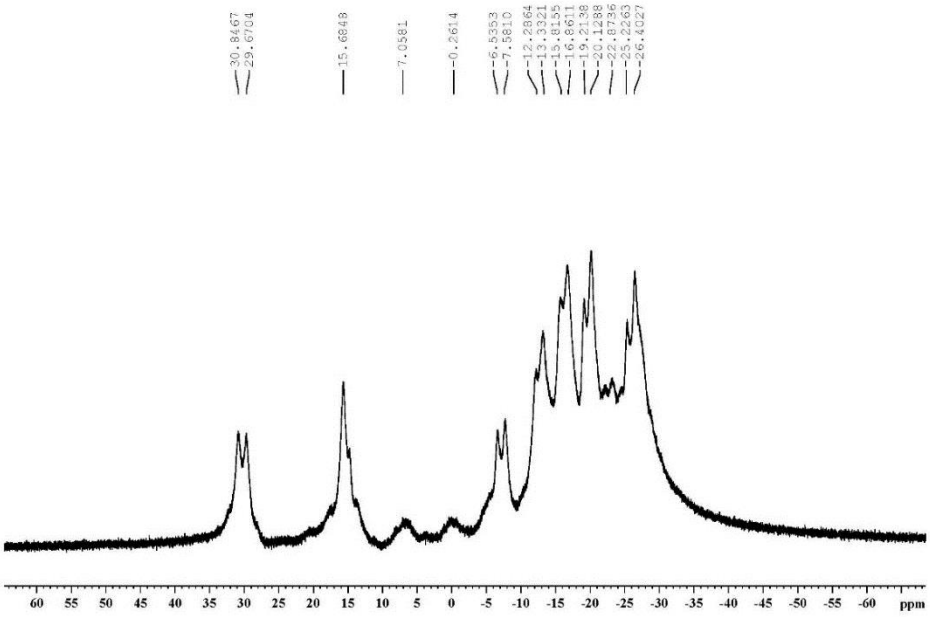

Figure 27: ^{11}B NMR spectrum of the product of the oxidation of [*ae*-$B_{20}H_{17}CH_2CH_3]^{4-}$ ion to form the [*trans*-$B_{20}H_{17}CH_2CH_3]^{2-}$ ion.

4.5 Investigation of Oxidation Mechanism of the $[B_{20}H_{17}X]^{4-}$ Ion to the $[B_{20}H_{17}X]^{2-}$ Ion With Electrophiles.

The [*trans*-$B_{20}H_{18}]^{2-}$ ion, first reported by Kaczmarczyk[15] in 1962, is susceptible to nucleophilic attack at the two electron-deficient, three-center, two-electron bonds, producing a reduced substituted ion of the form $[B_{20}H_{17}X]^{4-}$ where X is –OH, [20,21] –OR,[20,21] $–NH_3$,[4] –NHRR′,[26] and –SH.[6] The proposed mechanism of nucleophilic attack was reported by Hawthorne in 1965 using the hydroxide ion as the nucleophile.[1] The reaction was initiated by the attack of the equatorial boron in one of the electron-deficient, three-center, two-electron bonds by the hydroxide ion followed by a migration of one of the cages. A second equivalent of the nucleophile is required to remove the bridging hydrogen and convert the $[B_{20}H_{18}X]^{3-}$ ion into the $[B_{20}H_{17}X]^{4-}$ ion. The kinetic isomer of the product, $[B_{20}H_{17}X]^{4-}$, is characterized by an apical-equatorial connection between the two boron cages and is designated [*ae*-$B_{20}H_{17}X]^{4-}$. Single crystals of the $[B_{20}H_{17}X]^{4-}$ isomers suitable for characterization by X-ray crystallography have been challenging to obtain and, as a result, very few crystal structures have been reported. Aqueous oxidation of the $[B_{20}H_{17}OH]^{4-}$ ion using ferric chloride was reported by Hawthorne in 1965.[6,20] Crystallographic data of the $[B_{20}H_{17}OH]^{4-}$ ion and $[B_{20}H_{17}OH]^{2-}$ ion have not been reported in the literature. In an effort to investigate the location of the substituent as well as the oxidation reaction itself, both the $[B_{20}H_{17}OH]^{4-}$ ion and $[B_{20}H_{17}OH]^{2-}$ ion were prepared.

The [*trans*-$B_{20}H_{18}]^{2-}$ ion was allowed to react with potassium hydroxide in aqueous solution at room temperature to produce [*ae*-$B_{20}H_{17}OH]^{4-}$. Quantitative

conversion was confirmed by $^{11}B\{^{1}H\}$ NMR spectroscopy (**Figure 28**). Both isomers, the *ae* and the a^2, are present in the spectrum. The presence of the apical-equatorial isomer was confirmed by the presence of three apical boron atom signals observed at 2.8, -2.0, and -9.4 ppm. The three apical boron atoms exhibit doublets in the proton-coupled ^{11}B NMR spectrum (**Figure 29**). The presence of the apical-apical isomer was confirmed by the presence of two apical boron atom signals observed at -5.4 and -8.5 ppm. The two apical boron atoms exhibit doublets in the proton-coupled ^{11}B NMR spectrum. The K_4[*ae*-$B_{20}H_{17}OH$] was dissolved in acidic water and treated with *p*-benzoquinone for 4 h at room temperature. The product was isolated as a methyltriphenylphosphonium salt. The $^{11}B\{^{1}H\}$ (**Figure 30**) and ^{11}B NMR spectra (**Figure 31**) of the product are consistent with results observed for similar oxidations with signals at 30.0 and 15.0 ppm. Single crystals of the oxidized product suitable for characterization by X-ray crystallography were obtained by slow vapor diffusion of diethylether into a solution of the salt in acetonitrile. The crystal structure verified (**Figure 32)** that the hydroxy substituent was located in the anticipated position on the equatorial belt adjacent to the electron-deficient bonding region. The B7–O1 distance of 1.400(6) Å is shorter than what Hawthorne observed in the bridging hydroxy-substituted ion $[\mu\text{-}B_{20}H_{17}OH]^{2-}$ (avg. B–O bonds lengths = 1.483 Å)[29] as can be expected for a terminal versus bridging substituent. In the absence of the acid, no oxidation was observed.

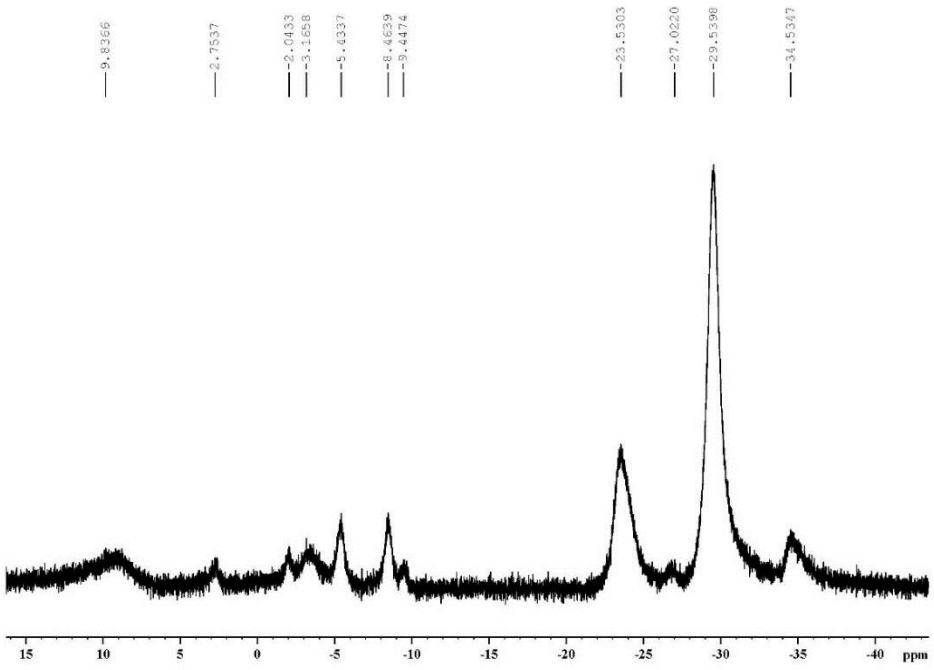

Figure 28: $^{11}B\{^{1}H\}$ NMR spectrum of the product of the reaction between KOH and the [*trans*-$B_{20}H_{18}$]$^{2-}$ ion.

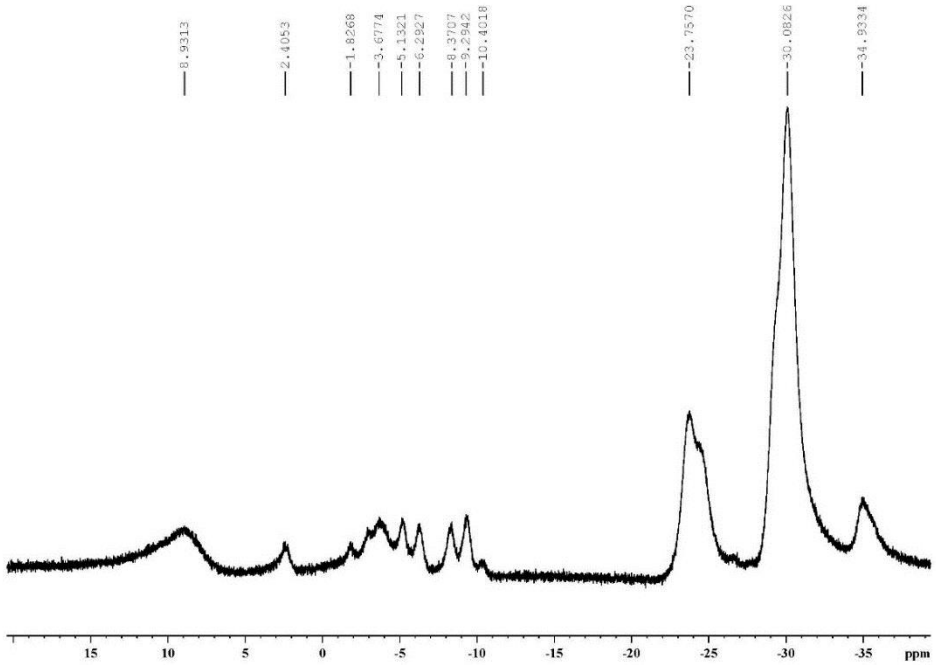

Figure 29: ^{11}B NMR spectrum of the product of the reaction between KOH and the [*trans*-$B_{20}H_{18}$]$^{2-}$ ion.

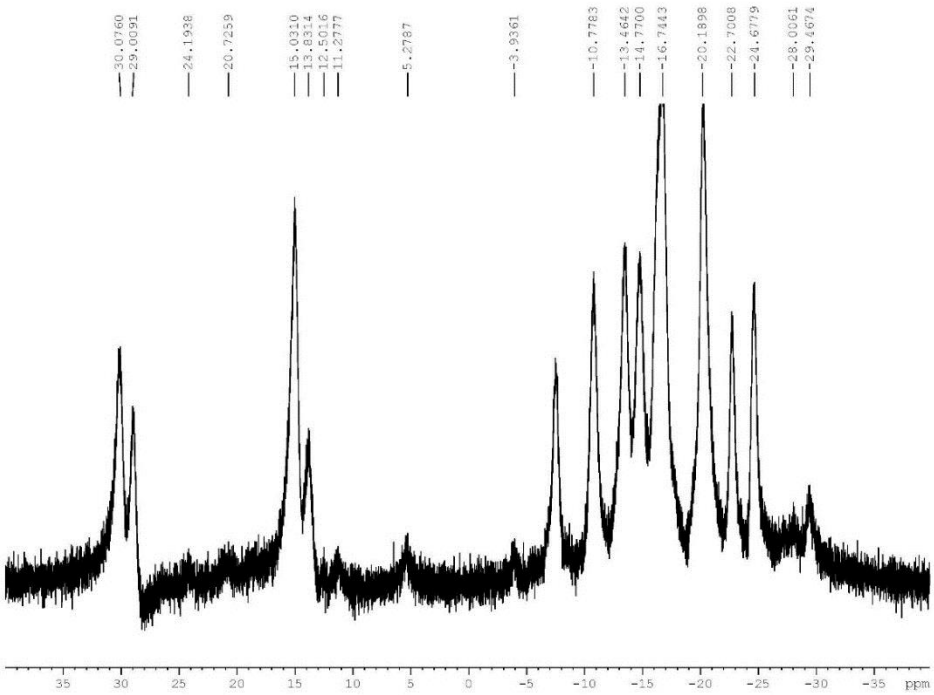

Figure 30: $^{11}B\{^{1}H\}$ NMR spectrum of the product of the oxidation of the $[B_{20}H_{17}OH]^{4-}$ ion to form the [*trans*-$B_{20}H_{17}OH]^{2-}$ ion.

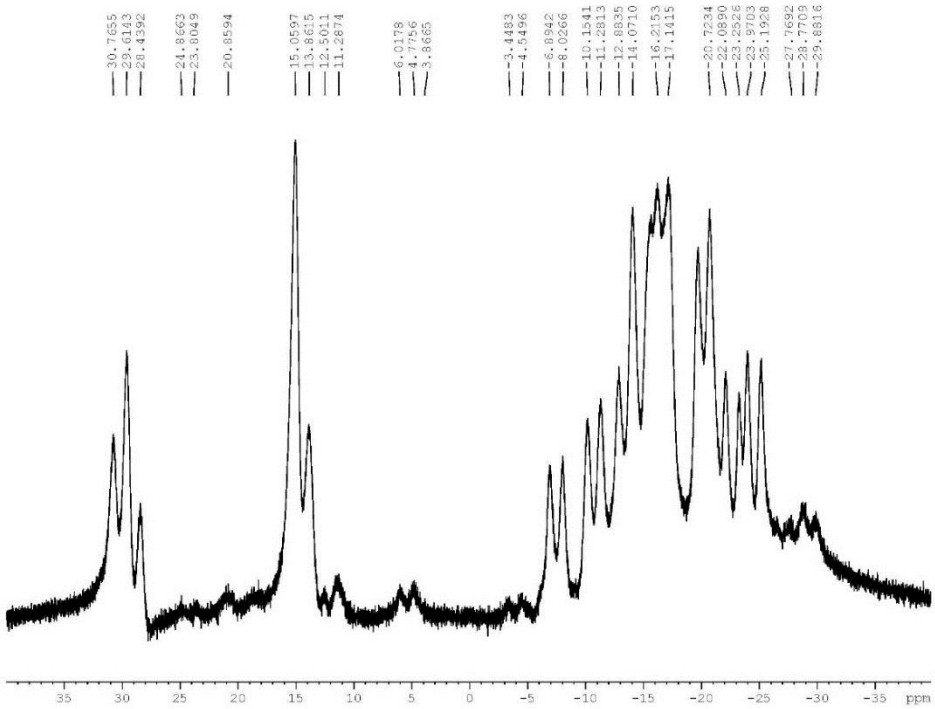

Figure 31: ^{11}B NMR spectrum of the product of the oxidation of the $[B_{20}H_{17}OH]^{4-}$ ion to form the [*trans*-$B_{20}H_{17}OH]^{2-}$ ion.

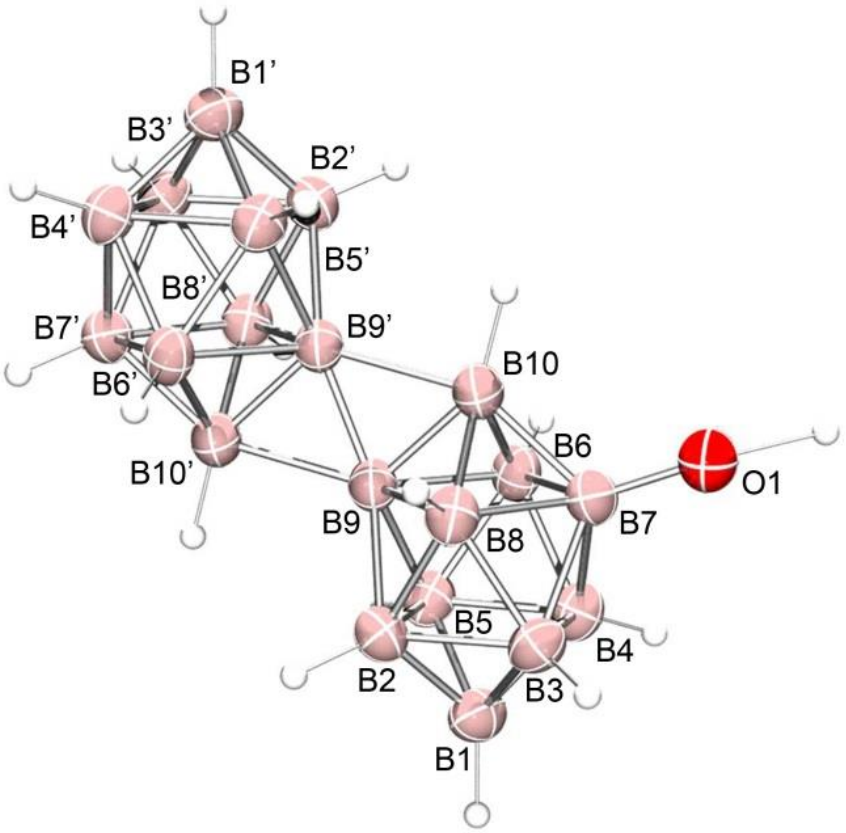

Figure 32: ORTEP drawing (ellipsoids set at 50% probability) of the crystal structure of the $[B_{20}H_{17}OH]^{2-}$ ion. Relevant bond lengths include: B7–O1 1.400(6) Å, B9´-B10 1.916(5) Å, and B9-B10´ 1.916(5) Å.

Based on the mechanism of nucleophilic attack proposed by Hawthorne[3] (**Scheme 3**) and the required presence of the acid, one would expect the oxidation process to be initiated by the protonation of the $[B_{20}H_{17}OH]^{4-}$ ion to form the $[B_{20}H_{18}OH]^{3-}$ ion. The hydrogen resulting from the protonation process would ultimately reside on one of the apical boron vertices which constitute the three-center, two-electron bonds characteristic of the $[\textit{trans}\text{-}B_{20}H_{18}]^{2-}$ ion and its derivatives. As a result, in the absence of the acidic solution, the oxidation process cannot proceed; however, in the presence of a suitable electrophile, the oxidation process should proceed and result in the addition of a

substituent at one of the apical boron vertices which constitute the three-center, two-electron bond. To investigate this hypothesis, the methyltriphenylphosphonium salt of the [*ae*-$B_{20}H_{17}OH]^{4-}$ ion was oxidized using *p*-benzoquinone in the presence of excess of electrophile. Iodomethane was the first electrophile investigated (**Scheme 15**). The investigation occurred by dissolving [*ae*-$B_{20}H_{17}OH]^{4-}$ ion in a mixture of dichloromethane and acetonitrile. Once dissolved, iodomethane (greater than two equivalents) was added to initiate the oxidation reaction. After stirring for five minutes *p*-benzoquinone was added and the reaction was refluxed for 12 h.

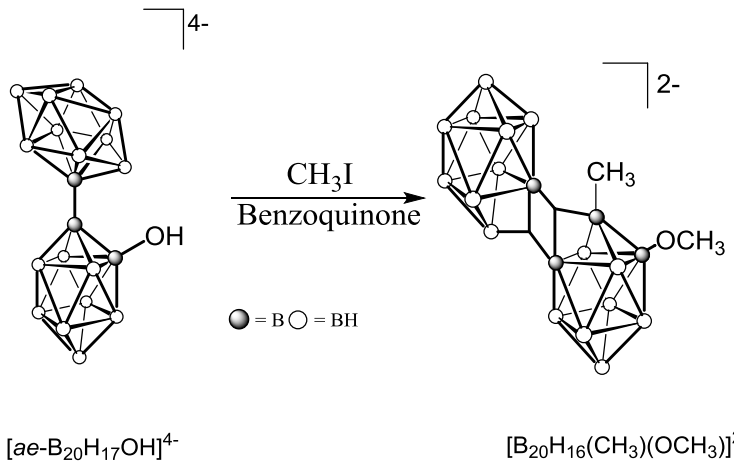

Scheme 15: Proposed oxidation of [*ae*-$B_{20}H_{17}OH]^{4-}$ in the presence of iodomethane to form the hypothesized $[B_{20}H_{17}(CH_3)(OCH_3)]^{2-}$ ion.

The $^{11}B\{^1H\}$(**Figure 33**) and ^{11}B NMR NMR spectra (**Figure 34**) of the oxidized product were consistent with the spectra observed for similar oxidation reactions with signals at ~30 and ~15 ppm . However other signals and splitting appeared that was not commonly observed. Further characterization by X-ray crystallography revealed the product, the [μ- OCH_3-$B_{20}H_{17}]^{2-}$ ion, contained both oxygen and hydrogen-bridge bonds (**Figure 35**). Formation of the bridging product is consistent with earlier observations that

the bridging isomer is formed when the reactions are completed in non-aqueous solutions.[21] The $[\mu\text{-}OCH_3\text{-}B_{20}H_{17}]^{2-}$ product has been reported earlier from the ferric chloride oxidation of the $[B_{20}H_{17}OR]^{4-}$ ion in anhydrous ethanol;[2] however, only the single crystal structure of the $[\mu\text{- }OH\text{-}B_{20}H_{17}]^{2-}$ ion has been reported.[32] The apical intercage B10–B20 separation in the $[\mu\text{-}OCH_3\text{-}B_{20}H_{17}]^{2-}$ ion is 1.916(5) Å,[32] and is consistent with that in the reported structure of the $[\mu\text{-}OH\text{-}B_{20}H_{17}]^{2-}$ ion (1.907(9) Å).[32] Additionally, the B9–O1 and B19–O1 distances of 1.481(4) and 1.488(4) Å, respectively, are both longer than what were observed with the terminal hydroxyl-derivative,(1.400(6) Å) $[B_{20}H_{17}OH]^{2-}$,[32] and similar to what Hawthorne reported in the bridging hydroxyl derivative (avg. B–O bonds lengths = 1.483 Å).[18]

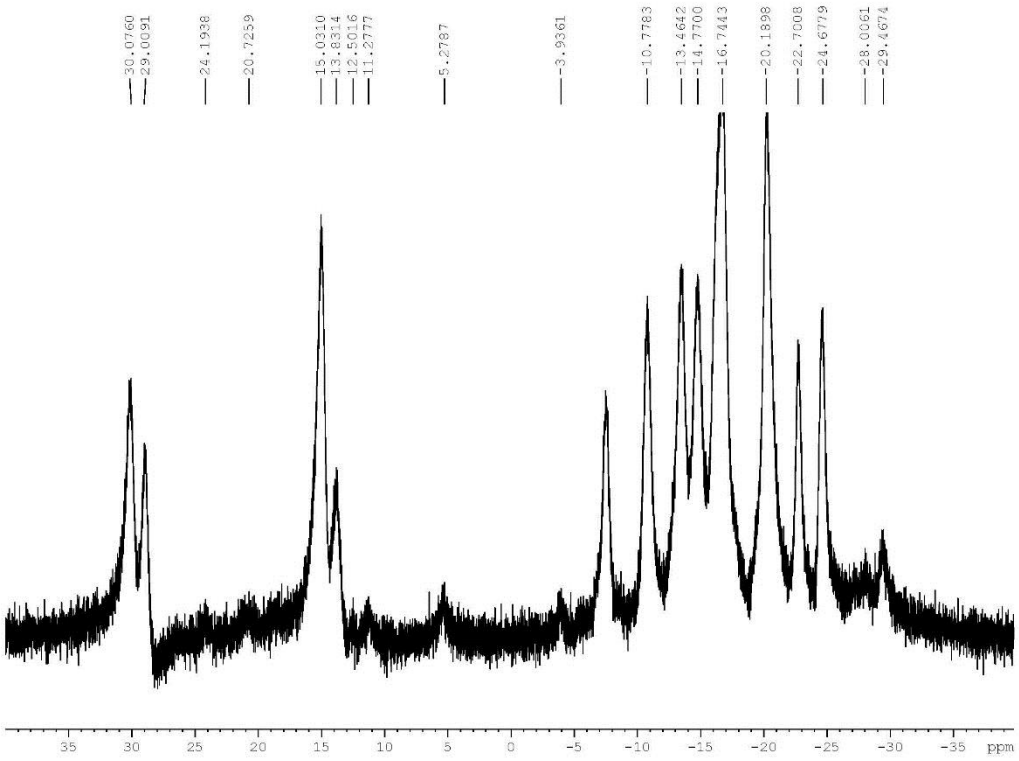

Figure 33: $^{11}B\{^1H\}$ NMR spectrum of the product of the oxidation of the [*ae*-$B_{20}H_{17}OH]^{4-}$ ion to form the [*trans*-$B_{20}H_{17}OH]^{2-}$ ion.

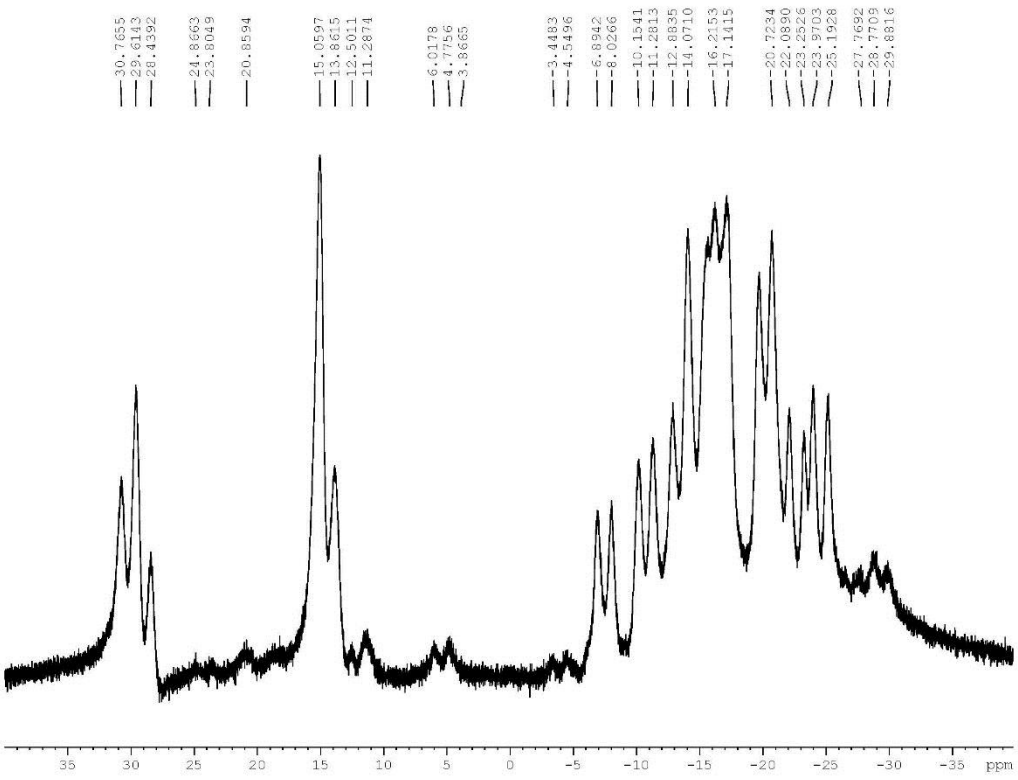

Figure 34: ^{11}B NMR spectrum of the product of the oxidation of the [*ae*-$B_{20}H_{17}OH]^{4-}$ ion to form the [*trans*-$B_{20}H_{17}OH]^{2-}$ ion.

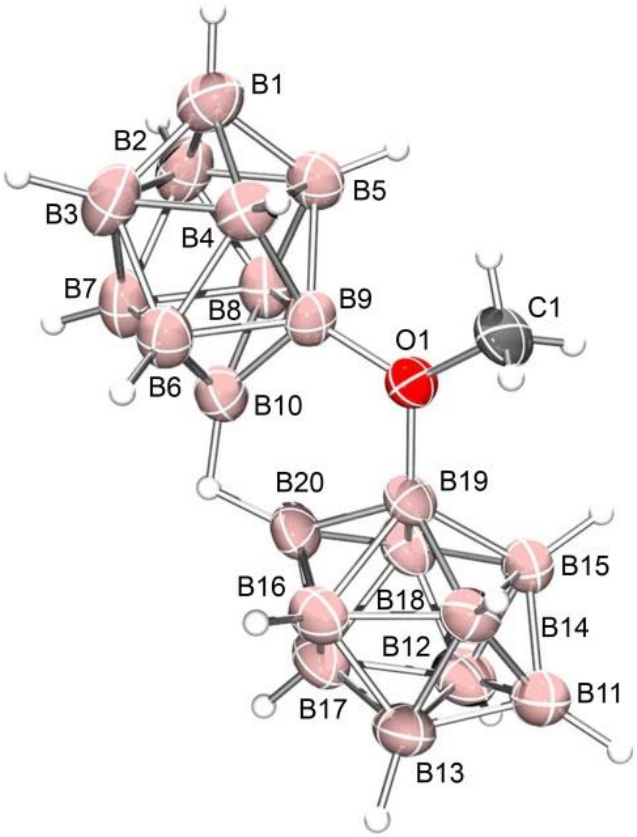

Figure 35: ORTEP drawing (ellipsoids set at 50% probability) of the crystal structure of the $[B_{20}H_{17}OCH_3]^{2-}$ ion. Relevant bond lengths include: B7–O1 1.400(6) Å, B9′-B10 1.916(5) Å, and B9-B10′ 1.916(5) Å.

Other electrophiles investigated included acetyl chloride (**Scheme 16**) and benzoyl chloride (**Scheme 17**). Reaction with benzoyl chloride and acetyl chloride were hypothesized to doubly substitute the boron cluster. However due to previous results observed, it is anticipated to yield a bridged product. The $^{11}B\{^1H\}$(**Figure 36**) and ^{11}B NMR spectra (**Figure 37**) of the acetyl products and the$^{11}B\{^1H\}$(**Figure 38**) and ^{11}B NMR spectra (**Figure 39**) spectra of the benzoyl products were consistent with results observed with similar oxidation reactions with signals at 32.9 and 13.9 ppm, and 31.1 and 15.8 ppm, respectively. Other signaling and splitting appeared that was not commonly

observed. X-ray crystallography has been unsuccessful to yield a definitive structure of either product because of the difficulty in growing single crystals. A table with a summary of crystal data, data collection and structural refinement of the $[B_{20}H_{17}OH]^{2-}$ ion and the $[\mu\text{-}B_{20}H_{17}OCH_3]^{2}\bullet CH_3CN$ ion can be observed in **(Table 2)**

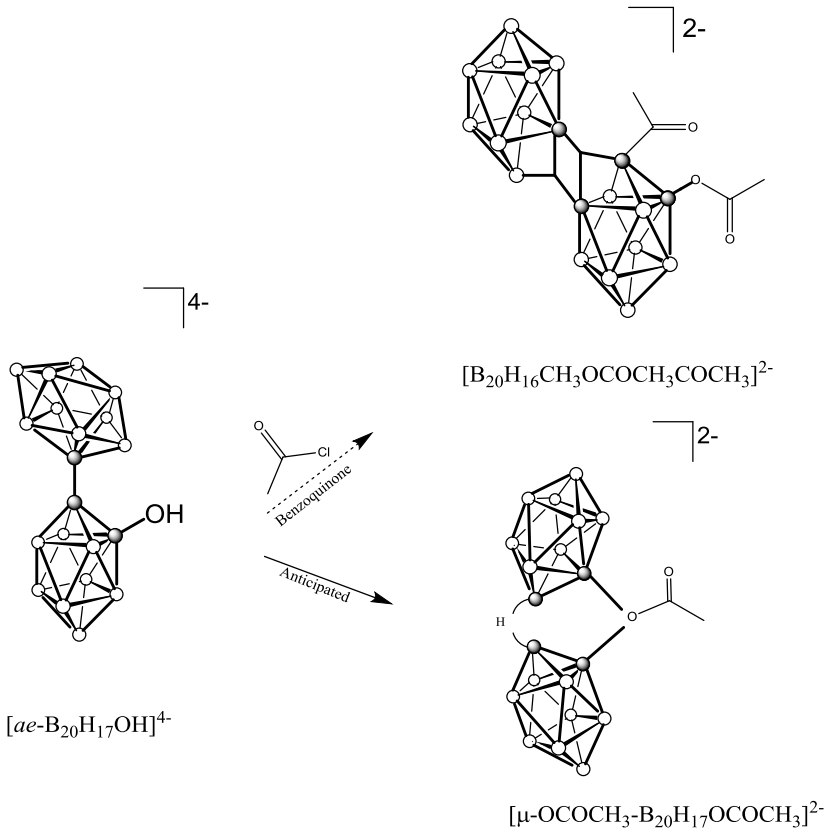

$[B_{20}H_{16}CH_3OCOCH_3COCH_3]^{2-}$

$[ae\text{-}B_{20}H_{17}OH]^{4-}$

$[\mu\text{-}OCOCH_3\text{-}B_{20}H_{17}OCOCH_3]^{2-}$

Scheme 16: Proposed and anticipated oxidation of $[ae\text{-}B_{20}H_{17}OH]^{4-}$ in the presence of acetyl chloride to form doubly substituted and bridged products.

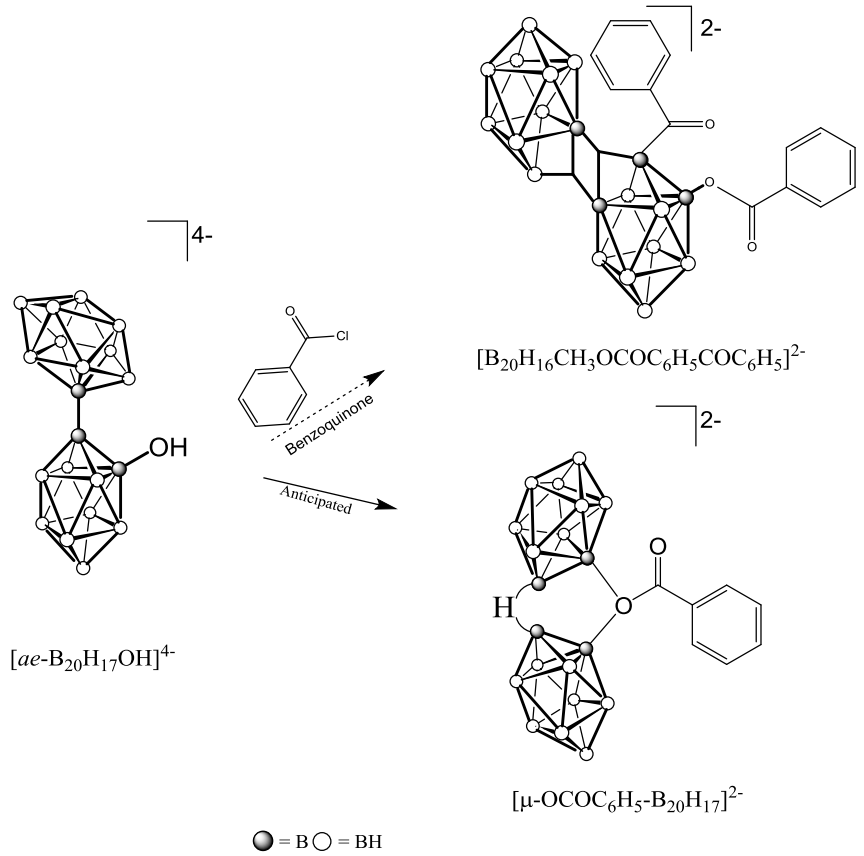

Scheme 17: Proposed and anticipated oxidation of [*ae*-$B_{20}H_{17}OH]^{4-}$ in the presence of benzoyl chloride to form doubly substituted and bridged products.

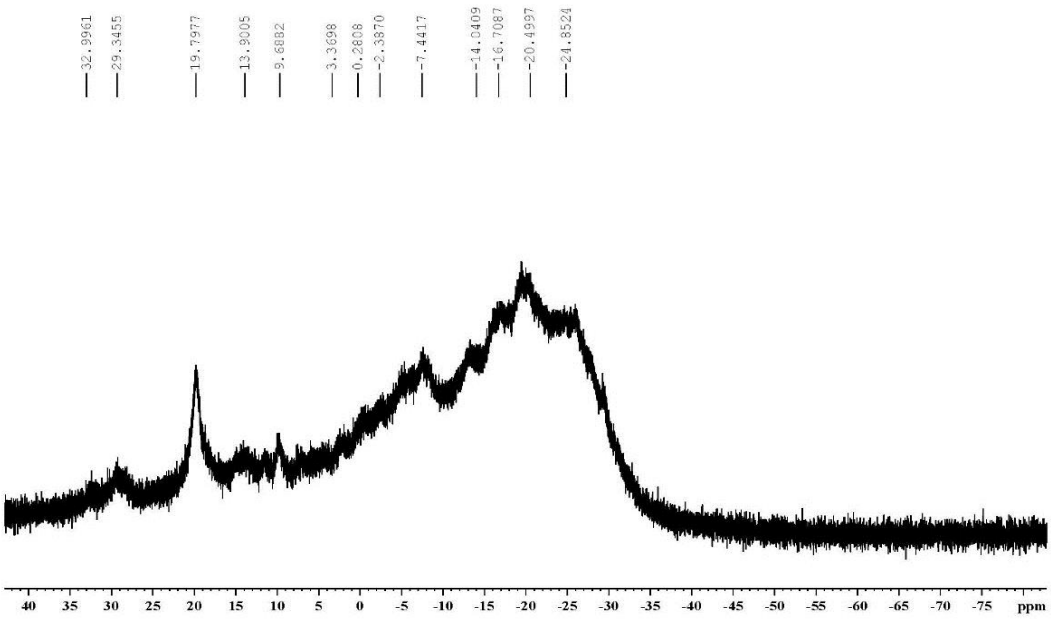

Figure 36: $^{11}B\{^{1}H\}$ NMR spectrum of the product of the oxidation of the [*ae*-$B_{20}H_{17}OH]^{4-}$ ion in the presence of acetyl chloride.

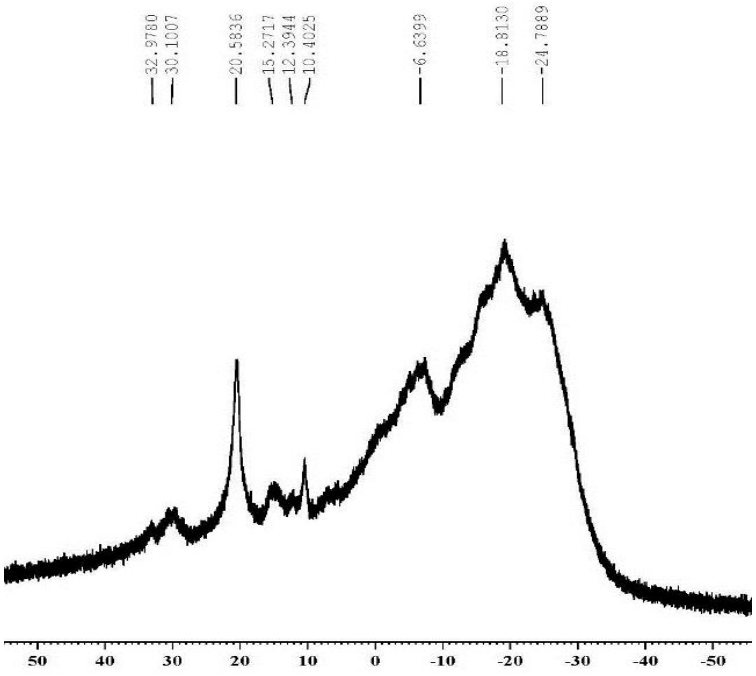

Figure 37: ^{11}B NMR spectrum of the product of the oxidation of the [*ae*-$B_{20}H_{17}OH]^{4-}$ ion in the presence of acetyl chloride.

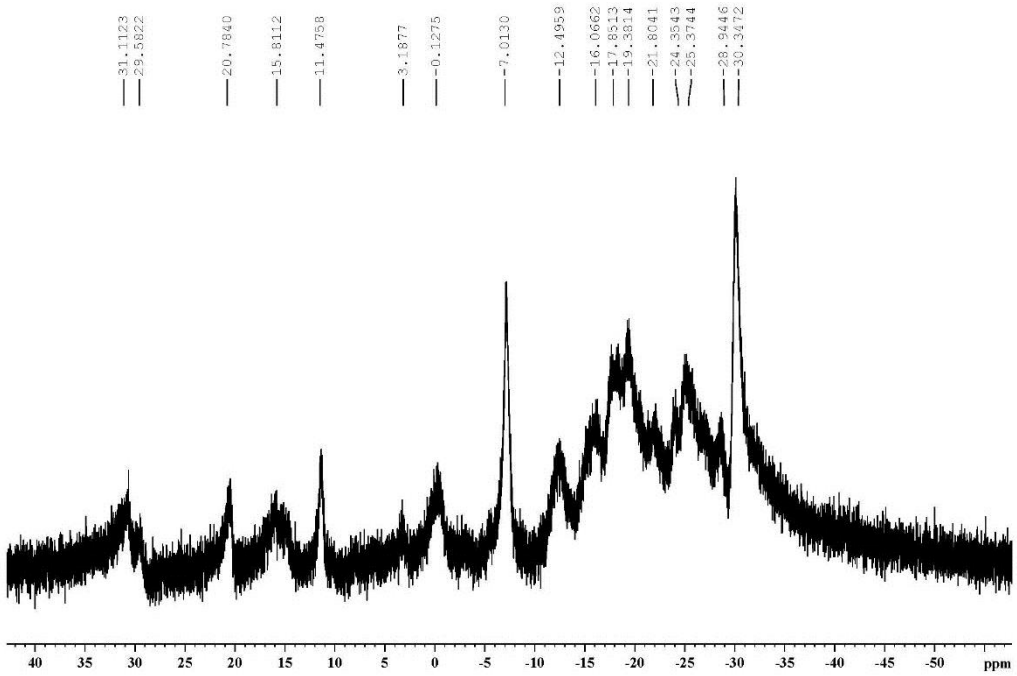

Figure 38: $^{11}B\{^{1}H\}$ NMR spectrum of the product of the oxidation of the [*ae*-$B_{20}H_{17}OH]^{4-}$ ion in the presence of benzoyl chloride.

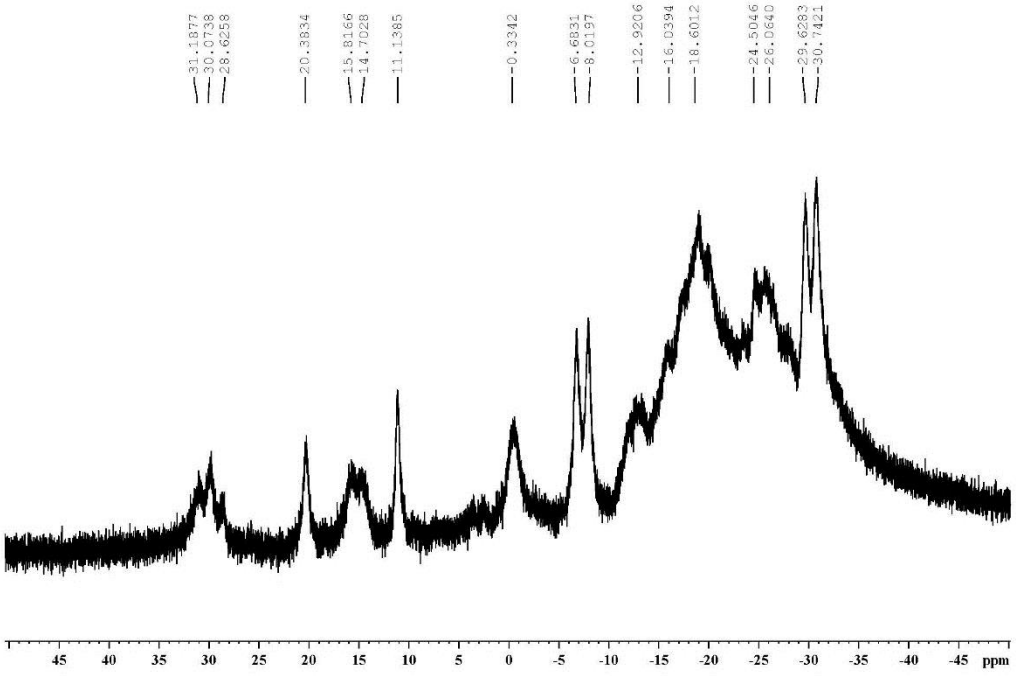

Figure 39: ^{11}B NMR spectrum of the product of the oxidation of the [*ae*-$B_{20}H_{17}OH]^{4-}$ ion in the presence of benzoyl chloride.

Table 2. Crystal Data, Data Collection and Structure Refinement for the $[B_{20}H_{17}OH]^{2-}$ ion and the $[\mu\text{-}B_{20}H_{17}OCH_3]^{2}\bullet CH_3CN$ ion.

Molecule	$[MePPh_3]_2[B_{20}H_{17}OH]$	$[MePPh_3]_2[\mu\text{-}OCH_3\text{-}B_{20}H_{17}]\bullet CH_3CN$
Empirical Formula	$C_{38}H_{53}B_{20}OP_2$	$C_{41}H_{59}B_{20}NOP_2$
Formula Weight	803.94	860.03
Temperature	100(2) K	100(2) K
Wavelength	0.71075 Å	0.71073. Å
Crystal System	Triclinic	Monoclinic
Space Group	P-1	P2(1)/c
Unit Cell Dimensions	a = 9.3043(17) Å b = 11.192(2) Å c = 11.213(2) Å α = 100.392(7)°. β = 90.238(6)°. γ = 92.200(7)°.	a = 20.4188(16) Å b = 14.8125(12) Å c = 16.4846(13) Å α = 90° β = 93.545(7)°. γ = 90°
Volume	1147.6(4) Å3	4976.3(7) Å3
Z	1	4
Density (calculated)	1.163 Mg/m3	1.148 Mg/m3
Absorption coefficient	0.127 mm-1	0.122 mm-1
F(000)	419	1800
Crystal size	0.1 x 0.1 x 0.1 mm3	0.1 x 0.1 x 0.1 mm3
Theta range for data collections	3.190 to 24.998°.	3.016 to 24.999°.
Index ranges	-11<=h<=11, -13<=k<=13, -13<=l<=13	-24<=h<=24, -17<=k<=17, -17<=l<=19
Reflections collected	8513	27097
Independent reflections	4000 [R(int) = 0.0645]	8732 [R(int) = 0.0649]
Completeness to theta = 26.00°	98.90%	99.60%
Refinement method	Full-matrix least-squares on F2	Full-matrix least-squares on F2
Data/restraints/parameters	4000 / 0 / 317	8732 / 0 / 663
GooF on F^2	1.01	1.013
Final R indices [I>2sigma(I)]	R1 = 0.0715, wR2 = 0.1726	R1 = 0.0626, wR2 = 0.1381
Largest diff. peak and hole	0.593 and -0.322 e.Å-3	0.245 and -0.204 e.Å-3

4.6 **Investigation of Novel Compounds**

In addition to the reinvestigation of the nucleophilic attack of sodium acetylide on the [*trans*-$B_{20}H_{18}$]$^{2-}$ ion, other carbon-containing nucleophiles were also investigated. In particular, the reaction of the [*trans*-$B_{20}H_{18}$]$^{2-}$ ion with deprotonated acetonitrile and copper (I) cyanide were investigated.

The $^{-}CH_2CN$ ion was formed by allowing *n*-butyl lithium to react with acetonitrile in diethylether at -78° C. The [*trans*-$B_{20}H_{18}$]$^{2-}$ ion was added to the deprotonated acetonitrile and the reaction allowed to take place (**Scheme 18**). Quantitative conversion to the reduced species was achieved as confirmed by $^{11}B\{^1H\}$ NMR. The isomeric assignment was confirmed by the presence of three apical boron atom signals in the spectrum at -0.35, -5.37, and -12.9 ppm (**Figure 40**). The reduced species was isolated and treated with the oxidizing agent, *p*-benzoquinone, in an acidic organic environment. The $^{11}B\{^1H\}$NMR (**Figure 41**) of the product were consistent results observed with similar oxidation reactions by the presence of signals at 30.4 and 14.6 ppm. Further characterization by X-ray crystallography has not been conducted due to difficulty of growing single crystals.

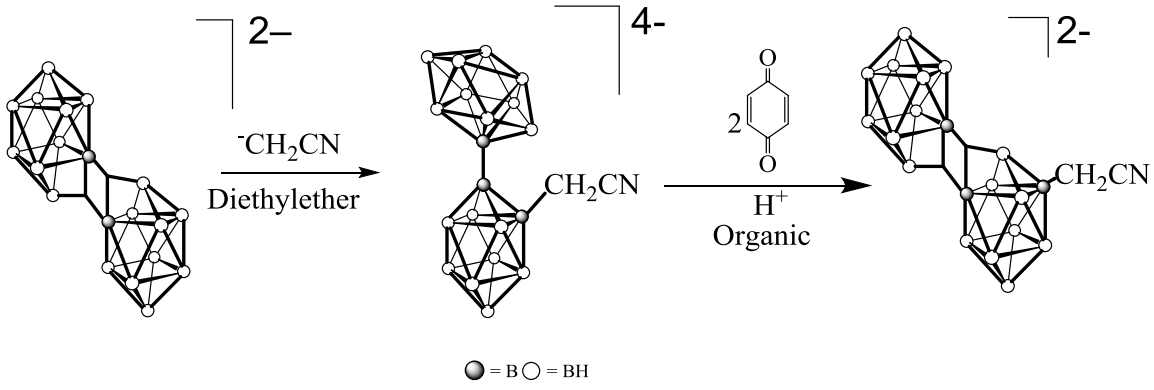

Scheme 18: Proposed reaction of the [*trans*-$B_{20}H_{18}$]$^{2-}$ ion with the acetonitrile ion and oxidation of the resulting product to form the [*trans*-$B_{20}H_{17}CH_2CN$]$^{4-}$ ion.

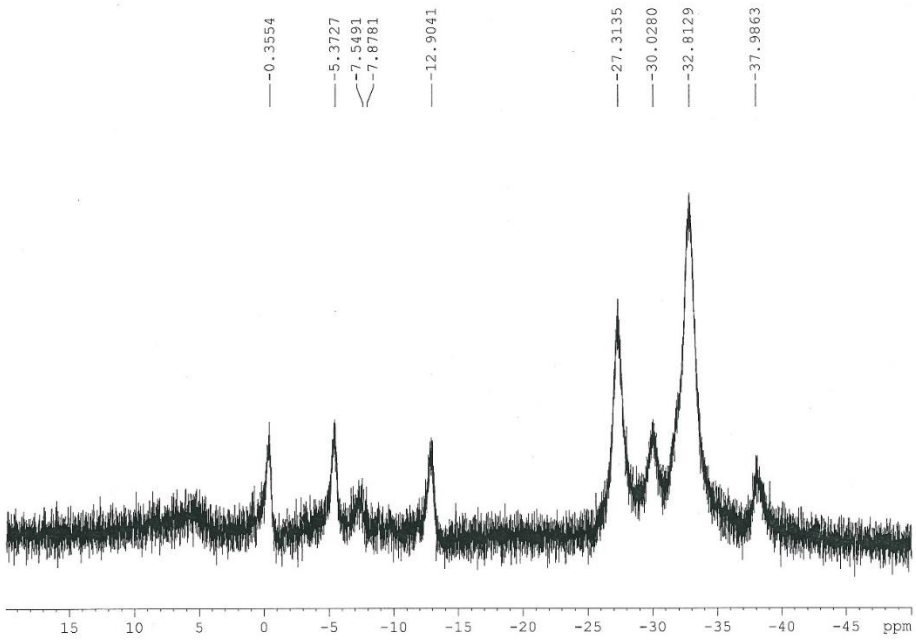

Figure 40: $^{11}B\{^{1}H\}$ spectrum of the product resulting from the nucleophilic attack of $^{-}CH_2CN$ on the $[trans\text{-}B_{20}H_{18}]^{2-}$ ion.

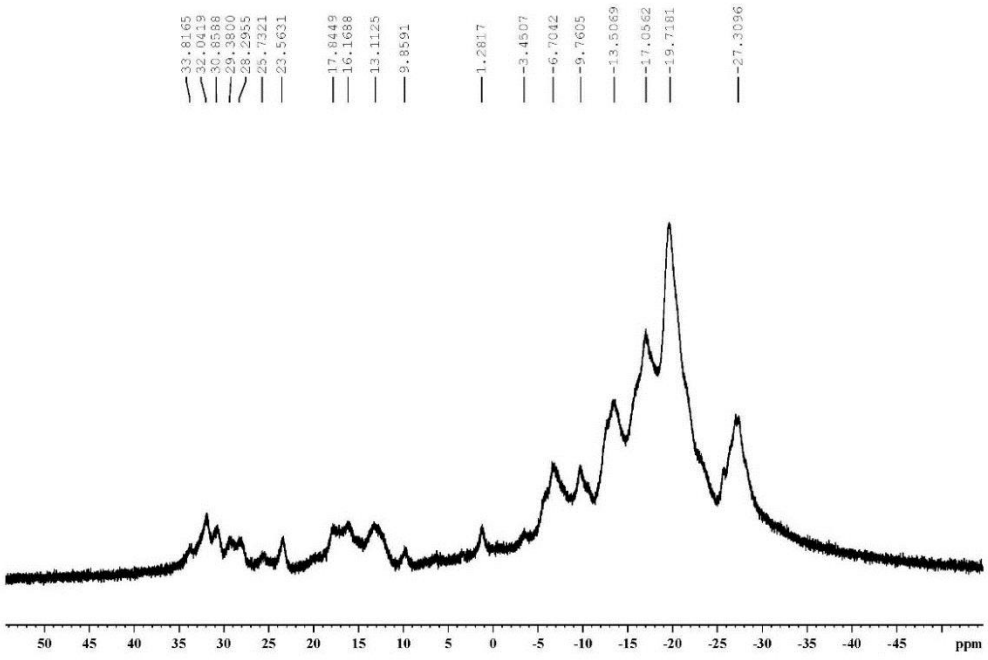

Figure 41: $^{11}B\{^{1}H\}$ NMR spectrum of the product of the oxidation of the $[ae\text{-}B_{20}H_{17}CH_2CN]^{4-}$ ion to form the $[trans\text{-}B_{20}H_{17}CH_2CN]^{2-}$ ion using *p*-benzoquinone in acidic organic oxidation.

The literature describes the use of carboranes as an attractive molecule for potential use in BNCT due to their richness of boron and stability in physiological conditions.[33] Specifically, Rosenbaum and coworkers iodinated a boron vertex of 1-carbo-*closo*-dodecaborate, and using microwave irradiation in the presence of copper (I) cyanide, the iodine was replaced by a cyano substituent. Juhasz further modified the cyano group by acid catalysis to convert the cyano group to a carboxylic acid.[36] The conversion of a cyano group to a carboxylic acid is ideal for coupling to biological molecules. The incorporation of a cyano group to the [*trans*-$B_{20}H_{18}]^{2-}$ ion seems plausible due to the susceptibility of the three center two electron bond's to nucleophilic attack. The reaction of the [*trans*-$B_{20}H_{18}]^{2-}$ ion with $^{-}$CN was achieved by allowing the [*trans*-$B_{20}H_{18}]^{2-}$ ion to react with copper (I) cyanide in dimethylformamide (DMF) at refluxing temperatures for six hours (**Scheme 19**).

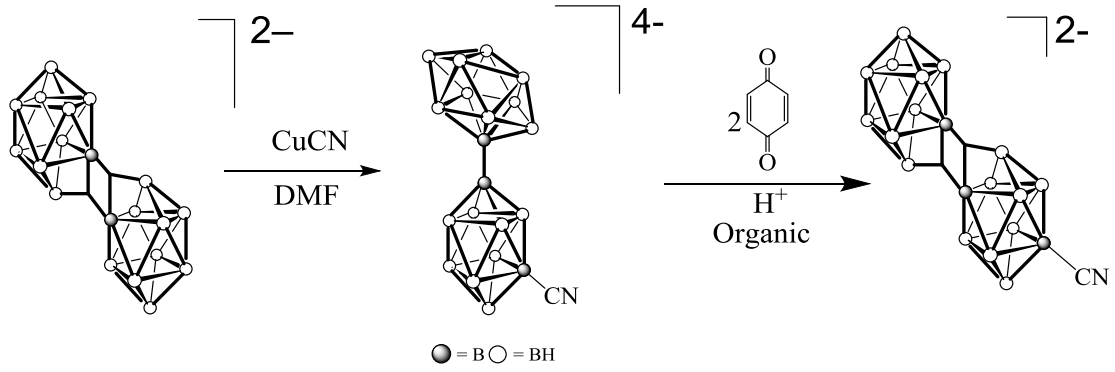

Scheme 19: Proposed reaction of the [*trans*-$B_{20}H_{18}]^{2-}$ ion with $^{-}$CN to form the [*ae*-$B_{20}H_{17}CN]^{4-}$ ion followed by oxidation of the product to form the [*trans*-$B_{20}H_{17}CN]^{2-}$ ion.

Quantitative conversion of the starting material to the reduced, substituted product was confirmed using $^{11}B\{^{1}H\}$ NMR spectroscopy (**Figure 42**). The isomeric assignment was

confirmed by the presence of three apical boron atom signals observed at 0.4, -3.2, and -4.2 ppm. The three apical boron atoms exhibit doublets in the proton-coupled ^{11}B NMR spectrum (**Figure 43**). The reduced species was isolated and treated with the oxidizing agent, *p*-benzoquinone, in an acidic organic environment. The $^{11}B\{^{1}H\}$ NMR (**Figure 44**) and ^{11}B spectra (**Figure 45**) of the oxidized product were consistent with spectra observed for similar oxidation products with signals at 29.3 and 14.8 ppm . Further characterization by X-ray crystallography has not been conducted due to the difficulty of growing single crystals.

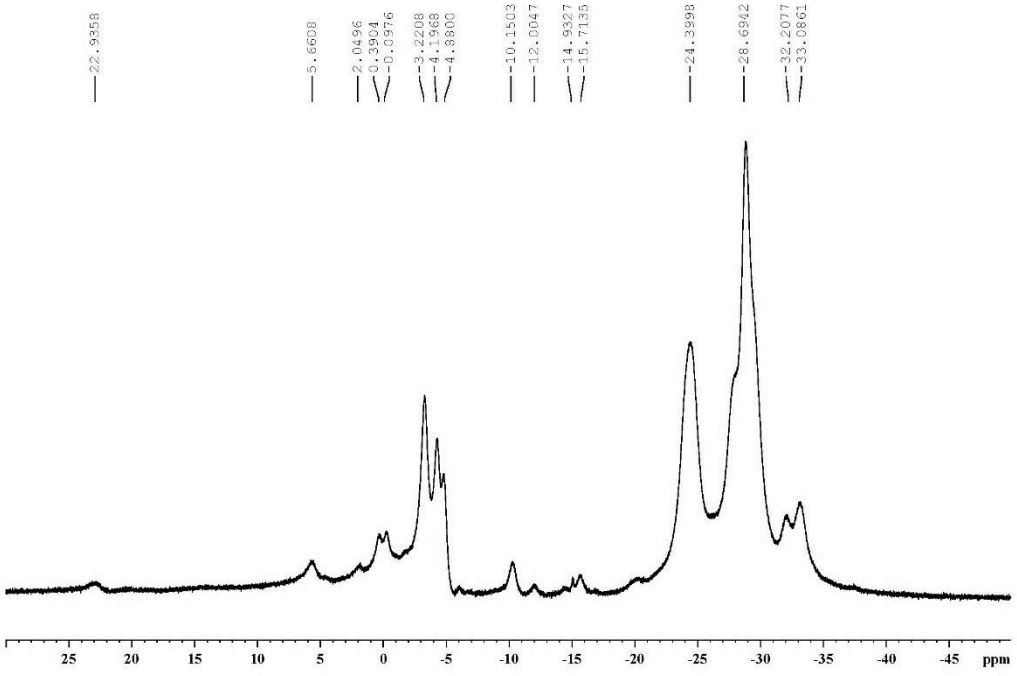

Figure 42: $^{11}B\{^{1}H\}$ spectrum of the product resulting from the nucleophilic attack of CuCN on $[trans\text{-}B_{20}H_{18}]^{2-}$ ion.

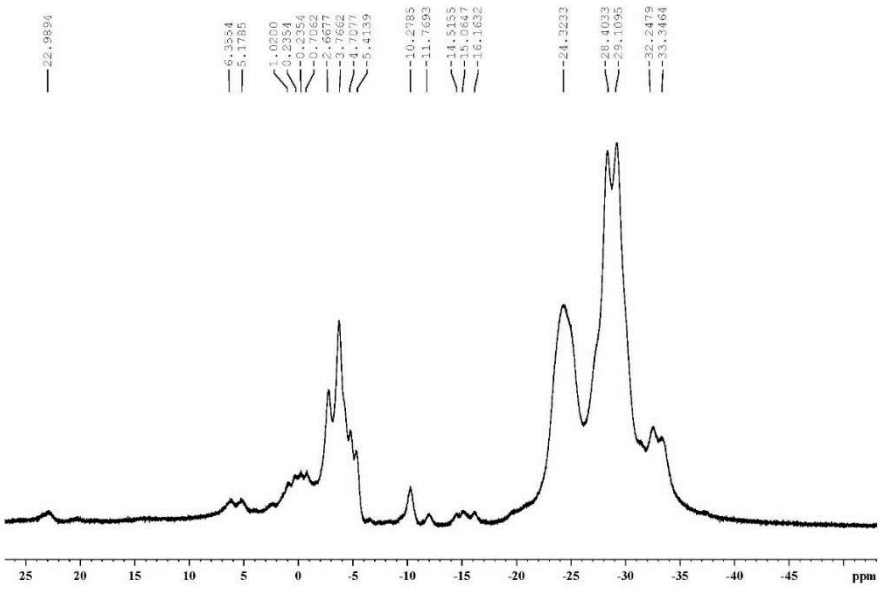

Figure 43: ^{11}B spectrum of the product resulting from the nucleophilic attack of CuCN on the [*trans*-$B_{20}H_{18}$]$^{2-}$ ion.

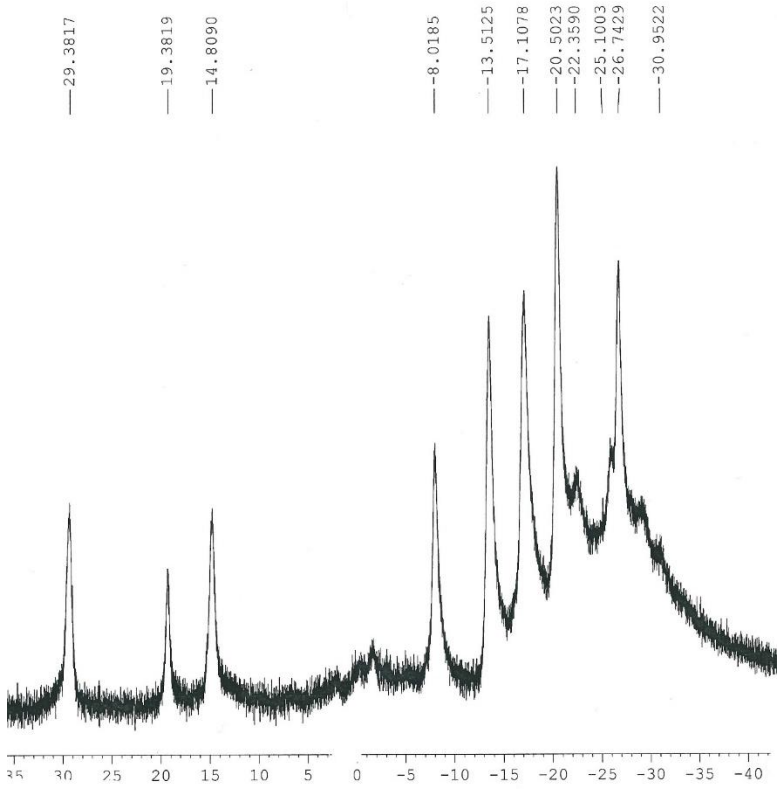

Figure 44: $^{11}B\{^{1}H\}$ spectrum of the product resulting from the oxidation of [*trans*-$B_{20}H_{17}X$]$^{4-}$ ion to [*trans*-$B_{20}H_{17}CN$]$^{2-}$ ion by *p*-benzoquinone acidic organic oxidation.

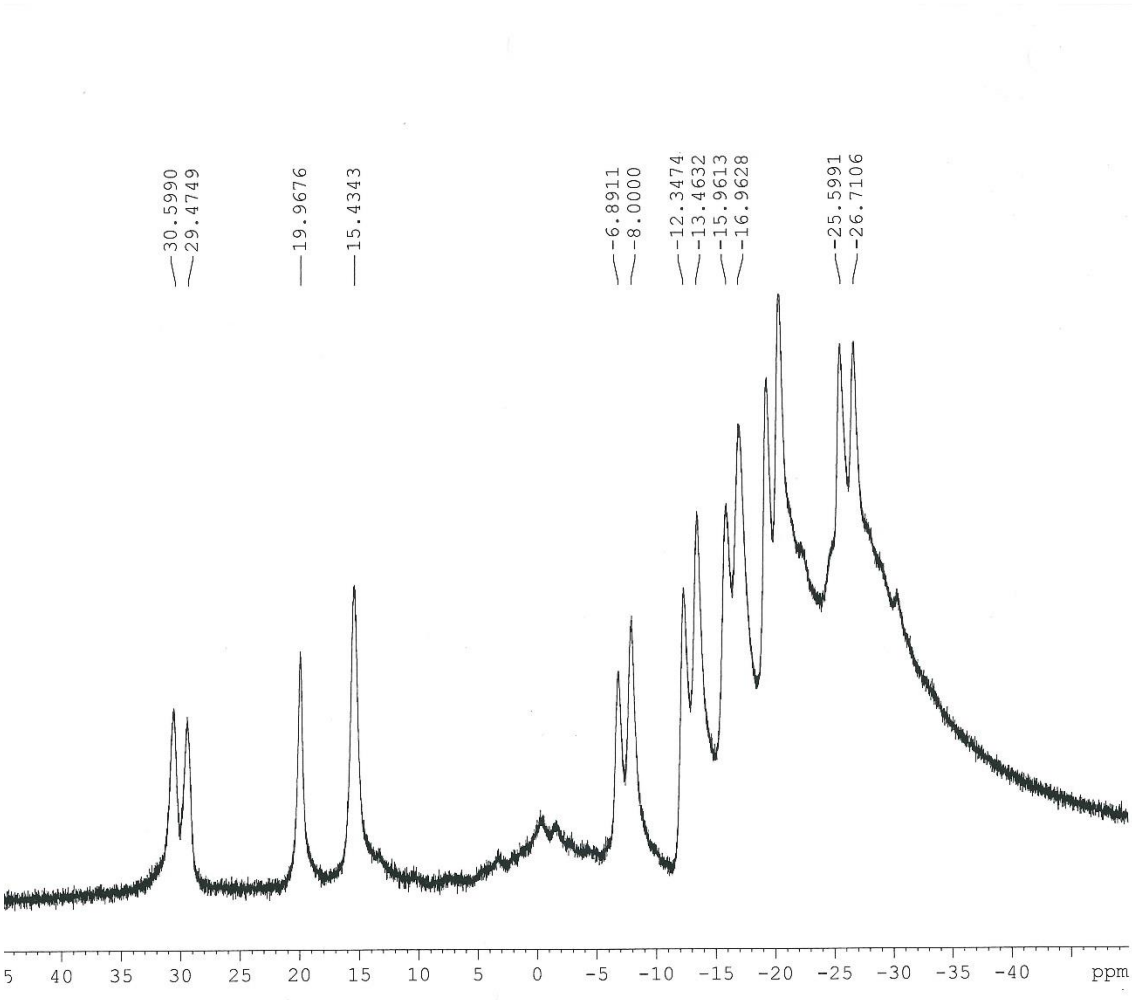

Figure 45: $^{11}B\{^{1}H\}$ NMR spectrum of the product resulting from oxidation of [*trans*-$B_{20}H_{17}X]^{4-}$ ion to [*trans*-$B_{20}H_{17}CN]^{2-}$ ion by *p*-benzoquinone acidic organic oxidation.

CHAPTER V

DISSCUSSIONS AND COMCLUSIONS

5.1 Reinvestigation of Reactions with Nucleophiles

The reaction of the [*trans*-$B_{20}H_{18}]^{2-}$ ion with sodium acetylide to form a reduced, substituted anion of the form [*ae*-$B_{20}H_{17}X]^{4-}$ was completed. The apical-equatorial isomeric assignment was confirmed by ^{11}B NMR spectroscopy; however, ^{1}H and ^{13}C NMR spectra provided no additional characterization information, presumably due to the coupling to the adjacent and neighboring boron atoms which have large quadrupolar moments and nuclear spins $I = 3/2$. Single crystals of the reduced product could not be obtained. Oxidation of the reduced product with the traditional ferric chloride solution resulted in removal of the substituent to form the [*trans*-$B_{20}H_{18}]^{2-}$ ion as confirmed by X-ray diffractometry. A milder oxidizing agent, *p*-benzoquinone, was used for the oxidation reaction and single crystals of the oxidized product were obtained and characterized using X-ray crystallography. The product of the reaction was the unanticipated [*trans*-$B_{20}H_{17}CH_3]^{2-}$ ion. The methyl substituent was located on the equatorial belt adjacent to the electron-deficient bonding region. Our original hypothesis for the formation of the methylated compound was that triple bond hydrolysis occurred as a result of the high reaction temperatures; however, this hypothesis is voided because the same product is obtained when the reaction is completed at room temperature. A second hypothesis is that the acetylide group is converted to a $–C(O)OCH_3$ substituent during the oxidation process, followed by the elimination of carbon dioxide. This hypothesis has not been tested. Single crystals of the reduced product would enable the determination of

whether the conversion to the methyl group occurs during the reaction to produce the reduced product or the reaction to produce the oxidized product. Regardless of how the methyl-substituted product was formed, the formation of the unexpected [*trans*-$B_{20}H_{17}CH_3]^{2-}$ ion led to the investigation of the reaction of three other carbon nucleophiles with the [*trans*-$B_{20}H_{18}]^{2-}$ ion.

5.2 **[*trans*-$B_{20}H_{17}CH_3]^{2-}$ Ion**

In an effort to rationally synthesize a methyl-substituted product, a unique reaction between the [*trans*-$B_{20}H_{18}]^{2-}$ ion and methyl Grignard reagent was investigated. Reaction of the [*trans*-$B_{20}H_{18}]^{2-}$ ion with $MgBrCH_3$ yielded a reduced, substituted species which was oxidized using *p*-benzoquinone. Single crystals of the oxidized product were obtained, confirming the formation of the desired [*trans*-$B_{20}H_{17}CH_3]^{2-}$ ion. The X-ray crystal structure of the product indicated that the methyl substituent was located on the equatorial belt adjacent to the terminal boron apex as opposed to the equatorial belt adjacent to the electron-deficient bonding region. The location of the substituent is consistent with the products formed from the nucleophilic attack of the [*iso*-$B_{20}H_{18}]^{2-}$ ion rather than the [*trans*-$B_{20}H_{18}]^{2-}$ ion. The only other report in the literature for this substituent location from the [*trans*-$B_{20}H_{18}]^{2-}$ ion was the reaction with a protected thiol nucleophile, $^{-}SC(O)C(CH_3)_3$. Single crystals of the thiol derivative were not obtained; however, two-dimensional ^{11}B NMR spectroscopy was used to determine the substituent location. The product of the thiol reaction was attributed to either the steric demand of the protecting group or the electronics of the sulfur atom; investigations not related to this work have been initiated to investigate the factors which determine the location of the

sulfur substituent. Results from the current investigation do not support the steric argument given that the methyl substituent is quite small as compared to the protected thiol group. Therefore, based on the current investigation, a new hypothesis is proposed. Nitrogen and oxygen nucleophiles are known to follow the mechanism proposed by Hawthorne which result in the substituent of the $[ae\text{-}B_{20}H_{17}X]^{4-}$ species being located on the equatorial belt adjacent to the intercage connection. This was also true for the reaction with the acetylide ion from the sodium acetylide source. In contrast, the sulfur nucleophile and now the methyl substituent resulting from the $MgBrCH_3$ source are located on the equatorial belt adjacent to the terminal boron apex. The new hypothesis is that the location of the substituent is dictated by hard-soft acid-base theory. We propose that the hard nucleophiles, such as the nitrogen and oxygen nucleophiles as well as the $NaC{\equiv}CH$, result in the substituent location on the equatorial belt adjacent to the intercage linkage and soft nucleophiles, such as the sulfur nucleophiles as well as the $MgBrCH_3$, result in the substituent location on the equatorial belt adjacent to the terminal apex of the boron cluster (**Scheme 20**).

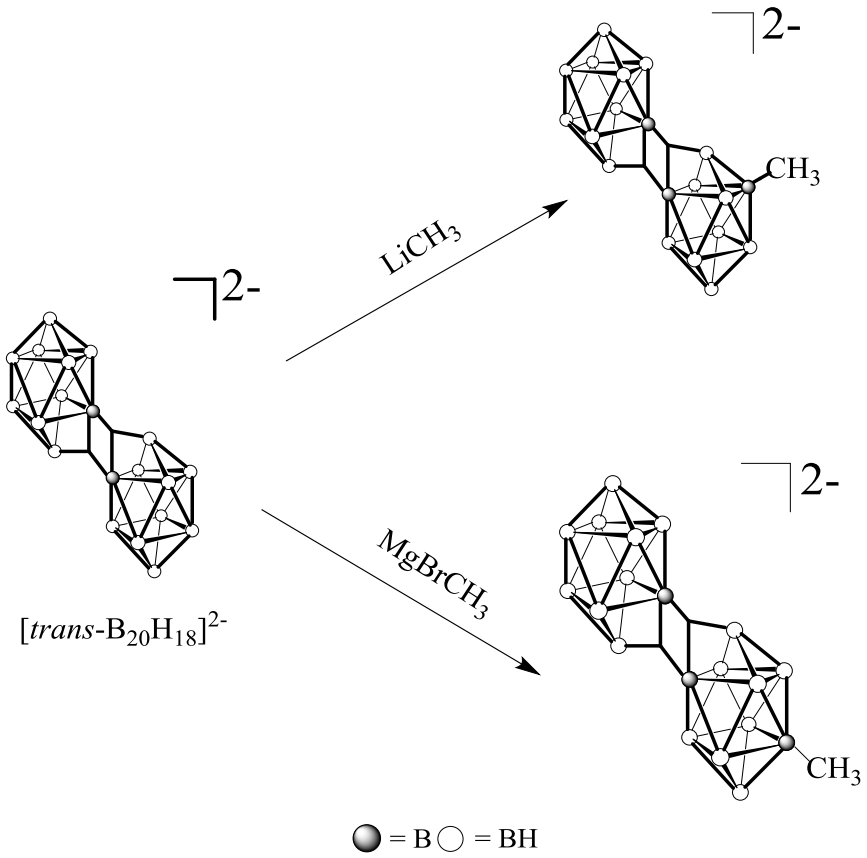

Scheme 20: Hypothetical scheme describing the placement of the substituent on the [*trans*-$B_{20}H_{17}X]^{2-}$ ions by based on hard and soft acids.

Once single crystals of the product of the methyllithium reaction and the product of the ethylmagnesium bromide reaction are obtained, we will have additional data for analysis. Based on the proposed hypothesis, the methyl substituent from the methyllithium reaction should be on the equatorial belt adjacent to the electron-deficient bonding region and the ethyl substituent from the Grignard reaction should be on the equatorial belt adjacent to the terminal boron apex.

5.3 **Oxidation with Carbon Electrophiles**

During the investigation of the oxidization reactions, two oxidizing agents were used: ferric chloride and *p*-benzoquinone. The ferric chloride tended to be too harsh for the reactions conducted and most reactions used *p*-benzoquinone. Investigations in other areas of the laboratory utilized substituents that are acid sensitive. As a result, the *p*-benzoquinone oxidation reaction was attempted in the absence of acid. In the absence of acid, no oxidation occurs regardless of solvent or reaction temperature. Therefore, the mechanism of the oxidation reaction was investigated. Based on the initial proposed mechanism of nucleophilic attack by Hawthorne,[15] one might anticipate that the oxidation reaction is initiated by the protonation of the $[B_{20}H_{17}X]^{4-}$ ion to form the $[B_{20}H_{17}X]^{3-}$ ion. The hydrogen resulting from the protonation process would ultimately reside on one of the apical boron vertices which constitute the three-center two-electron bonds characteristic of the oxidized ions. As a result, in the absence of the acidic solution, the oxidation process cannot proceed; however, in the presence of suitable electrophile, the oxidation process should proceed and result in the addition of a substituent at one of the apical boron vertices which constitute the electron-deficient bond (**Scheme 21)**.

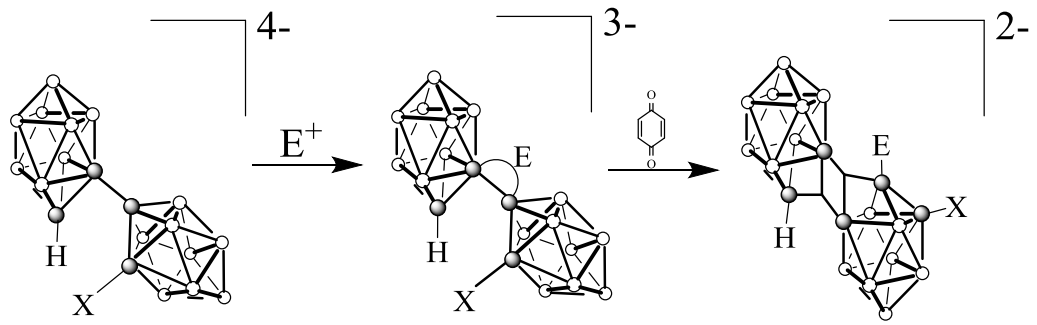

● = B ○ = BH X = Nucleophilie E = Electrophile

Scheme 21: Hypothetical scheme describing the oxidation of a reduced species resulting in a doubly substituted oxidized species.The hypothesis was tested by investigating the oxidation of the known.

$[B_{20}H_{17}OH]^{4-}$ ion with iodomethane and *p*-benzoquinone. An excess of iodomethane was used because the first equivalent of iodomethane was anticipated to alkylate the hydroxyl group and the second equivalent of iodomethane was anticipated to complete the oxidation reaction. The product of the reaction was isolated by recrystallization and single crystals were grown for X-ray crystallographic analysis. Rather than obtaining the anticipated doubly-substituted $[B_{20}H_{16}(CH_3)(OCH_3)]^{2-}$ product, the $[\mu\text{-}OCH_3\text{-}B_{20}H_{17}]^{2-}$ (**Figure 35**) ion, containing both oxygen and hydrogen-bridge bonds, was obtained. Formation of the bridging product is consistent with earlier observations that the bridging isomer is formed when the oxidation reactions are completed in non-aqueous solutions.[2] The $[\mu\text{-}OCH_3\text{-}B_{20}H_{17}]^{2-}$ product has been reported earlier from the ferric chloride oxidation of the $[B_{20}H_{17}OR]^{4-}$ ion in anhydrous ethanol. Based on the observed reactivity, it appears that both the hydrogen ion in the acidic solution and the iodomethane in the non-aqueous solution are functioning as electrophiles and initiate the oxidation reaction. Reactions using other electrophiles, benzoyl chloride

and acetyl chloride, have been conducted; however single crystals have not been obtained for the complete characterization using single crystal X-ray crystallography.

5.4 **Novel Reactions with Carbon Nucleophiles**

In addition to the reactions described above, reactions with additional carbon nucleophiles were investigated. Specifically, the reaction between the [*trans*-$B_{20}H_{18}]^{2-}$ ion and the $^{-}CH_2CN$ ion and the reaction between the [*trans*-$B_{20}H_{18}]^{2-}$ ion and the ^{-}CN were investigated. In both cases, the ^{11}B NMR spectrum of the product confirms the presence of a reduced, substituted apical-equatorial isomer of the form $[B_{20}H_{17}X]^{4-}$. Oxidation of both products has been achieved using *p*-benzoquinone, as confirmed by ^{11}B NMR spectroscopy. These substituents were chosen for their ability to be further modified to a carboxylic acid or an amide. Further characterization will be needed to confirm results prior to the derivatization of the products.

CHAPTER VI

FUTURE WORK

Although the polyhedral borane anions have been known for many years, the chemistry of the [*trans*-$B_{20}H_{18}$]$^{2-}$ ion remains relatively unexplored. The results from recent experiments not only enhance the understanding of the mechanism of nucleophilic attack, but also successfully demonstrate that the [*trans*-$B_{20}H_{18}$]$^{2-}$ ion is susceptible to nucleophilic attack by a carbon nucleophile. The ability of the [*trans*-$B_{20}H_{18}$]$^{2-}$ ion to react with carbon-based nucleophiles paves the way for compounds to be developed which can be used in several areas of research and develop specific novel target materials. A series of reactions and experiments has been proposed which help fully characterize and confirm previous results, investigate the reactivity of the [*trans*-$B_{20}H_{18}$]$^{2-}$ ion with a variety of carbon nucleophiles, and suggest modifications that may lead to more specific compounds for potential application in BNCT and drug delivery.

6.1 **Extension of Current Project**

The reactions of the [*trans*-$B_{20}H_{18}$]$^{2-}$ ion with sodium acetylide and methyl magnesium bromide gave rise to a hypothesis that potentially explains the location of the substituent group on the polyhedral borane ion and disproves the original hypothesis that the substituent location is controlled by steric effects. Therefore, the reactions conducted with methyllithium and ethylmagnesium bromide should be repeated in an effort to grow single crystals of the products for characterization by X-ray crystallography. Likewise, the unanticipated formation of [*trans*-$B_{20}H_{17}CH_3$]$^{2-}$ from the reaction of the [*trans*-

$B_{20}H_{18}]^{2-}$ ion and the acetylide ion, followed by oxidation of the reduced product, remains a mystery. Either an elemental analysis of the reduced ion or characterization of the reduced ion by X-ray crystallography is necessary to evaluate the reaction mechanism. If the reduced product has the acetylide substituent, the transformation occurs during the oxidation process. If the reduced product has the methyl substituent, the transformation occurs during the nucleophilic attack reaction. Reaction of the [*trans*-$B_{20}H_{18}]^{2-}$ ion with a series of terminal alkynes (such as 1-hexyne or phenylacetylene) would assist in the investigation to determine if the cleavage of the triple bond occurs and if cleavage can be prevented by protecting the triple bond by the presence of a longer alkyl chain.

The reactions investigating the use of electrophiles in the oxidation of [*trans*-$B_{20}H_{17}X]^{4-}$ ion to [*trans*-$B_{20}H_{17}X]^{2-}$ ion also need to be continued. The products of the reaction should be characterized by either elemental analysis or X-ray crystallography to confirm the identity of the products. The reactions developed to investigate the $^{-}CH_2CN$ and ^{-}CN nucleophiles have the potential to develop starting materials to investigate further modifications and allow for the synthesis of compounds with increased specificity for potential use in BNCT. Both reactions require further optimization along with complete characterization of the products.

6.2 **Potential Projects**

The current project establishes a basis by which new projects can be developed which further expand the understanding of the reactivity of the [*trans*-$B_{20}H_{18}]^{2-}$ ion along with producing new products that may be potentially used in BNCT.

6.2.1 **Modified Acetonitrile Derivatives**

Synthesis of either the $[B_{20}H_{17}CH_2CN]^{2-}$ ion or the $[B_{20}H_{17}CN]^{2-}$ ion would open an area of investigation to develop the chemistry of the substituent group and make the compounds more biologically relevant. Based on previous work conducted by Spievogel and coworkers with cyano-substituted boranes, both the $[B_{20}H_{17}CH_2CN]^{2-}$ ion and the $[B_{20}H_{17}CN]^{2-}$ ions could be treated with triethyloxoniumtetrafluoroborate to produce an intermediate salt.[34] When the intermediate is treated with hot water, the intermediate salt is hydrolyzed into a carboxylic acid and when treated with a hot base the intermediate is converted into an amide.[30] Along with the initial experiments, the length of the alkyl chain could be modified to prevent the substitution of the intermediate salt substituent with a base on the boron cluster. Transformation of the -CN group to a carboxylic acid also may also be accomplished though acid catalyzed hydrolysis.[33,34]

6.2.2 **Modified Acetylide Derivatives**

Carboxylic acids are a primary target for compounds with biological relevance to give the ability to couple to amino acids**.** Polyhedral borane anions are known to interact with serum albumins, primarily due to the electrostatic interactions; however, only the $[B_{20}H_{17}SH]^{4-}$ ion is bound to the protein covalently.[35]

Terminal alkynes can be treated with O_3 to form a carboxylic acid.[36] Therefore, a reaction is proposed to treat the [*trans*-$B_{20}H_{17}C{\equiv}CH]^{2-}$ ion with O_3 **(Scheme 22)**. The basic conditions of reaction may also lead to nucleophilic attack by the base in solution. To minimize the nucleophile reaction, a longer chain with a terminal alkyne may result in

a preference for the reaction at the terminal alkyne as opposed to the boron cluster because of steric access.

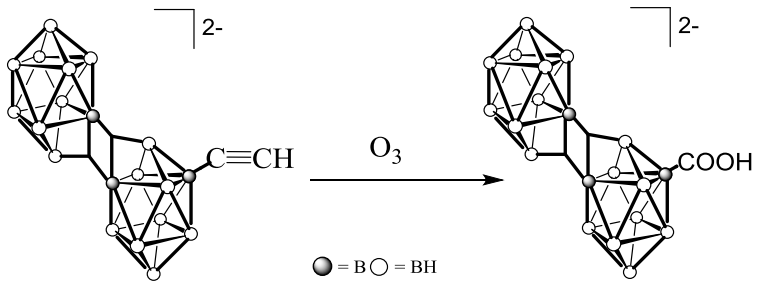

Scheme 22: Conversion of acetylide to carboxylic acid.

6.2.3 **Amino Acid Coupling**

A goal in the development of molecules for potential application in BNCT is to make the molecules more specific to the target to allow for more effective use of the molecule and reduce adverse effects. One way to accomplish this goal is by coupling the molecule to an amino acid that may be present in the substrate of the target. Peptides are linked together by hydrogen bonds between a carboxyl group and an amine depending on pH of the system. Therefore, if a [*trans*-$B_{20}H_{18}]^{2-}$ ion is substituted with a carboxylic acid or an amine, it should be possible to couple the molecules with amino acids. Dicyclohexylcarbodiimide (DCC) and 4-dimethylaminopyridine (DMAP) can be used to couple the desired compounds.[35] Therefore, a reaction is proposed to couple [*trans*-$B_{20}H_{17}COOH]^{2-}$, [*trans*-$B_{20}H_{17}CH_2CONH_2]^{2-}$, [μ-OCOOH-$B_{20}H_{17}]^{2-}$ ion, or [μ-O $CHCONH_2$-$B_{20}H_{17}]^{2-}$ ions to an amino acid or a derivative of an amino acid (**Scheme 23**).

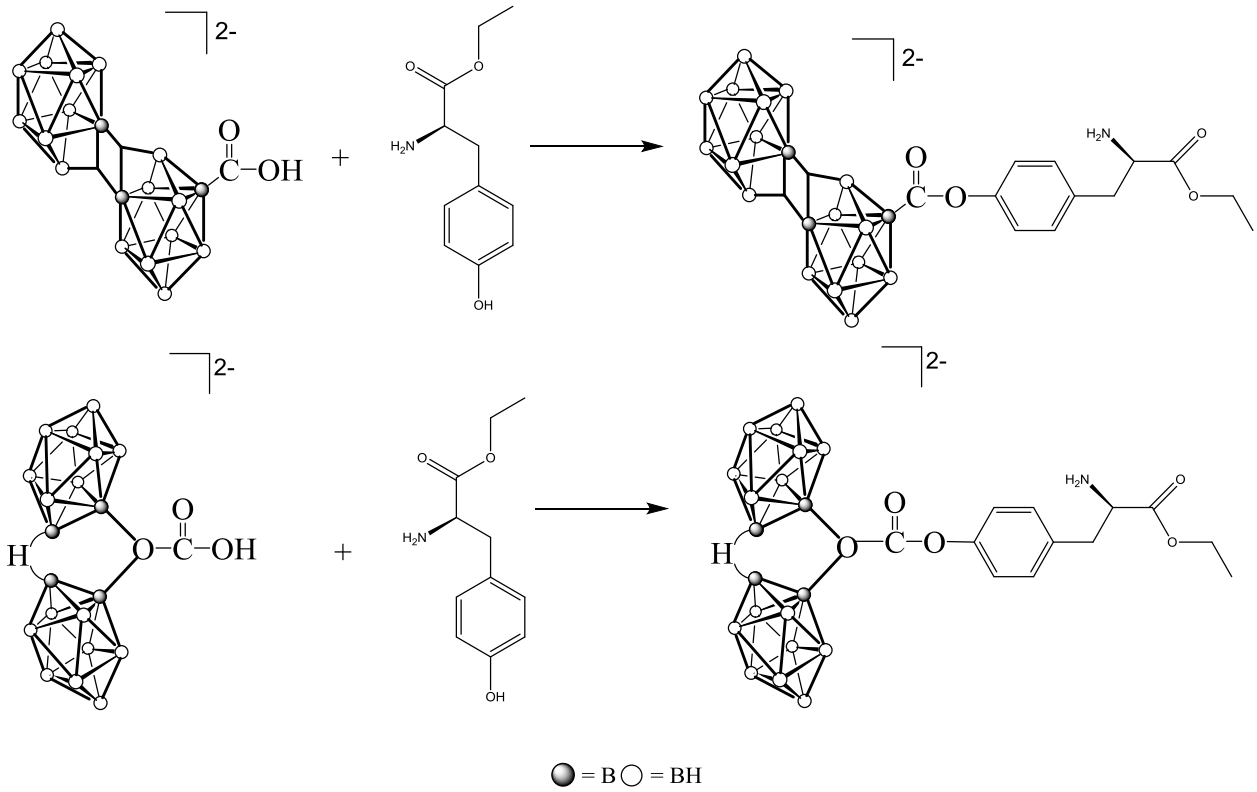

Scheme 23: Hypothetical coupling of [*trans*-$B_{20}H_{17}COOH]^{2-}$ and [μ-OCOOH-$B_{20}H_{17}]^{2-}$ ion and a carboxylic acid to and amino acid derivative, tyrosine ethyl ester.

6.2.4 **Synthesis of Amino Acid Ring**

Designing a coupling reaction between amino acids and protein is enhanced by a knowledge of a target protein. Target proteins vary depending on the disease, but a common target protein class is enzymes. When inhibited, enzyme functionality and substrate modification are disrupted. Substrates are modified by enzymes for use in other biological processes. Enzymes perform similarly to a catalyst in synthetic chemistry; they lower the activation energy to allow reaction to occur more readily. Enzymes contain a substrate binding site referred to as an active site. Substrates bind to the active site by bonding to the side chains of amino acids found within the active site. Replication of the

binding scheme is attempted when synthesizing a drug or molecule for treatment. This binding scheme may be possible with the [*trans*-$B_{20}H_{18}$]$^{2-}$ ion by coordinating amino acid substituents on the equatorial belt on both boron clusters which may lead to a linkage around half of the boron cluster complex. This would allow for multiple binding sites from one molecule of the substituted [*trans*-$B_{20}H_{18}$]$^{2-}$ ion (**Figure 46)**.

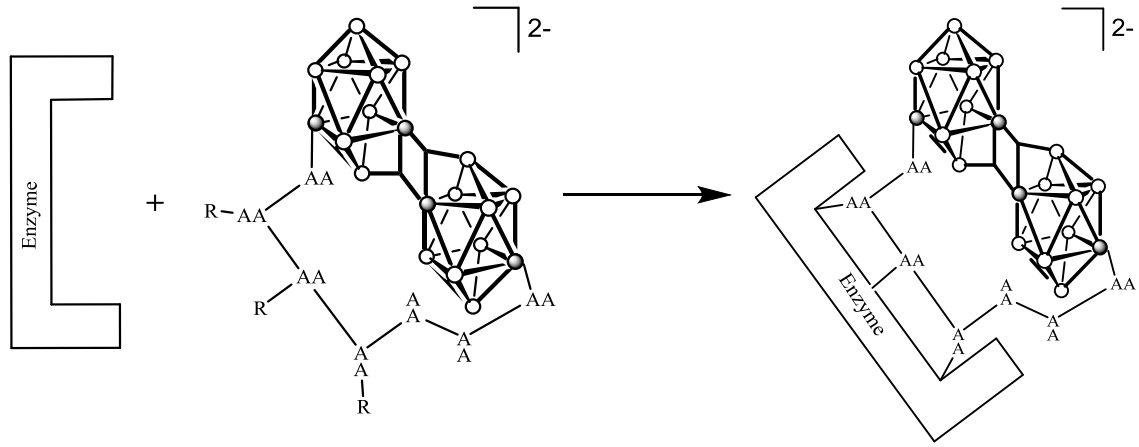

Figure 46: Hypothetical binding scheme of amino acid ring around [*trans*-$B_{20}H_{18}$]$^{2-}$ ion bond to a target enzyme AA- Amino acid or an amino acid derivative.

6.2.5 **[*trans*-$B_{20}H_{18}$]$^{2-}$ Ion Interaction with DNA**

The binding of a biological agent to an enzyme allows for more efficient targeting which aides the disruption of biological processes. This synthetic design allows for less side effects from treatment, along with other production and monetary benefits. However, when choosing a target for therapy, it is always best to choose the source of the disease. Several diseases involve a mutation with DNA. Molecules and drugs that are used to treat these diseases bind to DNA by an electrostatic interactions, groove binding, and/or intercalation. Intercalation takes advantage of pi stacking between the bases in the DNA

ladder and the aromatic component of a drug or treatment molecule. Polyhedral borane anions have been described as having three dimensional aromaticity. The proposed experiments are to synthesize a [*trans*-$B_{20}H_{18}]^{2-}$ ion with an aromatic substituent, create a competitive and noncompetitive environment, and observe if the cage or the substituent is involved in intercalation. An investigation of this nature would allow for multiple targets to be utilized, potentially eliminate the use of a drug delivery system, and observe the interactions of the substituted [*trans*-$B_{20}H_{18}]^{2-}$ ions with biological agents in a competitive environment.

LITERATURE CITED

1. Hawthorne, M. F.; Lee, M. W. A Critical Assessment of Boron Target Compounds for Boron Neutron Capture Therapy. *J. Neurooncol. 62* (1-2), 33–45.
2. Hawthorne, M. F.; Shelly, K.; Li, F. The Versatile Chemistry of the $[B_{20}H_{18}]^{2-}$ Ions: Novel Reactions and Structural Motifs. *Chem. Commun*. **2002**, No. 6, 547–554.
3. Barth, R. F.; Vicente, M. G. H.; Harling, O. K.; Kiger, W. S.; Riley, K. J.; Binns, P. J.; Wagner, F. M.; Suzuki, M.; Aihara, T.; Kato, I.; Kawabata, S. Current Status of Boron Neutron Capture Therapy of High Grade Gliomas and Recurrent Head and Neck Cancer. *Radiat. Oncol.* **2012**, *7* (1), 146.
4. Feakes, D. A.; Shelly, K.; Knobler, C. B.; Hawthorne, M. F. $Na_3[B_{20}H_{17}NH_3]$: Synthesis and Liposomal Delivery to Murine Tumors. *Proc. Natl. Acad. Sci. U. S. A.* **1994**, *91* (8), 3029–3033.
5. Shelly, K.; Feakes, D. A.; Hawthorne, M. F.; Schmidt, P. G.; Krisch, T. A.; Bauer, W. F. Model Studies Directed toward the Boron Neutron-Capture Therapy of Cancer: Boron Delivery to Murine Tumors with Liposomes. *Proc. Natl. Acad. Sci. U. S. A.* **1992**, *89* (19), 9039–9043.
6. Feakes, D. A.; Waller, R. C.; Hathaway, D. K.; Morton, V. S. Synthesis and *in Vivo* Murine Evaluation of $Na_4[1\text{-}(1'\text{-}B_{10}H_9)\text{-}6\text{-}SHB_{10}H_8]$ as a Potential Agent for Boron Neutron Capture Therapy. *Proc. Natl. Acad. Sci. U. S. A.* **1999**, *96* (11), 6406–6410.
7. Greenwod, N.N., Earnshaw, A. *Chemistry of Elements* 1st ed.; Emsoford: Ney York, 1986; pp 155-202.
8. Welch, A. J. The Significance and Impact of Wade's Rules. *Chem. Commun. (Camb).* **2013**, *49* (35), 3615–3616.
9. Kroto, H. W.; Heath, J. R.; O'Brien, S. C.; Curl, R. F.; Smalley, R. E. C60: Buckminsterfullerene. *Nature* **1985**, *318* (6042), 162–163.
10. Wade, K. The Structural Significance of the Number of Skeletal Bonding Electron-Pairs in Carboranes, the Higher Boranes and Borane Anions, and Various Transition-Metal Carbonyl Cluster Compounds. *J. Chem. Soc. D Chem. Commun.* **1971**, No. 15, 792.
11. Mingos, D. M. P. A General Theory for Cluster and Ring Compounds of the Main Group and Transition Elements. *Nature* **1972**, *236* (68), 99–102.
12. Lipscomb, W. N. The Boranes and Their Relatives. *Science* **1977**, *196* (4294), 1047–1055.
13. Johnson, W. C. Hydrides of Boron and Silicon (Stock, Alfred). *J. Chem. Educ.* **1934**, *11* (4), 256.
14. Stock, A. *Hydrides of Boron and Silicon*. Cornell University Press: Ithaca, NY, **1933**.
15. Kaczmarczyk, A.; Dobrott R. D., and Lipscomb, W. N. Reactions of $[B_{20}H_{18}]^{2-}$ Ion. *Proc. Natl. Acad. Sci.* **1962,** *48*, 729-733.
16. Pitochelli, A. R.; Lipscomb, W. N.; Hawthorne, M. F. Isomers of $B_{20}H_{18}^{-2}$. *J. Am. Chem. Soc.* **1962**, *84* (15), 3026–3027.

17. Hawthorne, M. F.; Pilling, R. L.; Stokely, P. F. The Preparation and Rearrangement of the Three Isomeric $B_{20}H_{18}^{-4}$ Ions. *J. Am. Chem. Soc.* **1965**, *87* (9), 1893–1899.
18. Li, F.; Shelly, K.; Knobler, C. B.; Hawthorne, M. F. A New Isomer of the $[B_{20}H_{18}]^{2-}$ Ion: Synthesis, Structure, and Reactivity of *cis*-$[B_{20}H_{18}]^{2-}$ and *cis*-$[B_{20}H_{17}NH_3]^-$. *Angew. Chemie Int. Ed.* **1998**, *37* (13-14), 1868–1871.
19. Hawthorne, M. F.; Pilling, R. L. Photoisomerization of the $B_{20}H_{18}^{-2}$ Ion. *J. Am. Chem. Soc.* **1966**, *88* (16), 3873–3874.
20. Hawthorne, M. F.; Pilling, R. L.; Stokely, P. F.; Garrett, P. M. The Isolation and Characterization of $B_{20}H_{19}^{-3}$ and $B_{20}H_{18}^{-4}$ Ions. *J. Am. Chem. Soc.* **1963**, *85* (22), 3704–3705.
21. Hawthorne, M. F.; Philling, R. L.; Garrett, P. M. A Study of the Reaction of Hydroxide Ion with $B_{20}H_{18}^{-2}$. *J. Am. Chem. Soc.* **1965**, *87* (21), 4740–4746.
22. Watson-Clark, R. A.; Hawthorne, M. F. An Exploratory Evaluation of the Reactions of Organic Oxidants with Polyhedral Borane Anions. *Inorg. Chem.* **1997**, *36* (23), 5419–5420.
23. Chamberland BL, Muetterties EL. *Inorg. Chem.* **1964**; 3: 1451.
24. Hawthorne, M. F. The Role of Chemistry in the Development of Boron Neutron Capture Therapy of Cancer. *Angew. Chemie Int. Ed. English* **1993**, *32* (7), 950–984.
25. Soloway, A. H.; Tjarks, W.; Barnum, B. A.; Rong, F. G.; Barth, R. F.; Codogni, I. M.; and Wilson, J. G. The Chemistry of Neutron Capture Therapy. *Chem. Rev.***1998,** *98* (4), 1515-1562.
26. Georgiev, E. M.; Shelly, K.; Feakes, D. A.; Kuniyoshi, J.; Romano, S.; Hawthorne, M. F. Synthesis of Amine Derivatives of the Polyhedral Borane Anion [B 20 H 18] 4 -. *Inorg. Chem.* **1996**, *35* (19), 5412–5416.
27. Smits, J. P.; Mustachio, N.; Newell, B.; Feakes, D. A. Synthesis and Investigation of $[B_{20}H_{17}O(CH_2)_5]^{3-}$, a Novel Solvent Complex of the $[B_{20}H_{18}]^{4-}$ Ion. *Inorg. Chem.* **2012**, *51* (15), 8468–8472.
28. Mantz, M. M.S. Thesis, Texas Reactivity of the $[B_{20}H_{18}]^{2-}$ Ion with Carbon Nucleophiles For Potential Application In BNCT Texas State University, **2013**.
29. Li, F.; Shelly, K.; Kane, R. R.; Knobler, C. B.; Hawthorne, M. F. ChemInform Abstract: Synthesis and Structure of the Polyhedral $(\mu\text{-}B_{20}H_{17}OH)^{2-}$ Borane Anion Containing Both Oxygen- and Hydrogen-Bridge Bonds. *ChemInform* **2010**, *27* (44), no – no.
30. Stasko, D.; Hoffmann, S. P.; Kim, K.-C.; Fackler, N. L. P.; Larsen, A. S.; Drovetskaya, T.; Tham, F. S.; Reed, C. A.; Rickard, C. E. F.; Boyd, P. D. W.; Stoyanov, E. S. Molecular Structure of the Solvated Proton in Isolated Salts. Short, Strong, Low Barrier (SSLB) H-Bonds. *J. Am. Chem. Soc.* **2002**, *124* (46), 13869–13876.
31. Kato, T.; Stoyanov, E.; Geier, J.; Grützmacher, H.; Reed, C. A. Alkylating Agents Stronger than Alkyl Triflates. *J. Am. Chem. Soc.* **2004**, *126* (39), 12451–12457.

32. Montalvo, S. J.; Hudnall, T. W.; Feakes, D. A. Exploring the Redox Reactivity of the $[B_{20}H_{18}]^{2-}$ Ion with Carbon-Based Nucleophiles and Electrophiles. *J. Organomet. Chem.* **2015**.
33. Rosenbaum, A. J.; Juers, D. H.; Juhasz, M. A. Copper-Promoted Cyanation of a Boron Cluster: Synthesis, X-Ray Structure, and Reactivity of 12-CN-*closo*-$CHB_{11}H_{10}^-$. *Inorg. Chem.* **2013**, *52* (19), 10717–10719.
34. Spielvogel, B. F.; Wojnowich, L.; Das, M. K.; McPhail, A. T.; Hargrave, K. D. Letter: Boron Analogues of Amino Acids. Synthesis and Biological Activity of Boron Analogues of Betaine. *J. Am. Chem. Soc.* **1976**, *98* (18), 5702–5703.
35. McVey, W. J.; Matthews, B.; Motley, D. M.; Linse, K. D.; Blass, D. P.; Booth, R. E.; Feakes, D. A. Investigation of the Interactions of Polyhedral Borane Anions with Serum Albumins. *J. Inorg. Biochem.* **2008**, *102* (4), 943–951.
36. Yang, N.-C. C.; Libman, J. Ozonation of Acetylenes and Related Compounds in the Presence of Tetracyanoethylene and Pinacolone. *J. Org. Chem.* **1974**, *39* (12), 1782–1784.